THE ELASTIC MODULI OF SOILS WITH DISPERESED OVERSIZE PARTICLES

by

Sebastian Lobo-guerrero

B.S. in C.E., Universidad de los Andes, 2002

Submitted to the Graduate Faculty of

the School of Engineering in partial fulfillment

of the requirements for the degree of

Master of Science

University of Pittsburgh

2002

UNIVERSITY OF PITTSBURGH

SCHOOL OF ENGINEERING

This thesis was presented

by

Sebastian Lobo-guerrero

It was defended on

October 29th, 2002

and approved by

Jeen-Shang Lin, Associate Professor, Civil and Environmental Engineering Department

Chao-Lin Chiu, Professor, Civil and Environmental Engineering Department

Thesis Advisor: Luis E. Vallejo, Associate Professor, Civil and Environmental Engineering Department

ABSTRACT

THE ELASTIC MODULI OF SOILS WITH DISPERSED OVRSIZE PARTICLES

Sebastian Lobo-guerrero, M.S.

University of Pittsburgh, 2002

To calculate the elastic deformations experienced by soils subjected to static or dynamic loads, knowledge of the elastic constants is required. The elastic constants (υ, E, G) are normally evaluated in the laboratory using conventional triaxial compressive tests on cylindrical samples. For meaningful test results, it is necessary to maintain a ratio of sample diameter to the maximum particle size of approximately 6 to 1 or greater. However, some soils have large and dispersed oversize particles that make it impossible for them to be tested in the conventional triaxial apparatus. This study presents the application of theoretical models that calculate the elastic properties of a composite made of an elastic matrix containing large dispersed particles.

The presented models require only knowledge of the elastic properties of the matrix coupled with the concentration by volume of the large particles in order to calculate the elastic properties of the mixture. These models were applied to different mixtures under different conditions of vertical pressure and moisture content. It was found that the models predict very well the measured elastic properties. The measurement of the elastic properties was carried out using an ultrasonic velocity apparatus.

It should be noticed that most of the tests presented in this research are related to the dynamic elastic properties of the mixtures; however, it was found that most of these models could be applied in order to predict the static elastic properties too.

PREFACE

I would like to express my sincere appreciation to my advisor Dr. Luis E. Vallejo, Associate Professor of the department of Civil and Environmental Engineering at the University of Pittsburgh, for his guidance and assistance at various stages of this investigation. The work described herein was supported by Grant No. CMS-0124714 to the University of Pittsburgh from the National Science Foundation, Washington, D.C. This support is gratefully acknowledged.

TABLE OF CONTENTS

LIST OF TABLES

LIST OF FIGURES

1.0 INTRODUCTION

Sediment and soil mixtures are the most important components of mudflows, glacial tills, debris flows, and colluvial soil deposits. The structure of these kinds of soil consists on a combination of large particles such as gravel fragments, and a soft matrix composed by clay or silt. Although some properties of these soils such as porosity and shear strength have been studied for several years [1] , there is not a general model explaining all the factors involved in predicting the elastic behavior of these compounds. Knowledge of the elastic properties (Young's modulus of elasticity, E; Poisson's ratio, ν; and shear modulus, G) is important, since they are required for the calculation of the elastic deformation experienced by soils when they are subjected to either static or dynamic loads. Although the stress-strain response of soils to static and dynamic loads may not be strictly represented as linear elastic, solutions based on linear elastic behavior are commonly used for the estimation of stresses or strains in the field.[2]

The elastic moduli are normally evaluated in the laboratory by using conventional triaxial compressive tests on cylindrical samples with a diameter of 7.1 cm, and a height of 14.2 cm. For meaningful test results, it is necessary to maintain a ratio of sample diameter to the maximum particle size of approximately 6 to 1 or greater. However, some soils have large and dispersed oversize particles that make it impossible for them to be tested in the conventional triaxial apparatus [3,4,1]. Sometimes the large particles (bigger than 1/7 of the sample diameter) are replaced with clay from the mixtures, affecting the agreement between the laboratory behavior and the field behavior since these samples do not represent the physical properties of the real components.

Thus, the main purpose of this research is to present and evaluate theoretical models that can be used to predict the elastic properties of a soil composite made of an elastic matrix containing large dispersed rigid particles. These models require only knowledge of the elastic constants of the matrix coupled with the concentration by volume of the large particles.

This research is organized as follows: Chapter 2.0 gives a briefly introduction to the topic of soil mixtures, presenting the results of the literature review about the different kinds of mixture structures and the models that are used on predicting mixtures properties such as porosity and hydraulic conductivity. Chapter 3.0 presents the theoretical models proposed by Hashin, Guth and Greszczuk in order to predict the elastic properties of mixtures.

Chapter 4.0 details the laboratory procedures and the equipment used in this research. Also, it includes a detailed description of the used materials. Chapter 5.0 studies the influence that the external pressure has on the performance of the theoretical models. Chapter 6.0 studies how the moisture content of the mixtures can affect the performance of the theoretical models. Chapter 7.0 and Chapter 8.0 focus on the influence that the size ratio of the particles has on the performance of these models. Chapter 9.0 attempts to study whether or not this models can be used in order to predict the static elastic properties of the mixtures, and how the assumption that these models have are affected. Chapter 10.0 presents the statistical analysis of the results obtained trough out this investigation, and finally, a summary of the major conclusions is presented in Chapter 11.0.

2.0 CONFIGURATION OF THE MIXTURE STRUCTURE

2.1 Kinds of Structures

Binary soil mixtures can present two different types of structure. The first one is called the "Contact Structure", and it occurs when the large particles of the mixture are in contact. The second one is termed as the "Floating Structure"; here, the large particles have a low concentration in the mixture, and they can be treated as disperse particles [5]. Figure 2.1 shows the two kinds of structures.

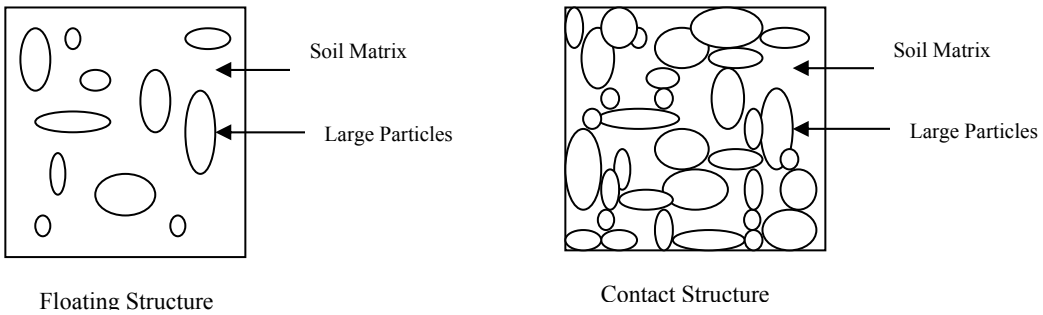

Figure 2.1 Soil Structures
(adapted from Innachione [5])

In a soil mixture, properties such as porosity, hydraulic conductivity, and shear strength are determinated by the interaction between the large particles and the fine particles. When the soil configuration presents a Contact Structure, the properties of the mixture depend mostly on the properties of the large particles. When the structure is floating, these properties depend mostly on the matrix characteristics. [6,7,5]

The gradual change between the two kinds of structures can be depicted by using two different approaches, the Ideal Packing Model and the Fractional Packing Model. Basically, the Ideal Packing Model assumes that only one

kind of structure will take place on the mixture, while the Fractional Packing Model suggests that the two kinds of structures can occur at the same time.

2.1.1 Principle of the Ideal Packing Model

This theoretical approach supposes that in a soil mixture the fine particles and the large particles interact without any kind of disturbance. In this way, three different stages function of the fines content can be noticed. Starting with a fine particles concentration of zero, the Contact Structure takes place while the fines are aggregated to the mixture, filling the voids between the coarse particles. At this point, the amount of voids between the large particles is higher than the volume of the fine particles. The second stage comes about when a critical fines content is produced at the moment of perfect fit. Finally, the third stage is produced when the fine particles start to separate the coarse particles, generating the Floating Structure [6,8,9]. The following figure illustrates this gradual interaction (Modified Vallejo and Mawby [10]).

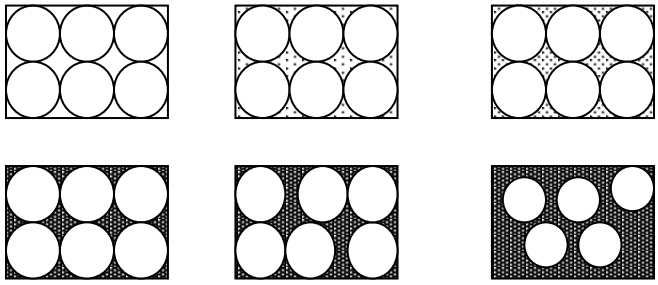

Figure 2.2 Soil Structure Under the Ideal Packing Model

Since this model only considers the geometric properties of the components, it could be used for different kinds of mixtures such as sandy clay or gravel-sand.

2.1.2 Principle of the Fractional Packing Model

The Ideal Packing Model suggests that only one kind of structure can occur in the soil at a certain moment. According to Marrion [8] and Kolterman and Gorelick [11] this assumption is only valid for a low or a very high coarse particle concentration. Thus, Kolterman and Gorelick [11] have proposed that soil can present two different structures at the same time. The Fractional Packing Model uses the same three stages and equations as the Ideal Packing Model, but it involves some correction factors.

2.2 Porosity in Soil Mixtures, Ideal Packing Model Approach

Porosity has been defined as the ratio between the voids volume and the solids volume inside a soil sample, giving a clear idea about the voids content. Several authors have found that porosity is controlled by the mixture's structure. In this way, the grain sorting, the fines content, and the external pressure determine this property in a soil mixture [12,13,6]. Using laboratory results, Vallejo and Mawby [14], Kolterman and Gorelick [11,13], Marrion [8], and Yin [6], have shown the following trend:

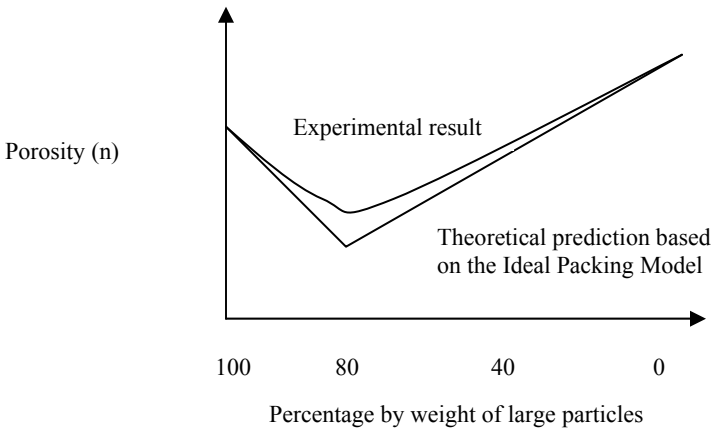

Figure 2.3 Observed Trend for Porosity in Binary Mixtures

Figure 2.3 shows the three stages that they found. The first one occurs when the voids volume inside the coarse material is higher than the volume of the fine particles, and the mixture structure is contact structure. The coarse

setup controls the mixture porosity, producing closer values to the pure large particles porosity. The second stage takes place when a minimum on porosity is reached. The fines perfectly fill the voids between the large particles, while porosity decreases to its minimum value. Finally, the third stage comes about when the fine particles volume is higher than the coarse particles voids. The setup of the packing is floating structure, since the fine particles start to separate the coarse material. Considering a unitary volume, the authors mentioned above matematicaly depict the three stages using the equations presented in Table 2.1:

Table 2.1 Expressions for porosity on binary soil mixtures

$C_f < n_c$	$C_f = n_c$	$C_f > n_c$
$n_{mix} = n_c - C_f(1-n_f)$	$n_{mix} = n_c n_f$	$n_{mix} = C_f n_f$

Where: C_f is the concentration by volume of the fine particles, n_c is the coarse material porosity, n_f is the fine particles porosity and n_{mix} is the mixture porosity. Moreover C_f can be found using the following weight relationships:

Table 2.2 Expresions for the fine particles concentration by weigth

$C_f <= n_c$	$C_f > n_c$
$W_f = C_f(1-n_f)\rho_f/(C_f(1-n_f)\rho_f + (1-n_c)\rho_c)$	$W_f = C_f(1-n_f)\rho_f/(C_f(1-n_f)\rho_f + (1-C_f)\rho_c)$

Where: W_f is the fine particles concentration by weight; ρ_f and ρ_c are the densities of the fine and coarse particles.

Making tests on Kaolinite clay and Ottawa sand, Vallejo and Mawby [15] reported values for the large particles concentration by weigth between 0.75 and 0.78, as the range where the minimum porosity occurs. In the same way, using the same kind of mixtures, Marrion [8] established a range between 0.8 and 0.6 of large particles concentration as the interval where the minimum porosity takes place. They recognized that this range varies with the effect of the external pressure.

Kolterman and Gorelick [11], and Marrion [8] attempt to explain the observed differences between the ideal packing model and the laboratory resuslts focus on the erroneous assumption that this model has, about that only one kind of structure ocurrs at a certain moment in the soil. They believe that one component is always disturbing

the arrangment of the other. The following sketch illustrates the gradual change on the mixture setup based on the principle that only one kind of structure takes place at a certain moment (modified from Marrion [8]):

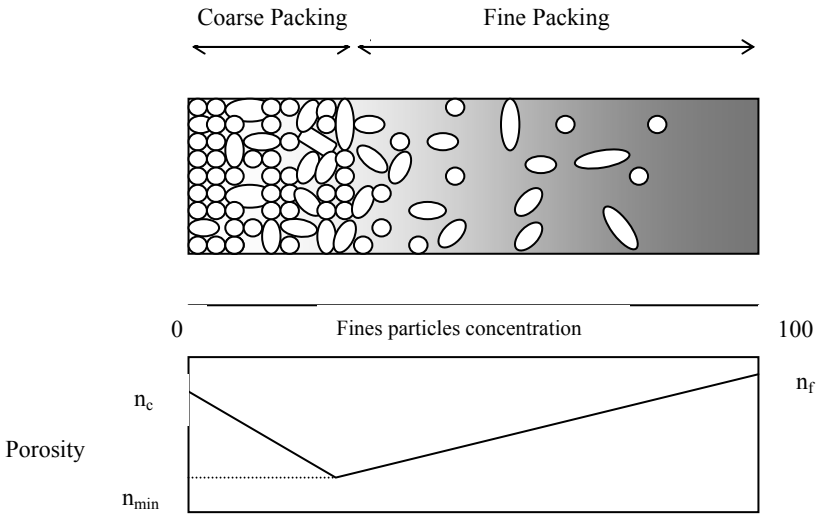

Figure 2.4 Ideal Packing Model for Porosity
(Modified from Marrion)

2.3 Hydraulic Conductivity in Soil Mixtures

In the civil engineering practice, this coefficient is found by conducting laboratory tests as the Constant Head test and the Falling Head Permeability test, or by doing field tests regardless the kind of structure that the soil has. However, several empirical correlations and analytic equations predicting the soil permeability have been proposed based on geometrical factors of the soil structure. A brief summary is presented in Table 2.3.

Table 2.3 Empirical correlations and analytic equations for the hydraulic conductivity
(modified Das [16] , Kolterman and Gorelick [17], Yin [6])

Equation	Author	Conventions
$K = C(d_{10})^2$	Hazen for loose sands	K [cm/s] Permeability; C:empirical factor (100); d_{10}: grain diameter for which 10% pf particle are smaller [cm]
$K= 0.35(d_{15})^2$	Hazen for dense sands	d_{15}: grain diameter for which 15% particle are smaller [cm]
$K= 0.05(n^2/(1-n)^2)(d_{10})^2$	Terzaghi	n: porosity of the soil
$K= \varphi^3/ (2S^2)$	Darcy – Poisville	φ: porosity of the soil; ; S_{sa}: Surfaced area exposed to the fluid per unit volume of solid.
$K= \varphi^3/ (5S^2)$	Carman	Darcy – Poisville modificated under the hydraulic radius model.
$K =(1/8\pi)R_1^4$	Darcy – Poisville for pipe modelation	R_1^2: φ:/π
$K= \varphi^3/ (k_0T^2S^2)$	Carman	K_0: empirical constant, T: tortuosity;
$K= (9.66E-04)(760d_g^2)EXP(-1.31\sigma_g)$	Krumbein and Monk	d_g: geometric mean grain diameter; σ_g= geometric mean standard deviation
$K= (g/\nu)(\varphi^3)/(C_tTS_{sa}^2)$	Kozeny modified by Collins	ν : dynamic viscosity; C_t=Coefficient for pore shape and packing; T= tortuosity
$K = (g/\nu)(d^2 \varphi^3)/(180(1-\varphi)^2)$	Kozeny –Carman	D: representative grain diameter
$K= (g/\nu)(\varphi^3)/(C_0S_{sa}^2(1-\varphi^2))$	Kozeny-Carman Modifieded	C_0= factor reflecting pore shape and packing.
$K= \varphi^3/ ((45(1-\varphi)^2(V_s/R_s + V_c/R_c)^2)$	Yin	V_s: volume of sand particles; V_c:volume of clay particles: R_s: radio of sand particles; R_c: radio of clay particles

Most of the equations presented above, involve a representative grain diameter. This value is assumed as the d_{10}, the d_{50}, the geometric mean or the harmonic mean of the sort [18]. According to Kolterman and Gorelick [18], the

Kozeny-Carman equation is the best equation that can be used to predict the hydraulic conductivity in soil mixtures, since it includes in the porosity and the representative particles size the effect of the external pressure and the soil structure. Based on laboratory tests and values predicted by using this equation, they have identified the trend showed in Figure 2.5:

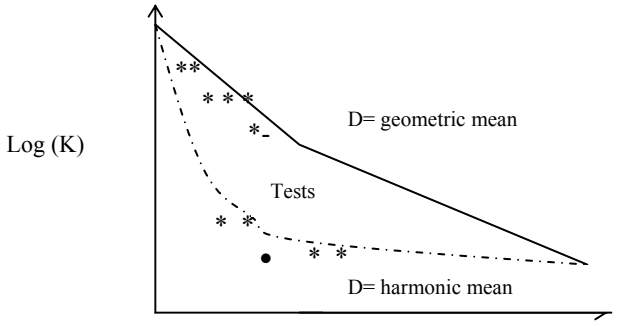

Figure 2.5 Observed Trend in the Soil Mixture's Permeability
(Modified Kolterman and Gorelick [17])

An abrupt change in the permeability behavior is noticed exactly at the time when a minimum porosity occurs, and the soil changes its kind of structure. They explained this by using the following process: First, when the fine particles concentration is negligible, the mixture arrangement is controlled by the large particles, and the mixture permeability corresponds to the pure coarse particles permeability. Then, while the fine particles concentration is increased, the hydraulic conductivity starts to diminish since the pore spaces are reduced. Finally, when the minimum porosity is reached, the soil changes its structure, and the fine particles start to control the mixture hydraulic conductivity. After this minimum is achieved, the hydraulic conductivity does not change in a substantial way. [18]

Using the Koseni-Carman equation, Kolterman and Gorelick [17,18] concluded that there does not exist a unique representative diameter able to predict the mixture permeability at every fine particles concentration. If the geometric mean is selected as the representative diameter, the Coseni-Karman equation accurately predicts the hydraulic conductivity values when the mixture presents contact structure, but over predicts the permeability during the floating structure. On the other hand, if the harmonic mean is used as the representative diameter, a constant under prediction is observed when the mixture presents contact structure. This situation can be explained based on

the statistical principle that the geometric mean weights higher values, while the harmonic mean weights smaller values .[17]

3.0 THEORETICAL MODELS PREDICTING THE ELASTIC BEHAVIOR OF SOIL MIXTURES

The reaction of a soil mass when it is subjected to an external load depends on the Elastic modulus (E), the Shear modulus (G) and the Poisson's ratio of the soil. Usually, these properties are evaluated in the laboratory by using triaxial cells. Since soil mixtures with oversized particles bigger than 0.5 inches cannot be tested in those machines, E, G, and the Poisson's ratio are estimated only with the matrix material of the soil or by using large triaxial cells, and large loading systems, making these tests more expensive and time consuming. In order to elude these problems, theoretical expressions predicting the elastic properties in soil mixtures have to be proposed.

3.1 Guth's Model

Based on the Einstein viscosity law, Guth [19] proposed expressions for the elastic moduli E and G in mixtures composed by disperse rigid particles embedded in a continuous matrix, regardless if the matrix is a fluid or a solid medium. Equation 3.1 is showing the Einstein's viscocity law, where η' and η are the viscosities of the emulsion and the solvent, and C is the concentration by volume of the disperse particles.

$$\eta' = \eta[1 + 2.5C] \qquad \textit{(3-1)}$$

Since Einstein's theory gives a pattern for the other physical properties, E and G can be estimated replacing in the viscosity equation the wanted property instead of viscosity [20]. In this way, the physical properties of the mixture (emulsion) can be known using the properties of the matrix (solvent) and the concentration by volume of the disperse particles. The Guth's model [20] supposes a Poisson's ratio of the mixture close to 0.5, meaning that the mixture can be treated as an almost perfect isotropic material. Moreover, it is assumed that the elastic moduli of the disperse particles is higher than the elastic moduli of the matrix particles.[20]

Although the equations proposed by Guth were not developed for soil particles, they can be used in soil mixtures since they are considered as uniform compounds of disperse rigid particles and a homogeneous matrix. The Guth equations are presented in table 3.1.

3.2 Greszczuk's Model

Greszczuk [21] has proposed expressions predicting the Poisson's ratio and the Elastic moduli in solid mixtures containing two materials. The proposed expressions are based on the following conditions [22]:

1. The matrix and the disperse particles are homogenous and isotropic materials that obey the Hook law.
2. There exists a perfect adhesion between both materials.
3. The disperse particles are uniformly distributed within the matrix.
4. There are no voids inside the mixture.

Thus, the Elastic Moduli and the Poisson's ratio of a solid mixture can be solved using the concept of compatible deformations between the components.

3.2.1 Poisson's ratio

The following procedure is presented in more detail in Greszczuk [23]:

- If a homogeneous and isotropic material is subjected to a strain ε_1, the correspondent strain ε_2 in an orthogonal plane will be

$$\varepsilon_2 = -\nu\varepsilon_1 \qquad (3\text{-}2)$$

  Where ν is the Poisson's ratio of the material.

- If a solid mixture is subjected to a stress in the direction "1_H", then the total strain in the direction of the orthogonal plane "2_H" will be

$$\varepsilon_{2H} = \varepsilon_{2i}K + \varepsilon_{2m}(1-K) \qquad (3\text{-}3)$$

where i and m refer to the inclusions and the matrix particles, and K represents the volumetric content of the inclusions.

- Also $$\varepsilon_{1i} = \varepsilon_{1m} = \varepsilon_{1H} \quad (3\text{-}4)$$

and $$\varepsilon_{2i} = -\nu_i \varepsilon_{1i} \quad (3\text{-}5)$$

$$\varepsilon_{2m} = -\nu_m \varepsilon_{1m} \quad (3\text{-}6)$$

$$\varepsilon_{2H} = -\nu_H \varepsilon_{1H} \quad (3\text{-}7)$$

- Substituting Equation 3.4 and Equations 3.5 to 3.7 in to Equation 3.3, the follow expression can be achieved:

$$\nu_H = \nu_i K + \nu_m (1-K) \quad (3\text{-}8)$$

3.2.2 Elastic Moduli

The following procedure is presented in more detail in Greszczuk [23]:

- Considering and homogenous and isotropic material subjected to a triaxial state of stress, the volumetric change ΔV, due to a loading condition can be expressed as

$$V = (1-2\nu)(3\sigma)/E \quad (3\text{-}9)$$

where E is the elastic modulus of the material, and σ is the applied stress.

- If the solid is composed by two different materials, the volumetric change of the mixture will be

$$\Delta V_H = \Delta V_m + \Delta V_i \quad (3\text{-}10)$$

- Moreover, the volume reduction of the inclusions and the volume reduction of the matrix can be expressed as

$$\Delta V_m \approx (1-K)(1-2\nu_m)(3\sigma)/E_m \quad (3\text{-}11)$$

$$\Delta V_i \approx K(1-2\nu_i)(3\sigma)/E_i \quad (3\text{-}12)$$

and $$\Delta V_H \approx (1-2\nu_H)(3\sigma)/E_H \qquad (3\text{-}13)$$

- Combining Equations 3.10 to 3.13 and Equation 3.8, E_H can be expressed as

$$E_H = E_m E_i[\, 1-2\nu_i K - 2\nu_m (1-K)] \,/\, [\, (1-K)(1-2\nu_m)E_i + K(1-2\nu_i)E_m \,] \qquad (3\text{-}14)$$

- Since ν_H and E_H can be known, the shear modulus (G) can be expressed assuming that the mixture behaves as an elastic material

$$G_H = E_H/[2(1+\nu_H)] \qquad (3\text{-}15)$$

According to Greszczuk [23], when the disperse particles in the mixture are treated as rigid particles, it can be assumed for a low concentration (K <0.5), that the mixtures properties are independent of the properties of the inclusions. In this way, the presented equations can be simplified. A summary of the Guth and Greszczuk simplified equations is provided in Table 3.1, where c refers to the compound, m refers to the matrix, and C_f is the disperse particles concentration by volume.

Table 3.1 Guth and Greszczuk simplified equations

Property	Guth Model	Greszczuk Model
ν	$\nu_c = \nu_m(1 + 2.5C_f)$	$\nu_c = \nu_m(1-C_f)$
E	$E_c = E_m(1 + 2.5C_f)$	$E_c = E_m(1-2\nu_m(1-C_f))/((1-C_f)(1-2\nu_m))$
G	$G_c = G_m(1 + 2.5C_f)$	$G_c = E_c/(2(1+\nu_c))$

Since the expressions presented above consider a mixture of disperse particles and a matrix, they just apply to low concentrations of separate particles (Floating structure). Thus, in a mixture of large and fine particles, if the

large particles concentration is below the critical point, the matrix will be the fine particles; otherwise, the large particles will become the matrix.

3.3 Hashin's Model

Based on the theory of elasticity, the theorems of the minimum potential energy and the minimum complementary energy, Hashin [24] developed expressions predicting the Poisson's ratio, and the elastic moduli E and G in mixtures containing solid particles. The following conditions are required: [25]

1. The matrix must be composed of an elastic, isotropic and homogeneous material.
2. The disperse particles must be rigid and spherical in shape.
3. There must be perfect adhesion between the disperse particles and the matrix.
4. The concentration by volume of the rigid particles is such that there is no contact between them.

In this way, Hashin achieved the following equations (all terms were defined before):

Table 3.2 Hashin's equations

Property	Hashin's Model
ν	$\nu_c = \nu_m + [3(1-\nu_m)(1-5\nu_m)(1-2\nu_m)/(2(4-5\nu_m))]C_f$
E	$E_c = E_m + [3(1-\nu_m)(5\nu_m^2 - \nu_m + 3)/((1+\nu_m)(4-5\nu_m))]C_f E_m$
G	$G_c = G_m + [15(1-\nu_m)/(2(4-5\nu_m))]C_f G_m$

The Hashin's equations for E and G can be expressed as $E_c = E_m(1+MC_f)$ and $G_c = G_m(1+MC_f)$, where M is only function of the Poisson's ratio of the matrix. Figure 3.1 shows how the Poisson's ratio of the matrix affects the M factor. It should be noticed that when ν_m is equal to 0.5, M becomes 2.5, and the resultant equations are the same obtained under the Guth approach. [26]

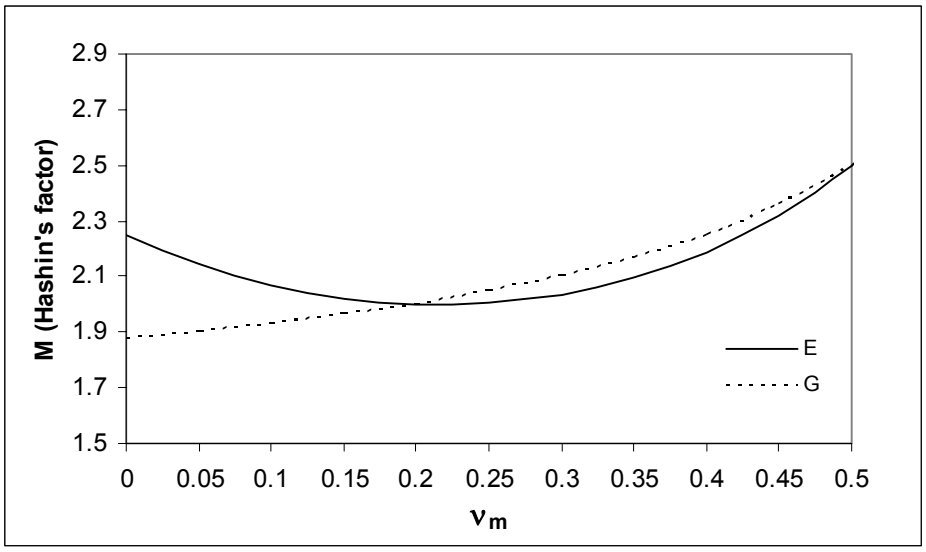

Figure 3.1 M vs Poisson's ratio of the Matrix

3.4 Summary

Theoretical models predicting the Poisson's ratio and the elastic moduli of binary mixtures have been presented. Although some of the constrains that these models have are not completely satisfied when considering soil mixtures, the equations proposed by these models might be applied under certain conditions. During the following chapters, laboratory tests will be presented in order to evaluate these models.

4.0 TEST PROCEDURES AND LABORATORY TECHNIQUES

This chapter explains the laboratory procedures used during the experiments presented in the follow chapters. Also, it has a detailed characterization of the materials and the equipment used on the tests.

4.1 Materials

Different mixtures of Kaolinite clay, Ottawa sand, coarse sand No.16, glass beads of diameter equal to 0.2cm, 0.5cm, and 1cm, were used in order to study the influence that the disperse particles concentration has on the elastic behavior of soil mixtures. Unsaturated and dry samples were prepared in the laboratory following the same procedure. The main properties of the tested materials are presented in Table 4.1

Table 4.1 Materials used on the tests

Material	Av. Diameter (mm)	Coefficient of uniformity C_u	Liquid limit (%)	Plastic limit (%)	Gs
Kaolinite Clay	0.0042	--	58	28	2.50
Ottawa Sand	0.59	1.3	--	--	2.65
Coarse Sand No.16	1.18	1	--	--	2.6
Glass Beads (2mm)	2	1	--	--	2.45
Glass Beads (5mm)	5	1	--	--	2.45
Glass Beads (10mm)	10	1	--	--	2.5

The different samples were prepared by mixing different proportions of the materials presented above. Most of the samples were made using just two materials. In this way, the mixtures presented in Table 4.2 were tested.

Table 4.2 Tested samples

Number of samples (C_f variable)	Moisture content	Matrix	Disperse particles	Number of tested pressures
2	Dry	Kaolinite clay	Air	14
10	Dry	Kaolinite clay	Ottawa sand	3
10	10%	Kaolinite clay	Ottawa sand	3
10	20%	Kaolinite clay	Ottawa sand	3
10	Dry	Kaolinite clay	Glass beads (10mm)	3
10	Dry	Coarse sand No 16	Glass beads (10mm)	3
10	Dry	Kaolinite + Ottawa sand	Glass beads (10mm)	3
10	Dry	Kaolinite + Ottawa sand	Glass beads (5mm)	3
10	Dry	Kaolinite + Ottawa sand	Glass beads (2mm)	3

4.2 Test Procedure

Unsaturated and dry samples were prepared in the laboratory following the same procedure: First, the calculated quantities for each component were carefully mixed trying to avoid the formation of flocks. After every mixture was prepared, it was placed in a transparent cylinder with an inside diameter that measured 5.1 cm; it was enclosed on top and bottom by a set of either P-wave transducers or S-wave transducers as shown in Figure 4.1. The sample, the cylinder and the transducers were weighted together, and the mass of the mixture was calculated.

After that, the sample was placed on a Versa Loader machine. The initial length was measured and the cables of the transducers were plugged to the Pundit. The sample was subjected to different values of a compressive stress, and finally the time required for the P-wave and the S-wave to travel through the sample, and the axial deformation due the load were measured. The travel time was used in conjunction with the length L ($L = L_{in}$ – deformation) of the sample in order to obtain the P-wave and the S-wave velocities.

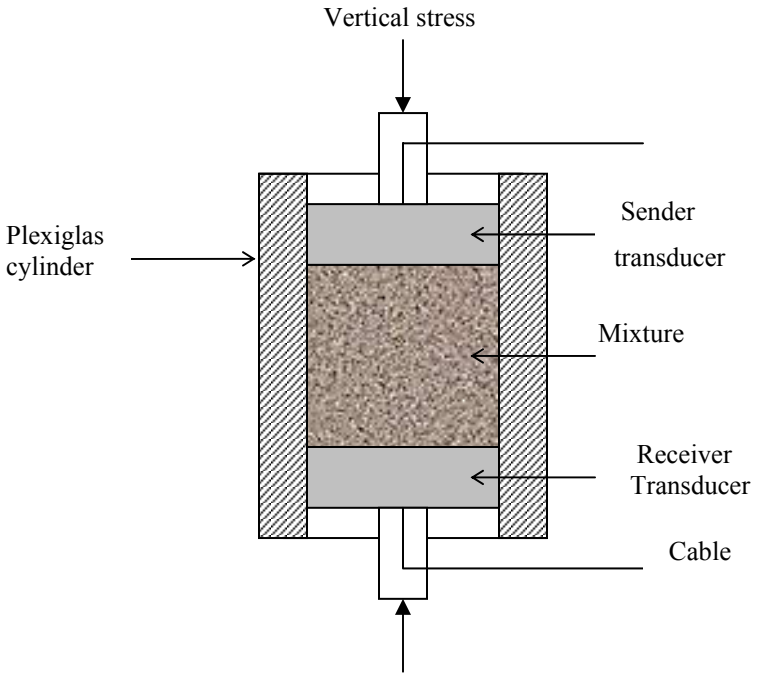

Figure 4.1 Laboratory Setup

4.3 Calculations

After a sample was tested, the information collected during the test was organized and the density, the compression wave velocity (Vp), the shear wave velocity (Vs), the elastic moduli E and G, and the Poisson's ratio of the sample were calculated. The density was computed by dividing the mass and the volume of the sample. The shear wave velocity and the compression wave velocity were computed by dividing the length of traveling, L, and the time, t, taken by the waves to travel the distance L.

Since the sample was confined, the elastic moduli were computed from the wave velocities using the following equations [27]:

$$\nu_c = \left(\frac{1}{2}\right)\left(\frac{V_p^2 - 2V_s^2}{V_p^2 - V_s^2}\right) \qquad \textbf{(4-1)}$$

$$E_c = \frac{V_s^2(3V_p^2 - 4V_s^2)(\rho_c)}{V_p^2 - V_s^2} \qquad \textbf{(4-2)}$$

$$G_c = \rho_c V_s^2 \qquad \textbf{(4-3)}$$

Where, ρ_c, is the density of the composite, and the other terms were defined before.

Using the obtained results, the theoretical models explained in Chapter 3 were evaluated. Since the theoretical approaches proposed by Guth, Greszczuk and Hashin, predict the elastic moduli and the Poisson's ratio of the mixtures based only on the matrix properties and the concentration by volume of the disperse particles, the concentration by weight was converted to concentration by volume using the following relation.[28]

$$C_f = \left(\frac{\rho_c}{\rho_p}\right)(C_w) \qquad \textbf{(4-4)}$$

Where, ρ_c, is the density of the composite, ρ_p, is the density of the rigid dispersed particles, and C_w is the concentration by weight of the rigid particles. This relationship can be easily demonstrated substituting the terms by their definition and canceling common factors.

4.4 Equipment

In order to measure the ultrasonic wave velocities, the PUNDIT apparatus was used. This device gives the travel time required for the compressive and the shear waves to cross the sample, with and accuracy of 0.1E-6 s. The PUNDIT is connected to two different transducers: the transmitting transducer and the receiver transducer. The transmitting transducer sends out the generated pulse while the receiver transducer passes on the received pulse to the receiving amplifier, which allows the apparatus to measure the time of travel. The transducers used for the compressive wave are different that those used for the shear wave. The central frequency of the P-wave and the S-wave transducers are 54 kHz and 180 kHz respectively. The transducers were cylindrical in shape and had a diameter equal to 5 cm. A self explained picture of the equipment is provided in Figure 4.2.

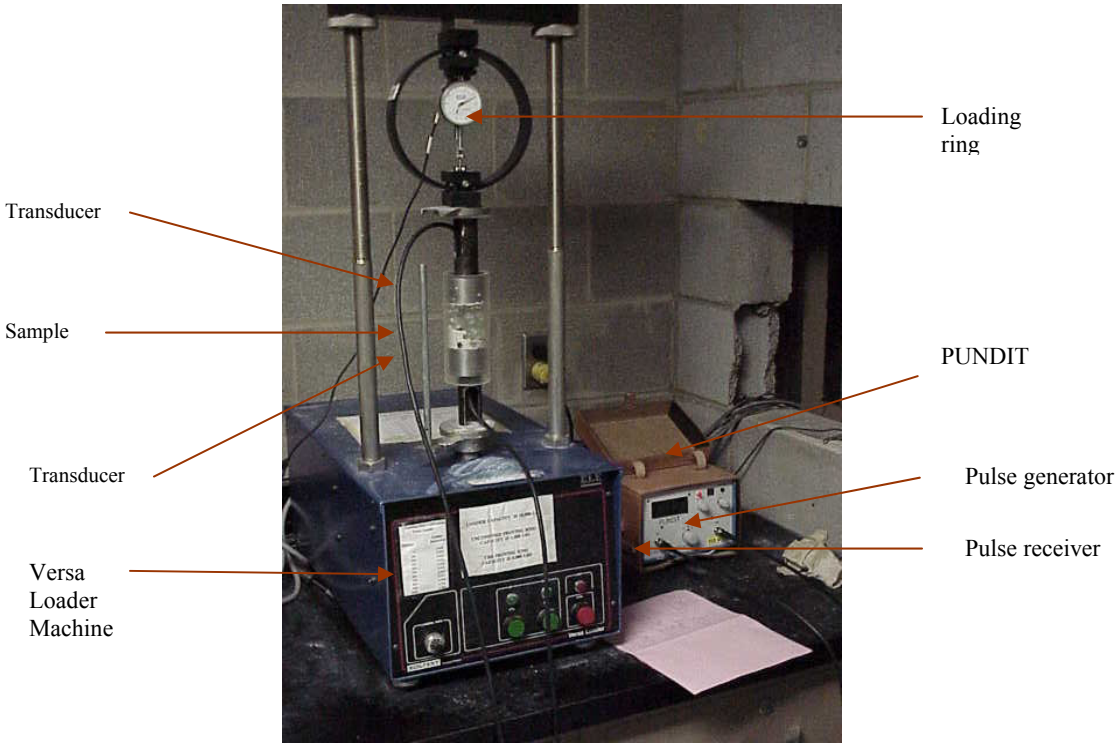

Figure 4.2. Equipment

5.0 INFLUENCE OF THE LOADING TIME AND THE VERTICAL PRESSURE ON E, G ,AND ν

5.1 Influence of the Loading Time on E and G

In order to study the influence of the loading time on the elastic moduli E and G, tests under different vertical pressures were carried out using dry kaolinite clay. The samples were subjected to a constant pressure during one hour, measuring E and G every 10 minutes. Figures 5.1 and 5.2 show the obtained results at 100 kPa, figures 5.3 and 5.4 show the obtained results at 200 kPa, and figures 5.5 and 5.6 show the obtained results at 500 kPa.

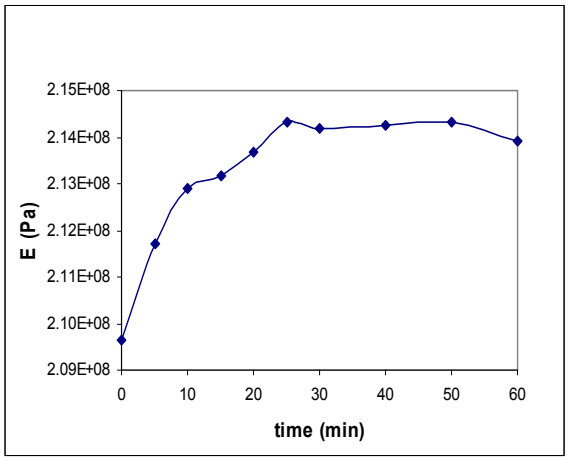

Figure 5.1. E at 100 kPa, Pure Kaolinite

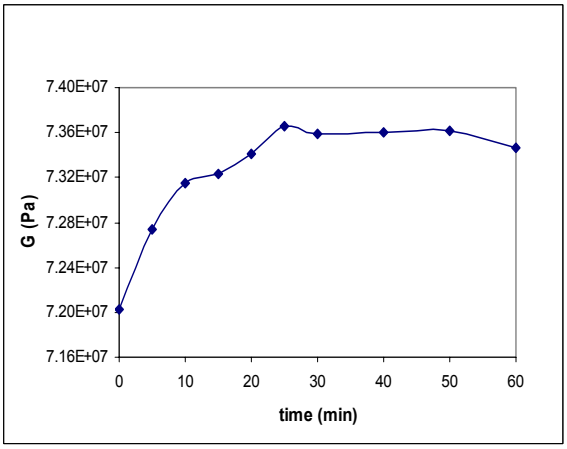

Figure 5.2. G at 100 kPa, Pure Kaolinite

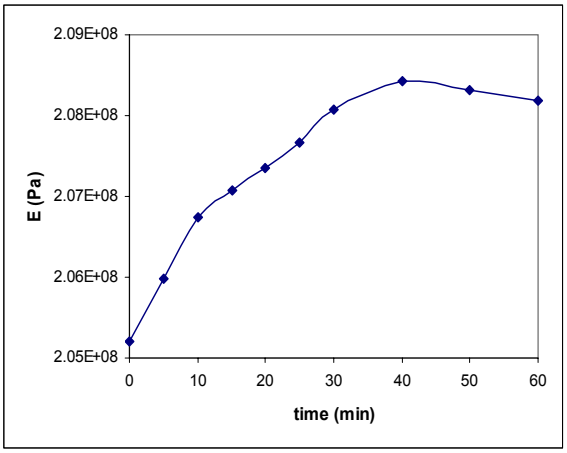

Figure 5.3 E at 200 kPa, Pure Kaolinite

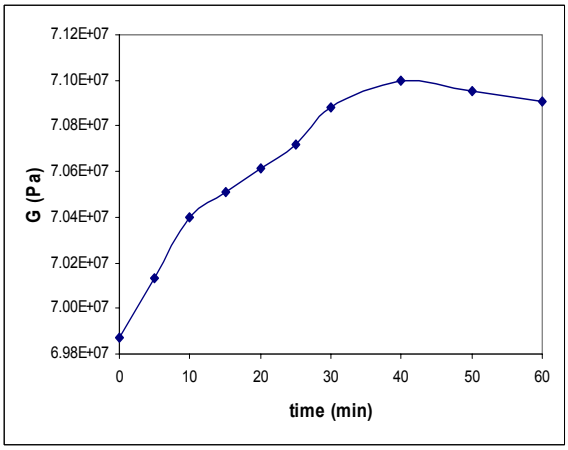

Figure 5.4 G at 200 kPa, Pure Kaolinite

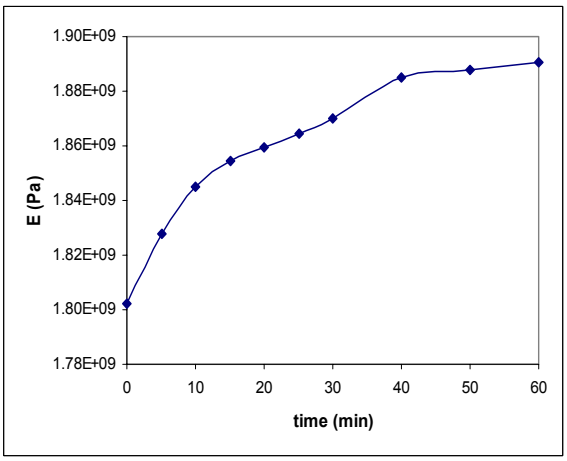

Figure 5.5 E at 500 kPa, Pure Kaolinite

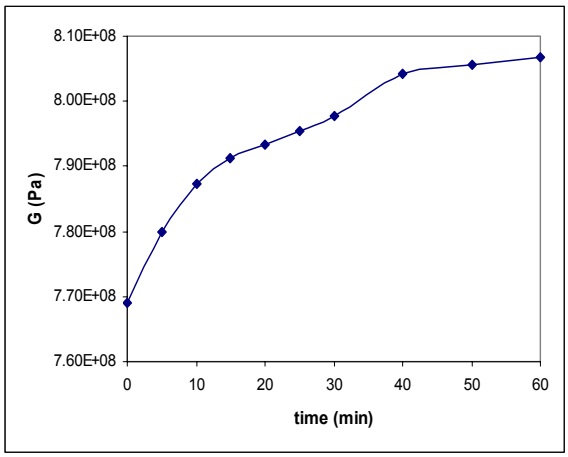

Figure 5.6 G at 500 kPa, Pure Kaolinite

It was observed that the samples achieved constant values of the elastic moduli E and G during the time of the test; however, the stabilization time changed with the magnitude of the vertical pressure. The small difference between the values recorded at the beginning of the test and the values recorded at the end of the hour show that there is not a considerable mistake to assume that the elastic moduli E and G on dry Kaolinite clay remain constant with time.

5.2 Influence of the Vertical Pressure on E and G, Pure Kaolinite

Marrion [8], using electrical conductivity techniques, found a strong correspondence between the number of particle contact points and the elastic moduli E and G. Since a high confining pressure produces more contact points than a low confining pressure, mixtures subjected to a high confining pressure will present a stronger reinforcement, having higher values of E and G. However, Marrion observed that in the case of the dynamic moduli, once a connected path of deforming contacts is created, the moduli do not change in a substantial way when increasing the number of contacts.

In order to gain some understanding about what happen with the dynamic elastic moduli E and G when increasing the vertical pressure, samples of pure Kaolinite clay were subjected to an increasing vertical pressure from 100 kPa to 1000 kPa. Fourteen points were recorded in this range. Figure 5.7 shows the influence of the

vertical pressure on the compressive and the shear waves velocities. It was observed that Vp increased almost linearly with the vertical pressure, while Vs presented a trend defined by three different zones. First, when the vertical pressure was lesser than 400 kPa, the shear wave velocity did not change with the vertical pressure. Then, when the sample was subjected to an increasing pressure between 400 kPa and 500 kPa, Vs considerable increased with a steep slope. Finally when the vertical pressure was higher than 600 kPa, the shear wave velocity started to increase with a mild slope.

Figure 5.8 shows the correspondent porosities of the mixtures at the vertical pressures showed in figure 5.7. It was observed that when porosity changed between 0.57 and 0.60, the velocity of the shear wave significantly decreased.

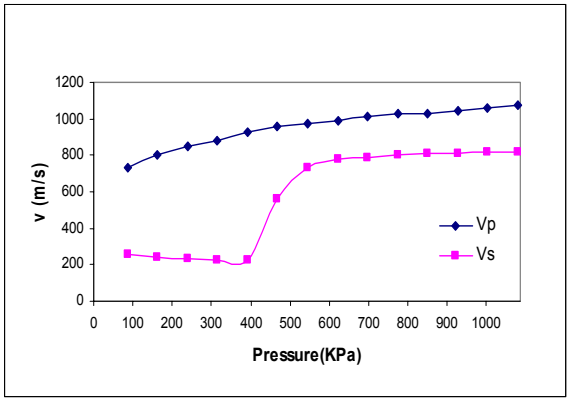

Figure 5.7 Vertical Pressure vs Wave Velocities, Pure Kaolinite

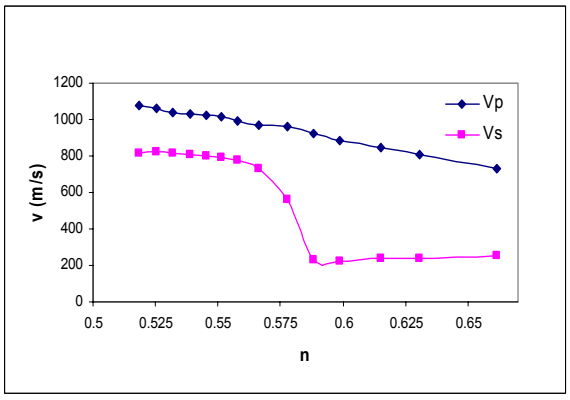

Figure 5.8 Porosity (n) vs Wave Velocities, Pure Kaolinite

Using the wave velocities showed in figure 5.8 and the obtained densities at the different pressures, the elastic moduli E and G were calculated. The results are showed in Figure 5.9. Since these moduli are function of the shear

wave velocity, the values correspondent to the samples having porosities between 0.57 and 0.60 showed a rapid drop. Moreover, it was observed that E started to decrease faster than G when porosity was higher than 0.53. However, the porosities obtained in the laboratory were restricted to a range between 0.52 and 0.63 due the limitations of the equipment (the maximum applied stress was 1000KPa). In order to measure porosities bellow 0.52, bigger loading systems would have to be used. Using data obtained by Yin [6] in a similar test on dry Kaolinite clay, Figure 5.9 was expanded to porosities between 0.5 and 0.2. Yin made his tests considering pressures between 2500 kPa and 50000 kPa.

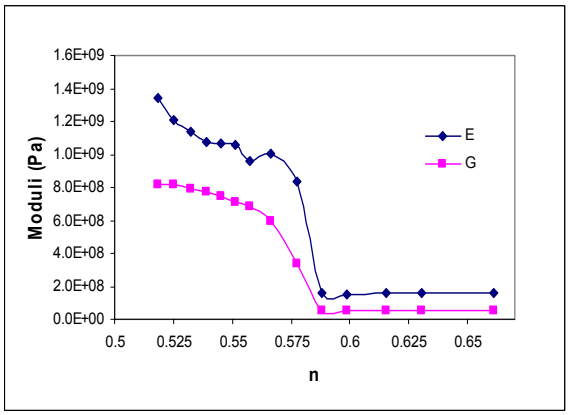

Figure 5.9 Porosity vs Moduli, n>0.5, Pure Kaolinite

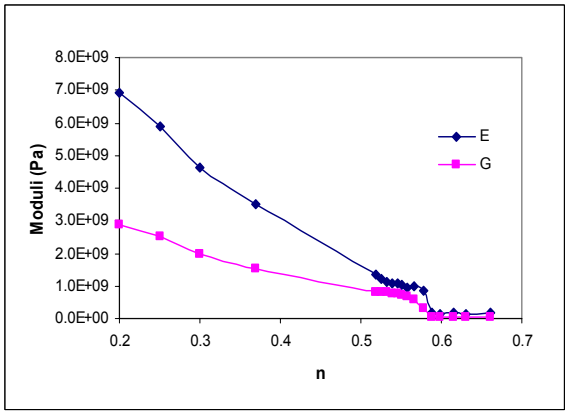

Figure 5.10 Porosity vs Moduli, Pure Kaolinite

Figure 5.10 shows the expanded curve for Figure 5.9, including the points obtained by Yin. It can be observed how the slopes for both moduli remain almost constant when porosity is lesser than 0.55.

Based on the experimental results presented before, it can be concluded that there exist three different stages in the formation of a structure in the dry Kaolinite clay. The first one takes place when porosity is higher than 0.6, in this stage the material is in a loose state and the elastic moduli are very small. After a certain vertical pressure is applied, new contacts are generated and an important transition is produced. This second stage corresponds to porosities between 0.6 and 0.57, where the elastic moduli strongly increment with small changes on porosity. Finally, when porosity is lesser than 0.57, the elastic moduli increment as almost linear functions of porosity.

In order to understand how the volume of the dry Kaolinite clay changes when increasing the vertical pressure, a graph showing the relationship between the specific volume of the sample and the natural logarithm of the vertical pressure was done. Figure 5.11 shows this relation. Once again the data obtained by Yin was added to the recorder values in order to expand the range of the vertical pressures. The obtained relation was a linear trend with a correlation of 0.976.

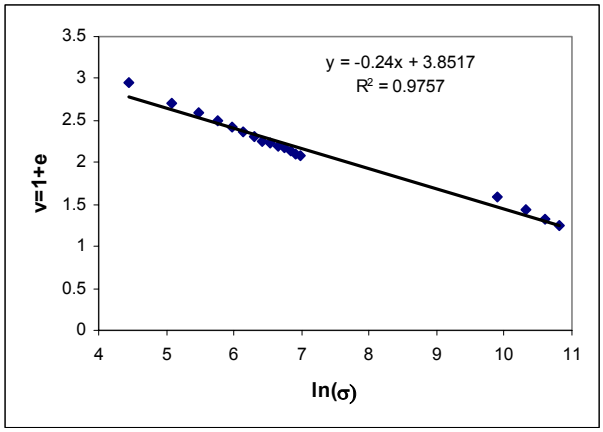

Figure 5.11 Vertical Pressure vs. Specific Volume.

5.3 Influence of the Vertical Pressure on υ, E, and G in Kaolinite-Ottawa Sand Mixtures, Theoretical Simulations

5.3.1 Samples Subjected to Vertical Pressures between 100 kPa and 500 kPa

In order to evaluate the performance of the theoretical models predicting the elastic behavior of soil mixtures under different vertical pressures, samples were prepared by mixing different concentrations of Kaolinite clay and

Ottawa sand; each sample was subjected to three different vertical pressures (100 kPa, 200 kPa, and 500 kPa). The change in density, wave velocities, elastic moduli, and Poisson's ratio as a function of the concentration by weight of the disperse particles and the vertical pressure is presented.

The change in density due an increasing percentage of fine particles (clay) and the vertical pressure is showed in figure 5.12. The maximum value at each pressure was obtained at an optimum concentration of sand particles between 70% and 80%. This critical value corresponds with the concentration where a change in the soil structure takes place. If the concentration of sand particles is below this limit, the structure of the sample is dominated by the clay that works as the matrix of the composite; otherwise, the sand particles start to behave as the continuous medium. It can be observed how the density of the samples rises when increasing the vertical pressure.

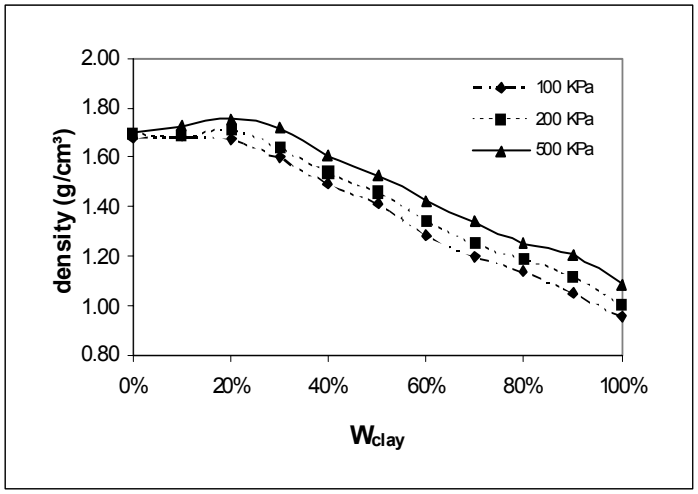

Figure 5.12 Density of the Kaolinite-sand Mixtures

The change of the wave velocities Vp and Vs as a function of the concentration by weight of the clay particles is not as clear as the trend observed in the density curves. Figure 5.13 shows the recorded values for Vp function of the clay particles concentration. It can be noticed how this velocity increases with the vertical pressure. Figure 5.14 shows the recorded values for Vs; it should be noticed that the maximum velocity took place close to the critical concentration observed in the density curves.

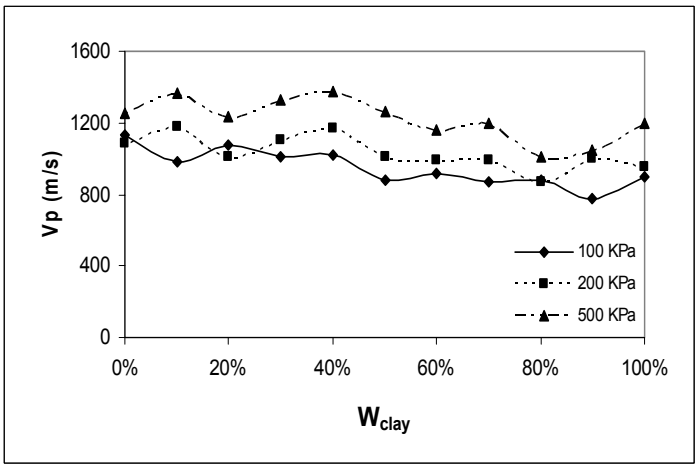

Figure 5.13 Vp of the Kaolinite-sand Mixtures

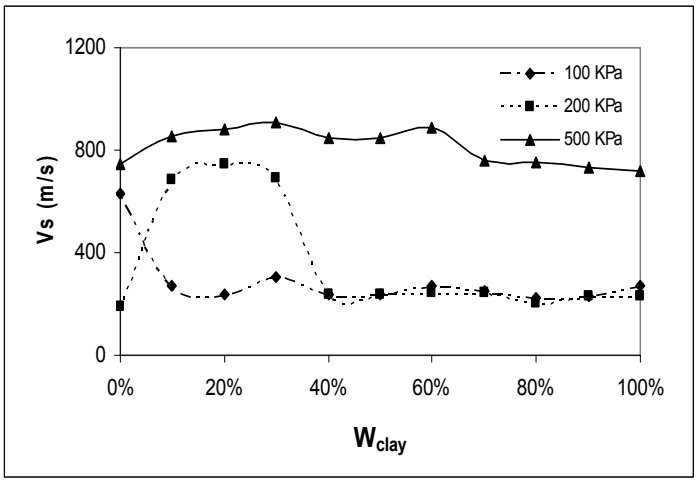

Figure 5.14 Vs of the Kaolinite-sand Mixtures

Using the results presented above, the laboratory values for the Poisson's ratio and the elastic moduli E and G were calculated. Also, the Hashin, Guth, and Greszczuk models were applied to the samples having a sand particles concentration between 0% and 70%. Figures 5.15, 5.16, and 5.17 show the comparison for the Poisson's ratio between the laboratory results and the values predicted by the models at vertical pressures of 100 KPa, 200 KPa and 500KPa. The Hashin's model satisfactory predicted the Poisson's ratio at every pressure, between a sand particles concentration of 0% and 70%. An average value of 0.45 was obtained at low vertical pressures (100KPa and 200Kpa), while at a high vertical pressure (500 KPa) the average was around 0.2. On the other hand, the Guth's model and the Greszczuk's model overpredicted and underpredicted the obtained laboratory results. It should be noticed that the Greszczuk's model improved when the vertical pressure took higher values.

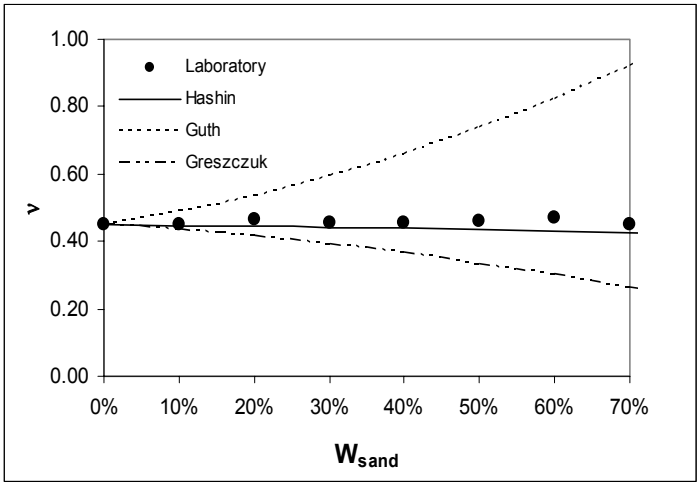

Figure 5.15 Poisson's Ratio of the Kaolinite-sand Mixtures at 100 kPa

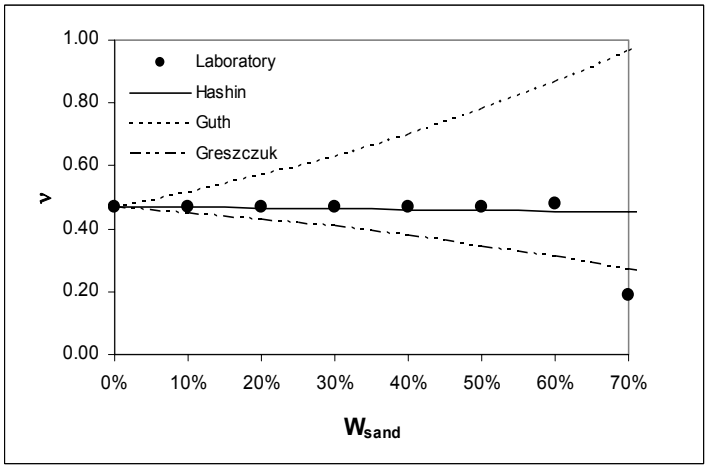

Figure 5.16 Poisson's Ratio of the Kaolinite-sand Mixtures at 200 kPa

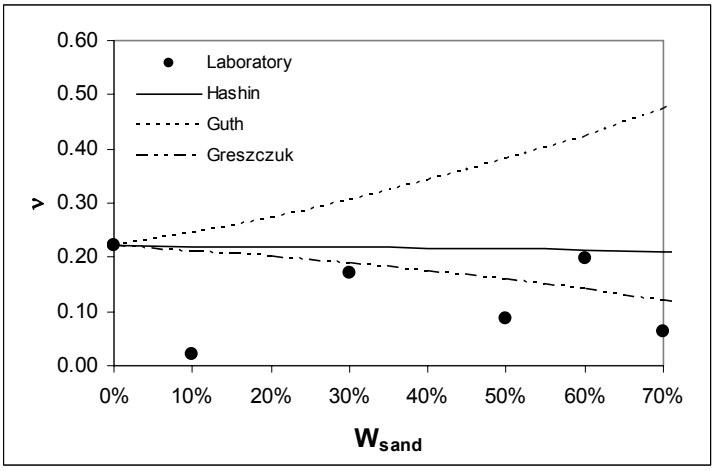

Figure 5.17 Poisson's Ratio of the Kaolinite-sand Mixtures at 500 kPa

The calculated elastic moduli E and G for the tested samples were compared with the results obtained by using the theoretical models. Figure 5.18, 5.19 and 5.20 show the comparison for the elastic modulus E. The Hashin and Guth models accurately predicted the elastic modulus E at the three vertical pressures. The Greszczuk model overpredicted the results at 100KPa and 200KPa, but it improved at 500KPa.

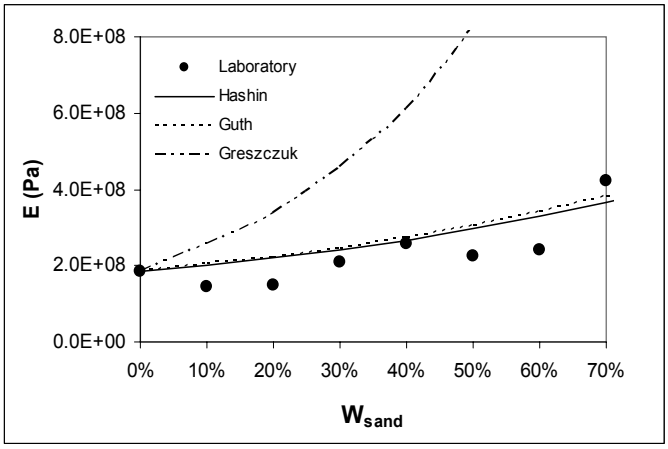

Figure 5.18 E of the Kaolinite-sand Mixtures at 100 kPa

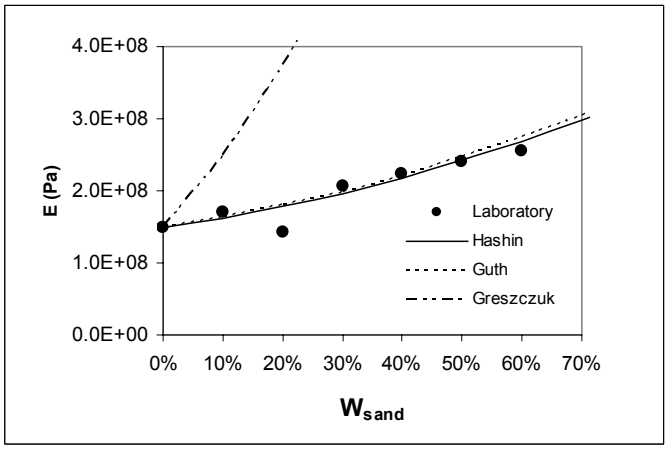

Figure 5.19 E of the Kaolinite-sand Mixtures at 200 kPa

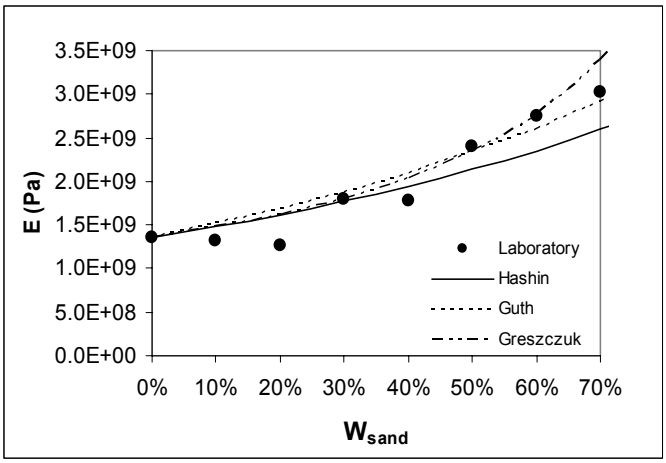

Figure 5.20 E of the Kaolinite-sand Mixtures at 500 kPa

The comparison between the laboratory results for elastic modulus G and the values predicted by using the theoretical models is showed in figures 5.21, 5.22, and 5.23. The trend observed in G was similar to the trend observed in E. A perfect agreement between the laboratory results and the predicted values by the Hashin and Guth models was observed. The Greszczuk's model only worked at 500 KPa.

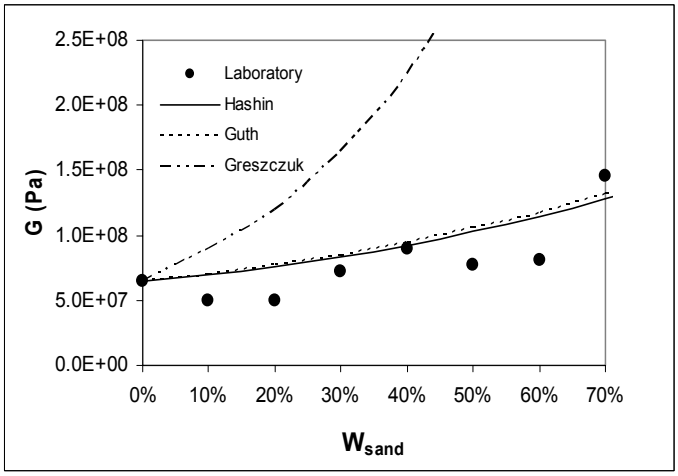

Figure 5.21 G of Kaolinite-sand Mixtures at 100 KPa

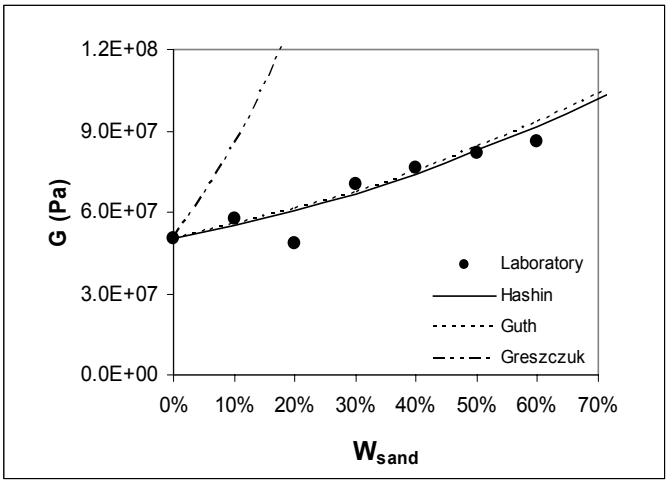

Figure 5.22. G of the Kaolinite-sand Mixtures at 200 KPa

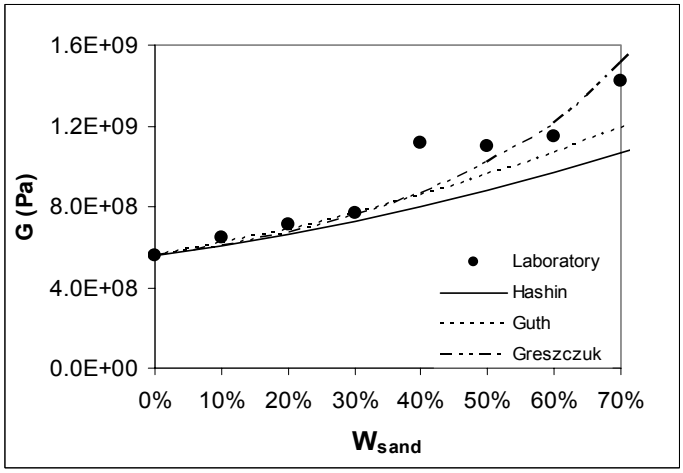

Figure 5.23. G of the Kaolinite-sand Mixtures at 500 KPa

Analyzing the results presented above, the follow trends can be summarized: there exist a disperse particles concentration when the soil changes its structure and the particles that used to be the disperse particles of the mixture become the matrix of the composite. This critical concentration depends on the vertical pressure, and it can be evidenced using the fine particles concentration vs density curves. Also, this critical concentration can be observed in the wave velocities curves. Thus, the theoretical models presented in Chapter 3 can be used in the range where the fine particles are the matrix of the compound. The Poisson's ratio can be satisfactory predicted by using the Hashin's model regardless the used vertical pressure. When the vertical pressure was lesser than 500 KPa, it was observed that the Poisson's ratio of the mixtures was close to 0.47 and it was not affected by the change in the disperse particles concentration. On the other hand, when the vertical pressure was equal to 500 KPa, the Poisson

ratio of the tested mixtures was lesser than 0.25. The Elastic moduli E and G were satisfactory predicted by using the Hashin and Guth models regardless the vertical pressure, while the Greszczuk model only worked at 500 KPa.

5.3.2 Samples subjected to Extremely High Vertical Pressures

Yin [6] presents values for Vp, Vs, and density in mixtures of Kaolinite clay and Ottawa sand subjected to confining pressures higher than 10 MPa. These pressures are considerably higher than the confining pressures used in the tests presented before. Using these data, the Poisson's ratio and the elastic moduli of the samples were calculated, and compared with the predicted values using the theoretical models.

Figure 5.24 shows the density curves function of the fine particles concentration and the confining pressure. As in the experiments presented in the last section (using vertical pressures between 100 KPa and 500 KPa), at each pressure the maximum density was obtained at a fine particles concentration close to 20%. Also, it can be noticed how the higher was the confining pressure, the higher was the value of the maximum density. An important shift to the right in the critical concentration of fine particles was observed when increasing the confining pressure.

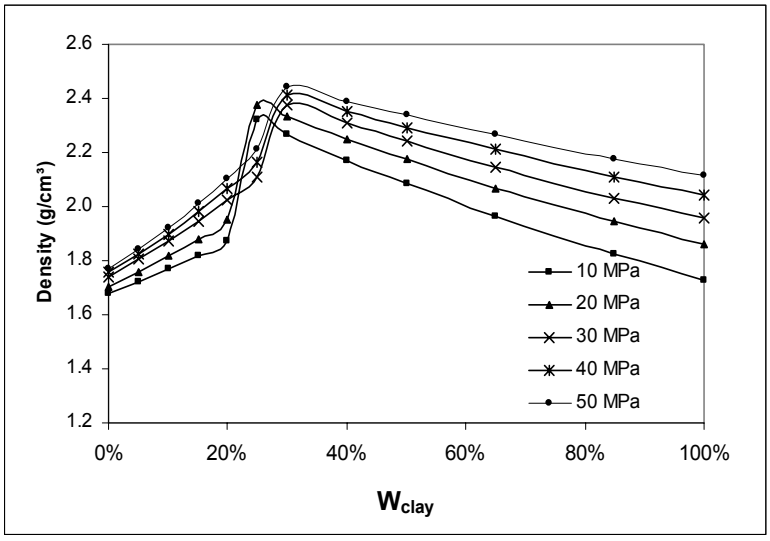

Figure 5.24. Density of the Samples, Yin tests

The calculated Poisson's ratios of the samples showed the same trend regardless the used confining pressure. Figures 5.25 and 5.26 show the results obtained at 20 MPa and 40 MPa. An average constant value of 0.3 was

observed. This value was close to the average value obtained on the tests made under a vertical pressure of 500 kPa. It should be noticed that in these tests the Poisson's ratio of the samples containing 100 % Kaolinite clay were considerably small compared to the Poisson's ratios of the other mixtures tested at the same confining pressure.

The theoretical models tended to underpredict the laboratory results for the Poisson's ratio. The difference between the values predicted by the theoretical models and the values obtained in the laboratory was bigger at the critical concentration of disperse particles, where a change in the kind of structure was taking place. However, it seems like this difference remained constant regardless the used confining pressure.

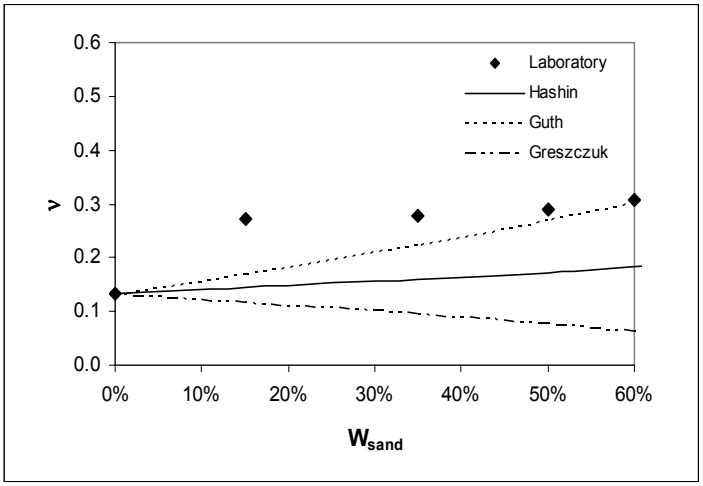

Figure 5.25 Poisson's ratio of the Samples at 20 MPa, Yin tests

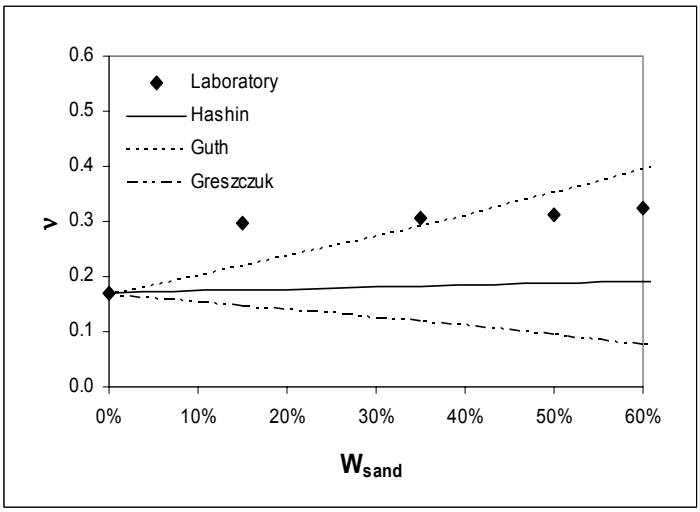

Figure 5.26 Poisson's ratio of the Samples at 40 MPa, Yin tests

The laboratory results and the values predicted using the theoretical models for the elastic modulus E at confining pressures of 20 MPa and 40 MPa are showed in figures 5.27 and 5.28. Although the measured elastic modulus E of the samples at 40 MPa are higher than the moduli obtained at 20 MPa, the observed trend is the same. The theoretical models tended to overpredict the laboratory results when increasing the disperse particles concentration. Thus, the models satisfactory predicted the recorded values while the disperse particles concentration was lower than 35%, but they tended to overpredict the laboratory results beyond this concentration. Moreover, the proportion of the overprediction at this concentration remained almost constant when increasing the confining pressure. It can be noticed that the three models produced closer values since the Greszczuk's model worked better at these pressures. Nevertheless, the agreement between the laboratory results and the values predicted by the Hashin and Guth models was better when the confining pressure was lower than 500 kPa.

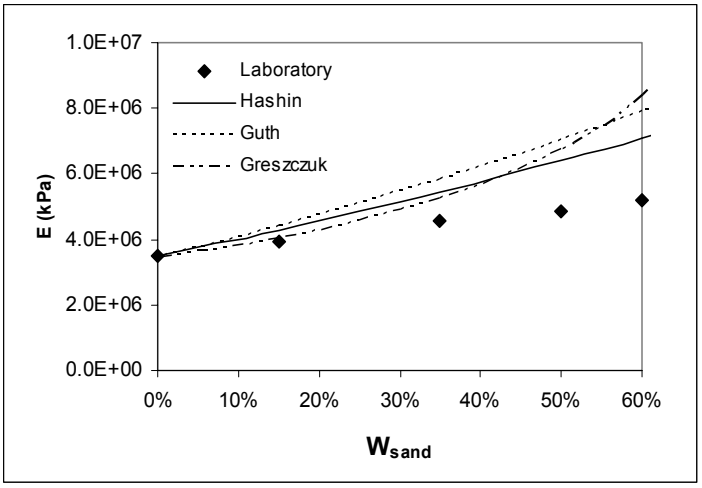

Figure 5.27 E of the Samples at 20 MPa, Yin tests

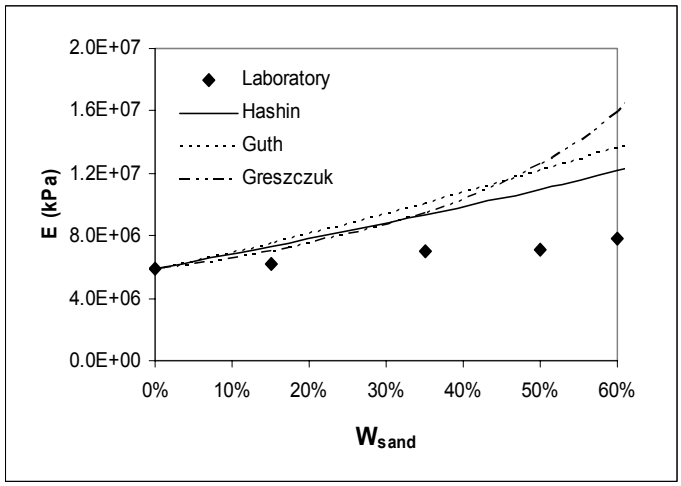

Figure 5.28 E of the Samples at 40 MPa, Yin tests

Figures 5.29 and 5.30 show the results for the elastic modulus G of the samples at confining pressures of 20 MPa and 40 MPa. The observed trend is the same trend obtained in the elastic modulus E. The theoretical models tended to overpredict the laboratory results when the disperse particles concentration was higher than 35%. This lack in accuracy remained almost constant when increasing the confining pressure.

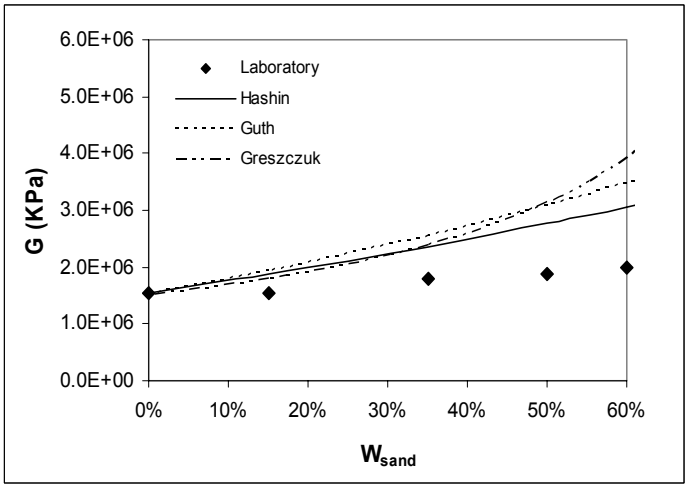

Figure 5.29 G of the Samples at 20 MPa, Yin tests

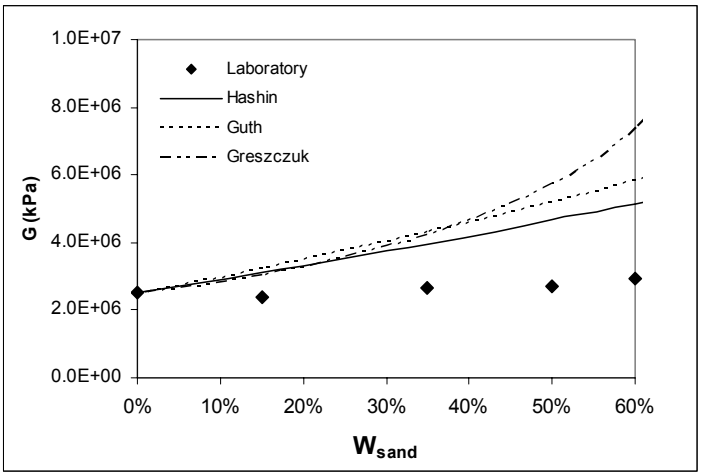

Figure 5.30 G of the samples at 40 MPa, Yin tests

Based on the results presented before, it can be concluded that the theoretical models work better when the applied confining pressure is not extremely high, indicating that the assumptions that these models have are not satisfied at all under this second condition.

5.4 Summary

The influence of the loading time and the vertical pressure on the elastic moduli of samples composed by 100% Kaolinite clay was studied. It was observed that for practical purposes it could be considered that the time of loading does not exert any influence on the elastic moduli of this material. On the other hand, it was found that the elastic moduli of these samples strongly depend on the applied vertical pressure. Graphs showing the behavior of the elastic moduli as a function of the porosity of the samples and the vertical pressure were developed.

Tests in dry mixtures of Kaolinite clay and Ottawa sand showed that the elastic moduli E and G are strongly related with the subjected vertical pressure and the concentration of the components. The densities of the mixtures and the wave velocities curves showed that there can be easily identified the concentration where the change in the soil structure takes place, and the particles that use to be the matrix become the disperse particles of the new arrangement. In this way, the theoretical models introduced in Chapter 3 were applied between a sand particles concentration of 0% and this critical point. These models took in count the effect of the vertical pressure since they are based on the properties of the matrix material at these conditions. It was observed that the Hashin and Guth models satisfactory predicted the elastic moduli in samples subjected to vertical pressures between 100 kPa and 500 kPa. The Greszczuk model overpredicted the laboratory results at these pressures since the constrains that this model has were not satisfied at all, except at 500 kPa.

Using experimental results reported by Yin[6] in the same kind of mixtures, a comparison between the recorded and the predicted values by the theoretical models at confining pressures between 10 MPa and 50 MPa was carried out. The three models predicted closer values since the Greszczuk model improved its performance; nevertheless, it was observed a constant overprediction in the elastic moduli when the disperse particles concentration was higher than 35%. The theoretical model satisfactory depicted the elastic moduli E and G of the samples below this concentration.

6.0 INFLUENCE OF THE MOISTURE CONTENT

The results obtained in the last chapter showed that both the Hashin and Guth models satisfactory work out in dry binary mixtures, while the Greszczuk's model has some problems since the constrains that this model has are not very often satisfied. However, soils are not dry in the field, being water one of their most important components. The three theoretical models do not have constrains about the moisture content if the structure of the soil is not affected. In this way, this chapter presents tests made on unsaturated mixtures of Kaolinite clay and Ottawa sand in order to evaluate the performance of the three models under these conditions. Tests at moisture contents of 10% and 20% are presented.

6.1 Tests at 10% of Moisture Content

Tests at vertical pressures of 100 kPa, 200 kPa and 500 kPa were carried out in mixtures having 10% of moisture content. Although the moisture content of the samples did not change during the tests, the degree of saturation (Sr) did not remain constant since the voids volume of the samples changed at each pressure and each concentration of disperse particles. A comparison between the laboratory results and the values predicted by the theoretical models for the Poisson's ratio and the elastic moduli E and G is presented.

The densities of the samples are presented in figure 6.1. At each pressure, the maximum density was observed at a fine particle concentration between 20% and 40%. This range is similar to the range obtained during the dry tests presented in the previous chapter. Also, as in the dry case, the concentration where the maximum density took place shifted to the right when the vertical pressure was increased. However, the value of the maximum density at each pressure was considerable higher than in the dry case. This can be explained since the water partially filled the spaces that air occupied before, allowing the particles to had a densely packed setup.

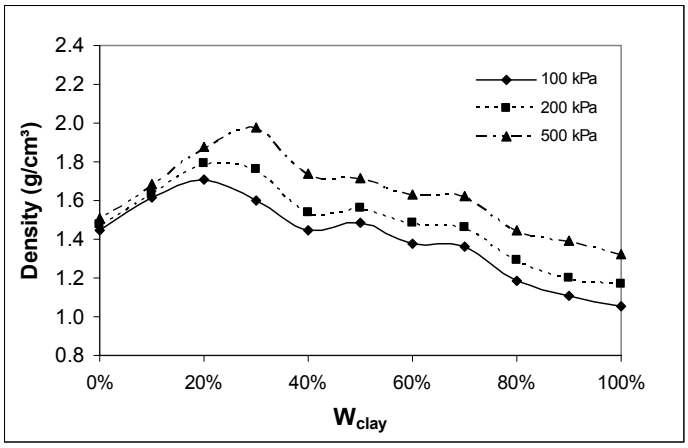

Figure 6.1 Density of the Kaolinite-sand Mixtures at w=10%

Figures 6.2 and 6.3 show the wave velocities Vp and Vs at each concentration of fine particles. At every vertical pressure, the maximum velocity can be identified at a fine particles concentration close to 30%. This value corresponds with the optimum concentration found in the density curves. In this way, this concentration was chosen as the limit for the theoretical simulation.

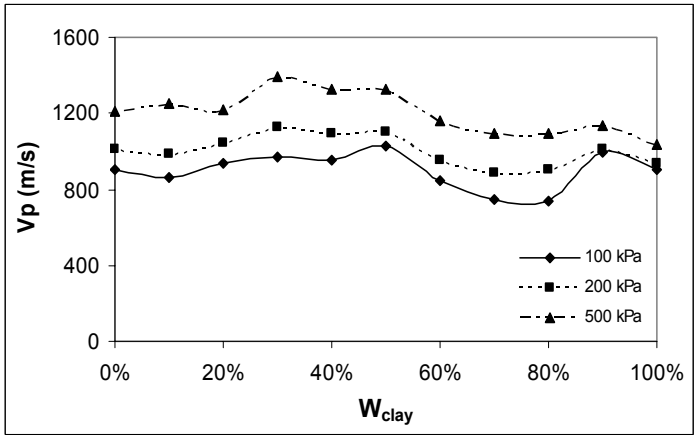

Figure 6.2 Vp of the Kaolinite-sand Mixtures at w=10%

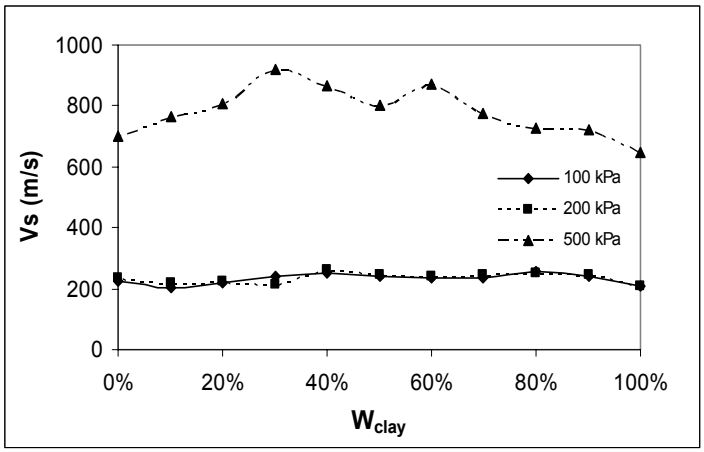

Figure 6.3 Vs of the Kaolinite-sand Mixtures at w=10%

The trend observed on the Poisson's ratio during these tests was similar to the trend observed during the dry tests in the previous chapter. Figures 6.4, 6.5 and 6.6 show the comparison between the laboratory results and the values predicted using the theoretical models. A constant average value of 0.45 was obtained during the tests developed at vertical pressures of 100 kPa and 200 kPa, while less than one half of this value was recorded as the average value when the samples were subjected to 500 kPa.

At every vertical pressure, the Hashin's model satisfactory predicted the Poisson's ratio of the tested samples. The agreement between the laboratory results and the predicted values by this model was almost perfect when the samples were subjected to vertical pressures of 100 kPa and 200 kPa. Nevertheless, a small flaw in accuracy was observed when the samples were subjected to 500 kPa. On the other hand, the Guth's model and the Greszczuk's model did not accurately predict this property of the mixtures since they went up and down when increasing the concentration of the disperse particles, while the laboratory results remained almost constant.

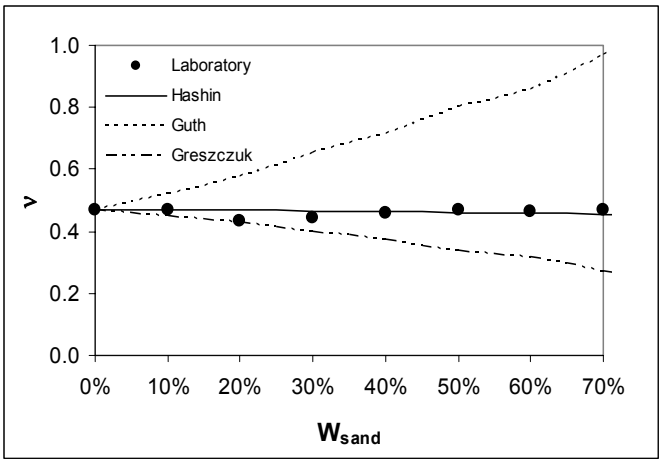

Figure 6.4 Poisson's Ratio of the Kaolinite-sand Mixtures (w= 10%) at 100 kPa

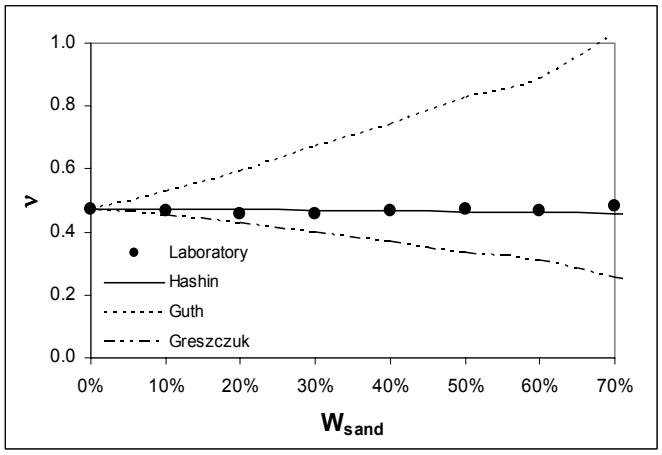

Figure 6.5 Poisson's Ratio of the Kaolinite-sand Mixtures (w=10%) at 200 kPa

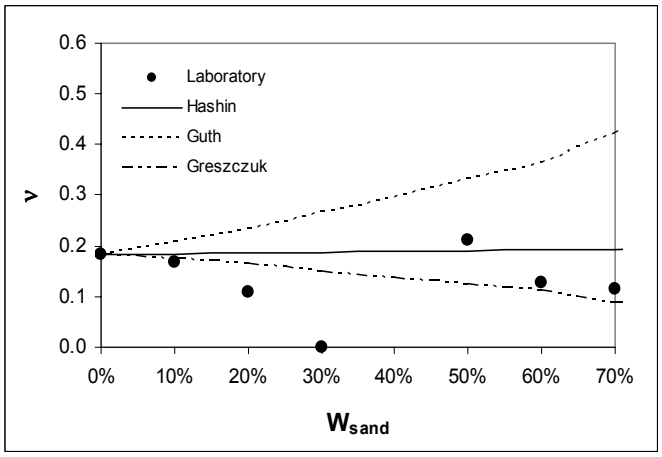

Figure 6.6 Poisson's Ratio of the Kaolinite-sand Mixtures (w=10%) at 500 kPa

Figures 6.7, 6.8 and 6.9 show the obtained results for the elastic modulus E of the samples. The obtained laboratory values were close to those obtained in the dry case. The Hashin and Guth models satisfactory predicted the values of the elastic modulus E at every disperse particles concentration, but no matter what pressure was used the two models tended to slightly underpredict the laboratory results. As in the dry case the Greszczuk's model only worked out when a vertical pressure of 500 kPa was used.

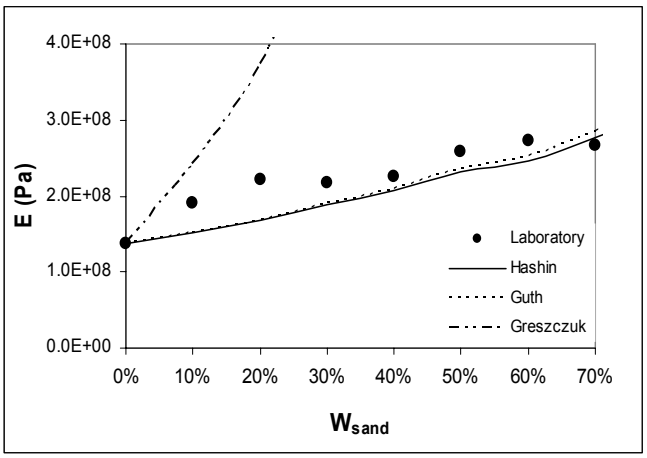

Figure 6.7 E of the Kaolinite-sand Mixtures (w= 10%) at 100 kPa

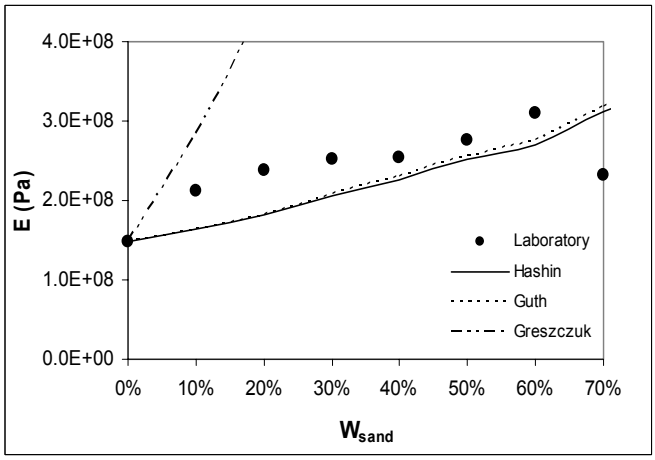

Figure 6.8 E of the Kaolinite-sand mixtures (w=10%) at 200 kPa

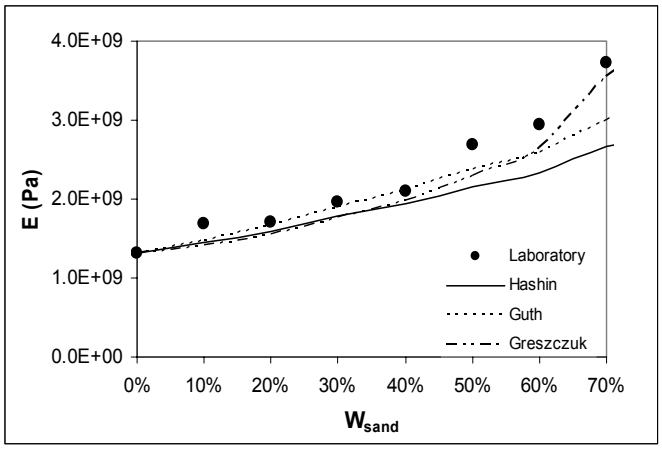

Figure 6.9 E of the Kaolinite-sand Mixtures (w= 10%) at 500 kPa

Regardless the used vertical pressure, the Hashin and Guth models accurately predicted the values of the elastic modulus G of the samples although they tended to slightly underpredict the laboratory results. On the other hand, only when the samples were subjected to a vertical pressure of 500 kPa, the Greszczuk's model presented a good agreement between the predicted values and the laboratory results. Figures 6.10, 6.11 and 6.12 show the obtained results.

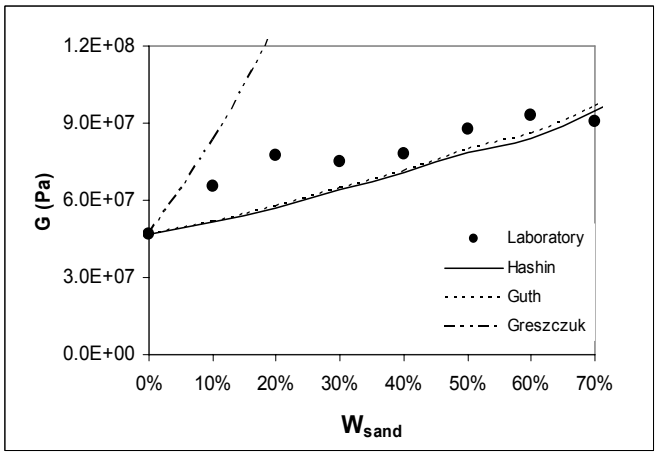

Figure 6.10 G of the Kaolinite-sand Mixtures (w=10%) at 100 kPa

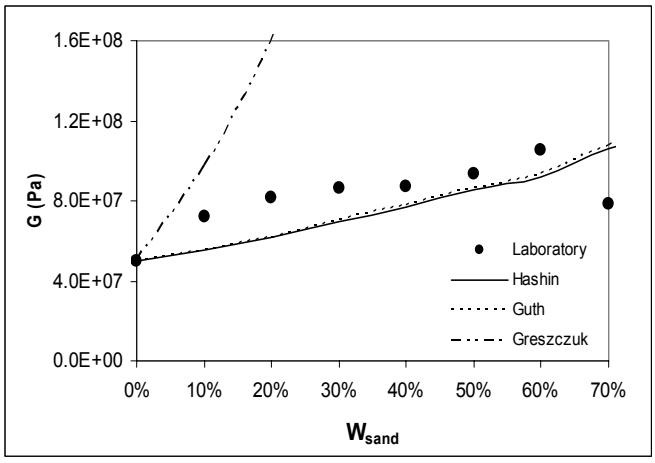

Figure 6.11 G of the Kaolinite-sand Mixtures (w= 10%) at 200 kPa

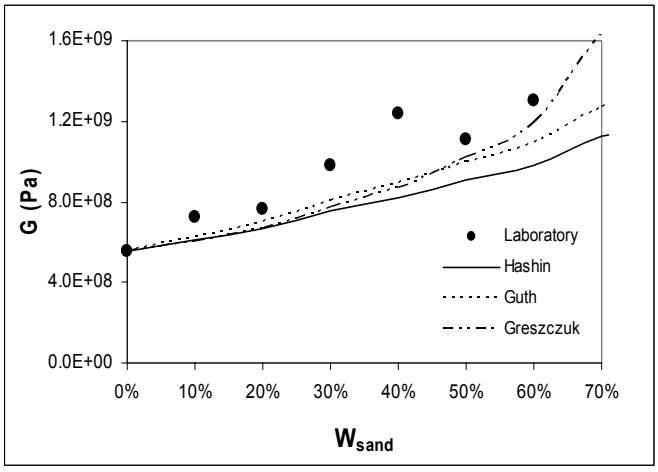

Figure 6.12 G of the Kaolinite-sand mixtures (w=10%) at 500 kPa

Based on the results presented before, it can be concluded that regardless the used vertical pressure, the Hashin's model accurately predict the Poisson's ratio and the elastic moduli of Kaolinite-sand mixtures when they have a low moisture content. Although the Guth's model accurately predicts the elastic moduli too, it fails when predicting the Poisson's ratio of these samples. On the other hand, the Greszczuk's model can be applied only in specific cases. During these and the previous tests, it was observed that the Greszczuk's model was only able to predict the elastic moduli when the samples were subjected to a vertical pressure of 500 kPa. It should be noticed that the Poisson's ratio of the mixtures at this vertical pressure was close to 0.25.

6.2 Tests at 20% of Moisture Content

In order to evaluate how the theoretical models work when the unsaturated mixtures have a high moisture content, samples with a fixed moisture content of 20 % were tested. This section attempts to study the effect that a high moisture content has on the structure of the binary mixtures, and how this effect is reflected by the considered models.

Figure 6.13 shows the density of the samples at the different concentrations of the fine particles. As in the previous cases, the samples were subjected to three different vertical pressures. The maximum density at each pressure was obtained at a fine particles concentration between 30% and 40%; range that is slightly different that the obtained in the previous cases. Thus, it can be noticed that when the moisture content is increased, the concentration of the fine particles that defines the structure transition shifts to the right, starting from 20% in the dry case and becoming closer to 40% when the moisture content is 20%. Moreover, The maximum density under each pressure is considerable higher than in the dry and 10%-moisture content cases.

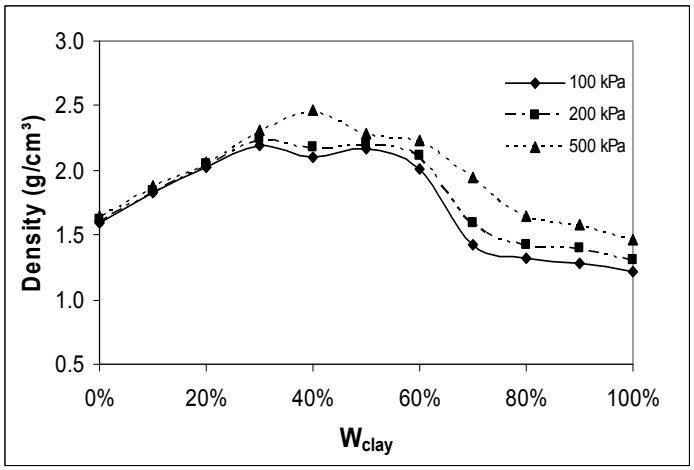

Figure 6.13 Density of the Kaolinite-sand Mixtures at w= 20%

Figures 6.14 and 6.15 show the wave velocities as functions of the fine particles concentration. Similarly to the density curves, the maximum values in Vp and Vs took place at a fine particles concentration close to 40%.

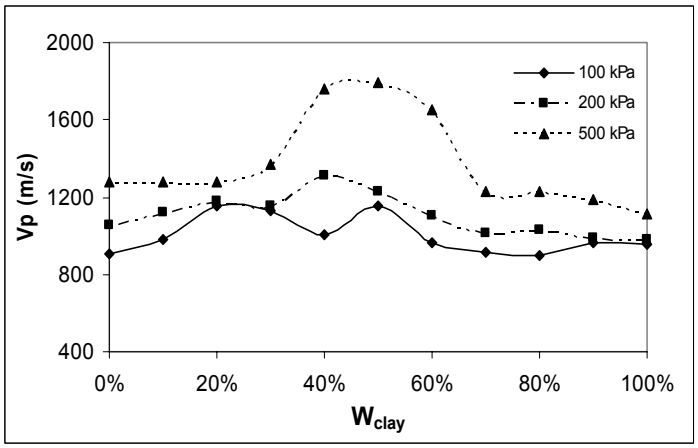

Figure 6.14 Vp of the Kaolinite-sand Mixtures at w= 20%

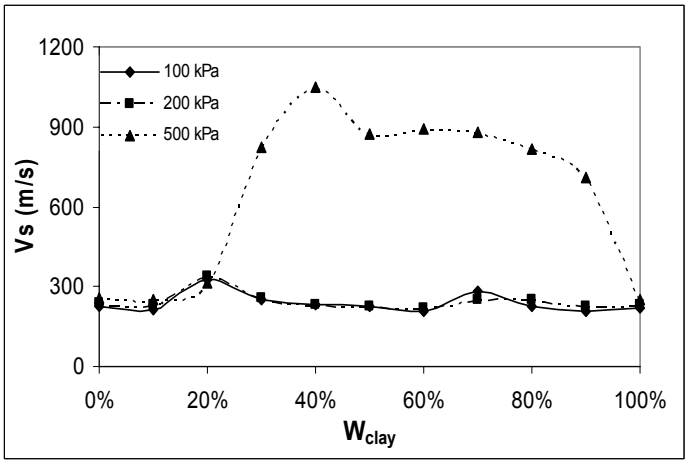

Figure 6.15 Vs of the Kaolinite-sand Mixtures at w= 20%

Using the results presented before, the Poisson's ratio and the elastic moduli of the mixtures were calculated, and compared to the values predicted by using the theoretical models. Figures 6.16, 6.17, and 6.18 show the obtained results for the Poisson's ratio. The general trend observed in the Poisson ratio during the dry and the 10%-moisture content cases was repeated again. When the samples were subjected to vertical pressures of 100 kPa and 200 kPa, the Poisson's ratio was close to 0.45, and it remained constant at the different concentrations of the disperse particles. However, when the vertical pressure was increased to 500 kPa, the Poisson's ratio had an average value close to 0.3, being higher than in the dry and 10%-m.c cases.

The Hashin's model satisfactory predicted the Poisson's ratio when the samples were subjected to 100 kPa and 200 kPa. Nevertheless, a lack on accuracy was observed when the vertical pressure was increased to 500 kPa; while

the Hashin's model predicted constant values, the laboratory values went down. As in the previous cases, the Guth's model overpredicted the Poisson's ratio regardless the vertical pressure, while the Greszczuk model tended to underpredict the laboratory results at 100kPa and 200 kPa. However, it should be noticed the good agreement between the values predicted by this model and the laboratory results at a vertical pressure of 500 kPa.

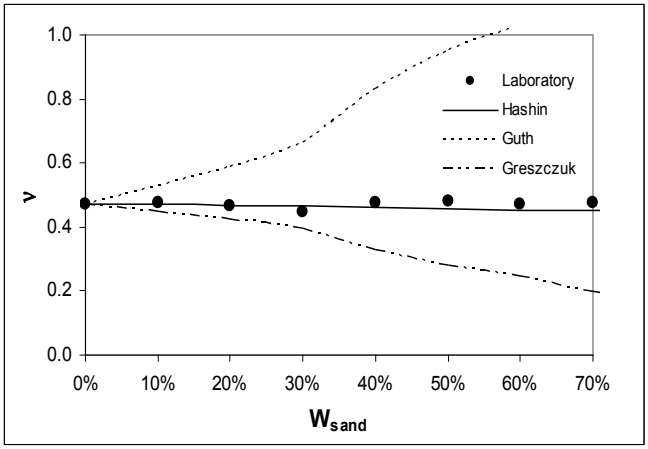

Figure 6.16 Poisson's ratio of the Kaolinite-sand Mixtures (w=20%) at 100 kPa

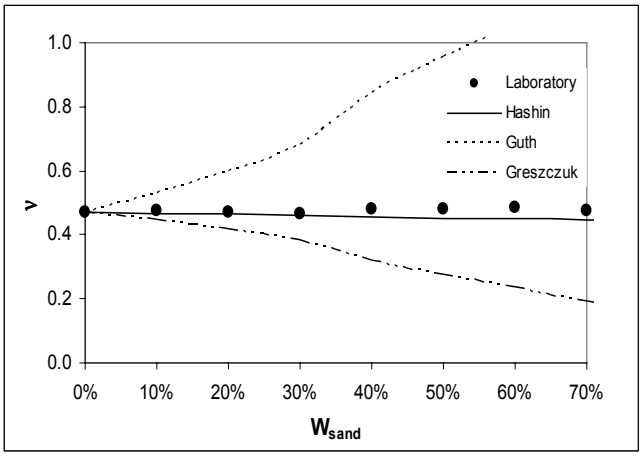

Figure 6.17 Poisson's ratio of the Kaolinite-sand Mixtures (w=20%) at 200 kPa

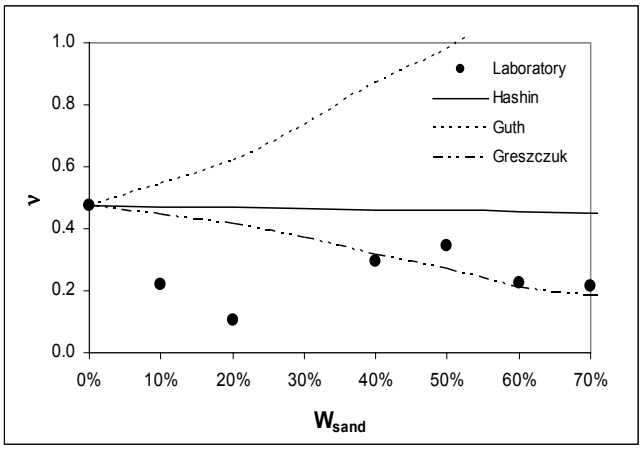

Figure 6.18 Poisson's ratio of the Kaolinite-sand Mixtures (w=20%) at 500 kPa

The calculated elastic moduli E and G of the samples were higher than the values presented in the previous cases. The comparison between the laboratory results and the values predicted by using the theoretical models for the elastic modulus E is showed in Figures 6.19, 6.20, and 6.21. The Hashin and Guth models accurately predicted the values of the elastic modulus E when the samples were subjected to vertical pressures of 100 kPa and 200 kPa, although these models tended to slightly overpredict the laboratory results at 200 kPa. In contrast, when the vertical pressure was increased to 500 kPa, they strongly underpredicted the laboratory results. It is clear that something happened in the mixture structure under these last conditions. On the other hand, the Greszczuk's model overpredicted the laboratory results at 100 kPa and 200 kPa, but it satisfactory worked out at 500 kPa, showing that at this last pressure the change in the mixture structure did not affect the performance of this model.

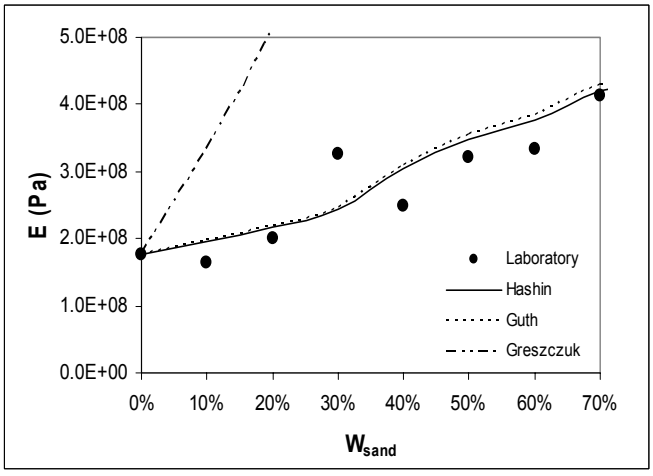

Figure 6.19 E of the Kaolinite-sand Mixtures (w=20%) at 100 kPa

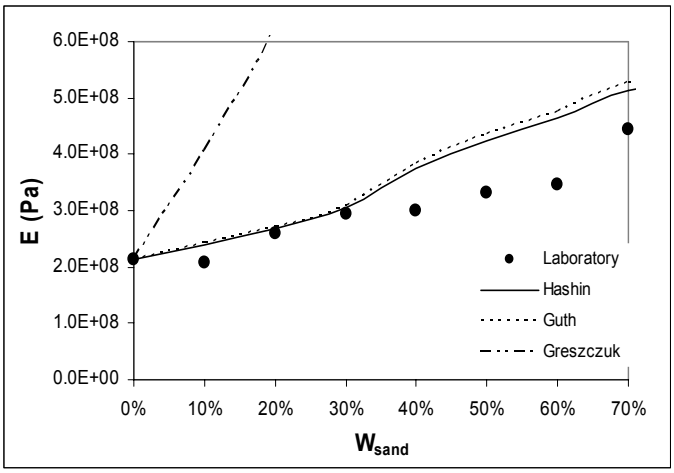

Figure 6.20 E of the Kaolinite-sand Mixtures (w=20%) at 200 kPa

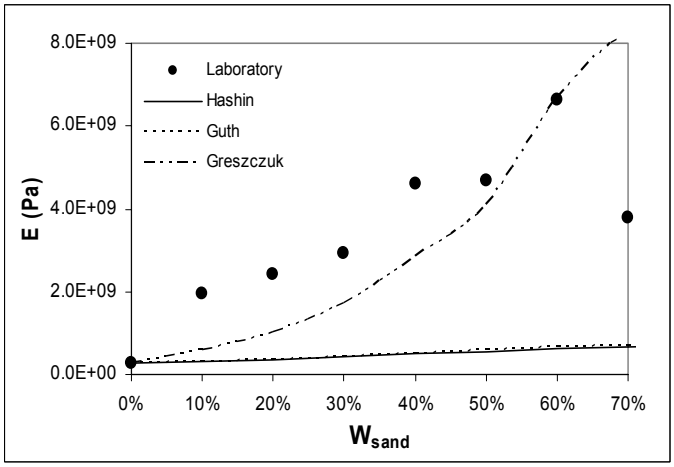

Figure 6.21 E of the Kaolinite-sand Mixtures (w=20%) at 500 kPa

Figures 6.22, 6.23 and 6.24 show the results obtained for the elastic shear modulus G of the samples. The observed trend for the elastic modulus E was repeated again in the elastic modulus G. The Hashin and Guth models satisfactory predicted the elastic shear moduli G when the samples were subjected to vertical pressures of 100 kPa and 200 kPa, but they underpredicted the laboratory values at 500 kPa. In the same way, the Greszczuk's model overpredicted the laboratory results at vertical pressures of 100 kPa and 200 kPa.

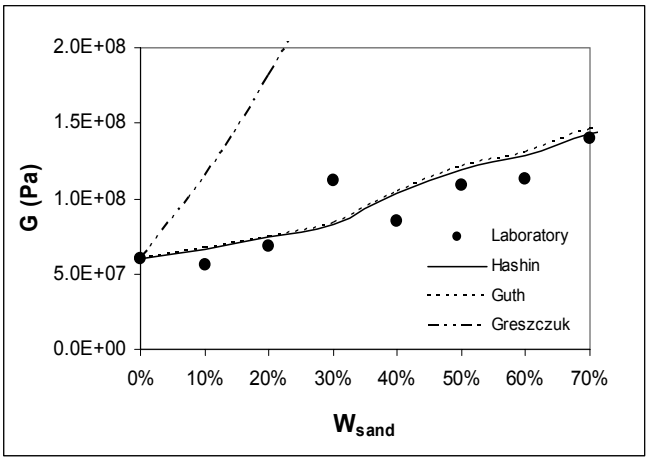

Figure 6.22 G of the Kaolinite-sand Mixtures (w=20%) at 100 kPa

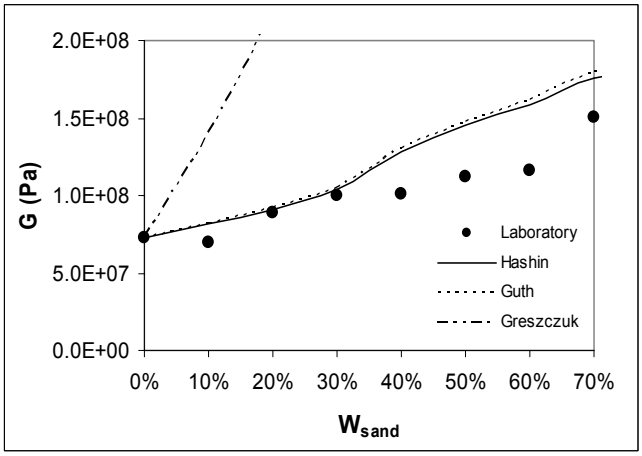

Figure 6.23 G of the Kaolinite-sand Mixtures (w=20%) at 200 kPa

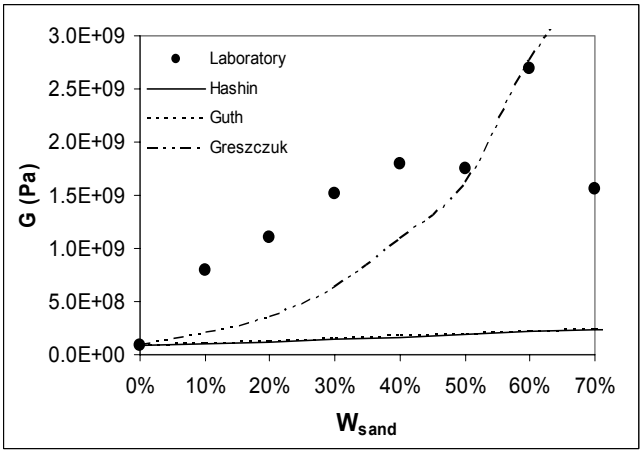

Figure 6.24 G of the Kaolinite-sand Mixtures (w=20%) at 500 kPa

The tests developed at a vertical pressure of 500 kPa have shown that the Hashin and the Guth models cannot be used in order to predict the elastic moduli of mixtures with a high moisture content when they are subjected to a high vertical pressure. It is clear that the vertical pressure alone does not produce the problem since these models satisfactory worked out when they were used at the same pressure in the dry and 10% m.c cases. It has to be a combined effect of the high vertical pressure and the high moisture content. The saturation degree of the mixtures was calculated, and it was found that when the samples containing a sand particles concentration higher than 30% were subjected to a vertical pressure of 500 kPa, they were saturated.

6.3 Tests Under High Confining Pressures and Saturated Condition

Yin[6] has presented the wave velocities and the density values of saturated samples made on Kaolinite clay and a variable concentration of Ottawa sand. These tests were carried out under different confining pressures, from 10MPa to 50 MPa. Using the results presented by Yin, the elastic moduli of the mixtures were calculated and compared with the values predicted by the theoretical models.

It was found that an important overprediction of the elastic moduli E and G takes place during these conditions. When the percentage of sand particles was increased, the laboratory values remained almost constant, while the results from the three models went up. The predicted values were almost two times the laboratory results. This effect can be explained since the developed high pore water pressure separates the particles forming the matrix, and the structure of the mixture it is no longer the structure assumed by the theoretical models. This phenomenon was observed at every confining pressure.

6.4 Summary

The tests presented during this chapter have shown the main features of the influence that the moisture content has on the agreement between the laboratory results and the theoretical simulations for υ, E and G. Three different stages produced by the combined effects of the vertical pressure and the moisture content were identified:

- Low vertical pressure and low moisture content:

The Hashin and Guth models satisfactorily predicted the elastic moduli of the samples with a low moisture content (less than 20%) when they were subjected to low vertical pressures; showing that the principles that these models are based on were not affected under these conditions. However, only the Hashin's model correctly predicted the Poisson's ratio of the samples. As observed in the previous chapter, the Greszczuk's model overpredicted the results when lower vertical pressures were used, since some constrains of this model were not satisfied.

- High vertical pressure and low moisture content:

When the samples having a low moisture content were subjected to higher vertical pressures, it was observed that all the three models satisfactory predicted the laboratory results for the elastic moduli. However, it was noticed that the Hashin and Guth models tended to slightly underpredict these values. Similarly, the Hashin and Greszczuk models acceptably predicted the Poisson's ratio of the samples. The Greszczuk's model was very accurate under these conditions.

- High vertical pressure and high moisture content:

It was observed that when the samples having a high moisture content were subjected to high vertical pressures, two different situations took place:

a. At 500 kPa, the Hashin and Guth models strongly underpredicted the laboratory results for the elastic moduli of the samples. On the other hand, the Greszczuk's model acceptably predicted those values.

Moreover, this model was the only one that satisfactory predicted the Poisson's ratio of the samples. Therefore, it seems like under these conditions only deformation compatibility can be correctly assumed.

b. Using results presented by Ying, it was found the three theoretical models strongly overpredicted the elastic moduli of saturated samples when they were subjected to extremely high confining pressures.

In this way, the Hashin and Guth models can be applied in order to predict the elastic moduli of unsaturated mixtures regardless the used vertical pressure. If the unsaturated mixtures are subjected to a high vertical pressure, the Greszczuk model will accurately predict these values too. However, it can generate a significant overprediction when the mixtures are subjected to low vertical pressures. On the other hand, if the mixtures are saturated or their degree of saturations is close to one, and they are subjected to extremely high vertical pressures, all the theoretical models will overpredict the elastic moduli.

7.0 INFLUENCE OF THE MATRIX PARTICLES SIZE

The previous chapters have shown that in general, the considered theoretical models can satisfactory predict the elastic moduli and the Poisson's ratio regardless the vertical pressure and the moisture content of the mixtures, with some exceptions when the mixtures are subjected to special conditions. However, until this moment all the tests have been developed in mixtures containing Kaolinite clay and Ottawa sand. The next two chapters attempt to explore the influence that the size ratio of the mixture components has on the accuracy of the theoretical simulations. In this chapter, tests on mixtures composed by Kaolinite clay and glass beads of 10 mm in diameter, and mixtures containing coarse sand No.16 and the same glass beads are presented. Also, the effects of particle interference, matrix compaction and matrix crushing are discussed.

7.1 Tests on Mixtures of Kaolinite Clay and Glass Beads (10mm)

The tests presented on the previous chapters were developed in mixtures containing Kaolinite clay and Ottawa sand, these mixtures had a size ratio of 140. In this section, tests that were carried out in mixtures composed by Kaolinite clay and glass beads of 10 mm in diameter are illustrated. These mixtures have a size ratio of 2381. They are presented in order to identify what happen with the theoretical simulations when the size ratio of the components is extremely high. Vertical pressures of 100 kPa and 200 kPa were used.

Figure 7.1 shows the density of the tested samples at each concentration of fine particles. At each vertical pressure, the maximum density was produced at a Kaolinite concentration between 20% and 30%. It should be notice that this maximum value was almost twice of the pure Kaolinite density.

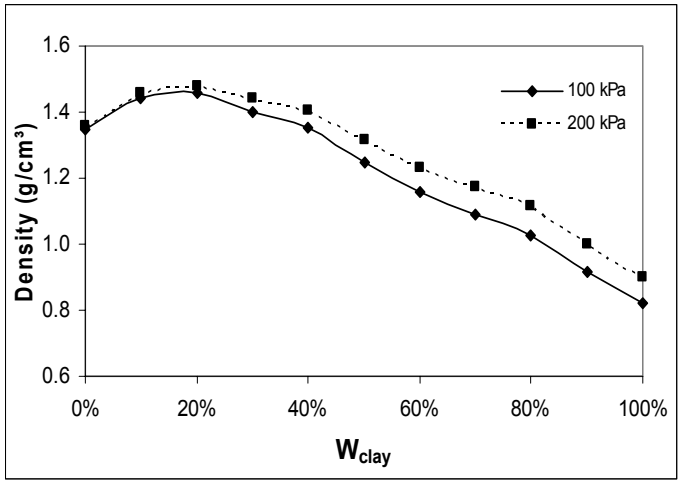

Figure 7.1 Density of the Kaolinite –Glass Beads Mixtures

The maximum values in Vp and Vs took place at a fine particles concentration between 20% and 30%. This range corresponds to the optimum concentration found in the density graphs. Figure 7.2 and 7.3 show the obtained results.

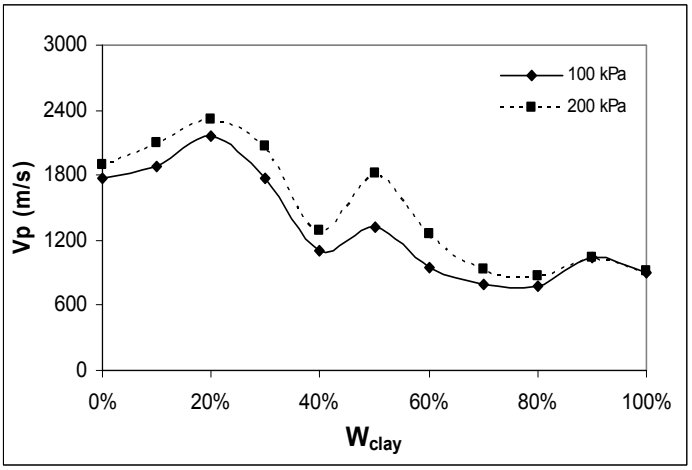

Figure 7.2 Vp of the Kaolinite –Glass Beads Mixtures

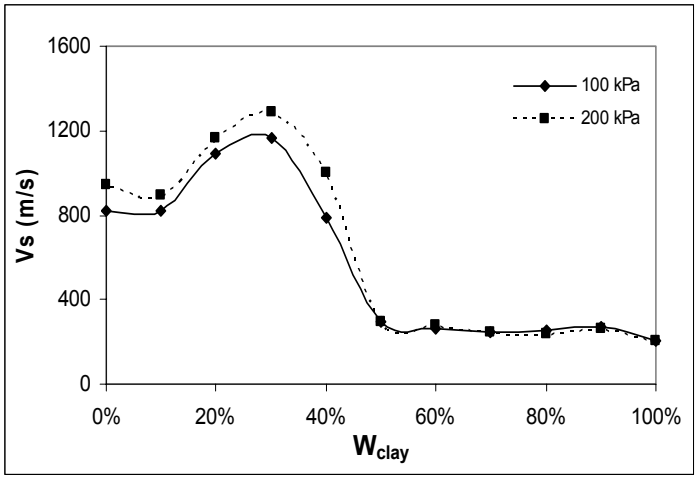

Figure 7.3 Vs of the Kaolinite –Glass Beads Mixtures

The comparison between the Poisson's ratio of the samples measured in the laboratory and those values obtained by using the theoretical models is showed in figures 7.4 and 7.5. The Poisson's ratio of the mixtures tended to remain constant when increasing the percentage of the disperse particles. An average constant value of 0.46 was observed when the samples were subjected to 100 kPa and 200 kPa. As observed in the tests developed on mixtures of Kaolinite clay and Ottawa sand, the Hashin's model satisfactory predicted the Poisson's ratio for the considered interval. Also, the Guth and Greszczuk models overpredicted and underpredicted respectively the laboratory results.

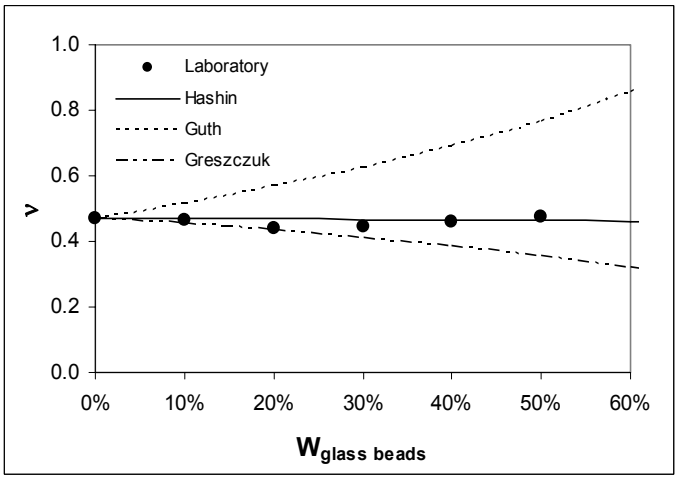

Figure 7.4 Poisson's ratio of the Kaolinite –Glass Beads Mixtures at 100 kPa

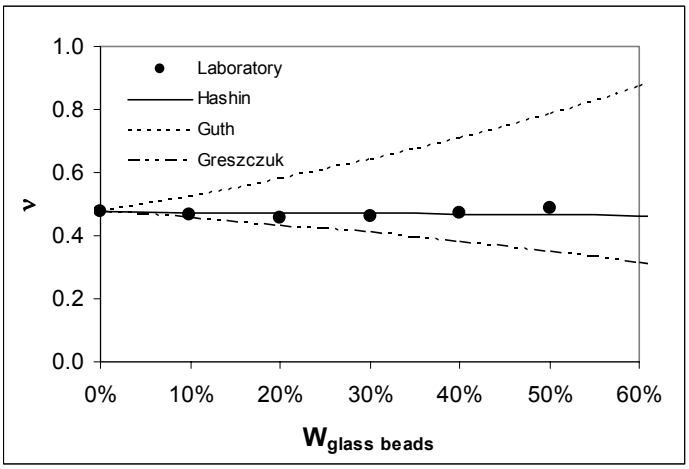

Figure 7.5 Poisson's ratio of the Kaolinite –Glass Beads Mixtures at 200 kPa

The observed trends on the elastic moduli E and G were considerably different that the observed trends during the tests made on mixtures of Kaolinite clay and Ottawa sand. The transition between the moduli at 0% of glass beads and the moduli at the concentration where the change in the kind of structure took place was not a gradual change. The results for the elastic modulus E are showed in Figures 7.6 and 7.7. First, an important change on this modulus was produced when increasing the glass beads concentration from 0% to 10%. Then, the correspondent values for the elastic modulus E at concentrations of glass beads between 10% and 30% were almost the same. In this way, the Hashin and Guth models underpredicted the laboratory results during low concentrations of glass beads. Near to a glass beads concentration of 40%, the values of this modulus were substantially increased; thus, for higher concentrations, these models strongly underpredicted the laboratory results.

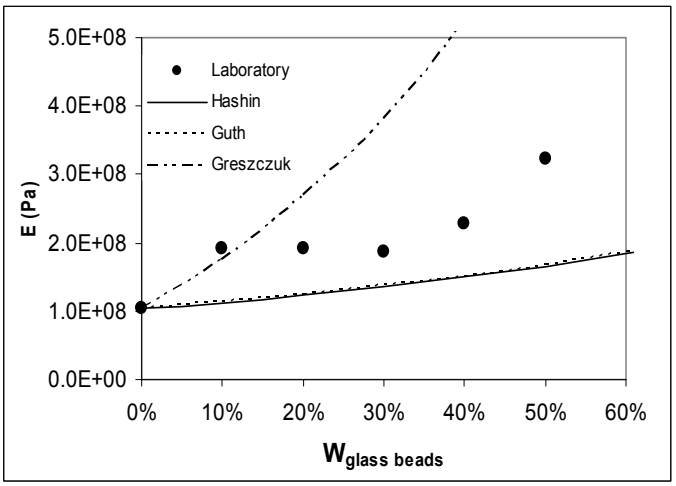

Figure 7.6 E of the Kaolinite –Glass Beads Mixtures at 100 kPa

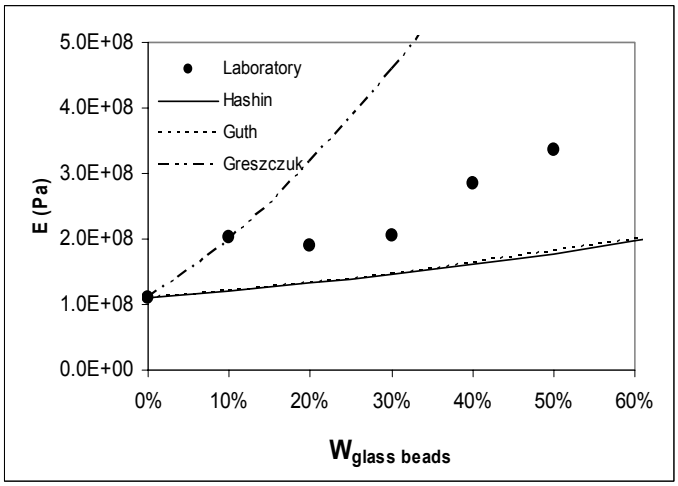

Figure 7.7 E of the Kaolinite –Glass Beads Mixtures at 200 kPa

The exhibited trend on the elastic modulus G was similar to the trend observed on the elastic modulus E. Figures 7.8 and 7.9 show the obtained results. The Hashin and Guth models underpredicted the laboratory results, while the Greszczuk model strongly overpredicted these values.

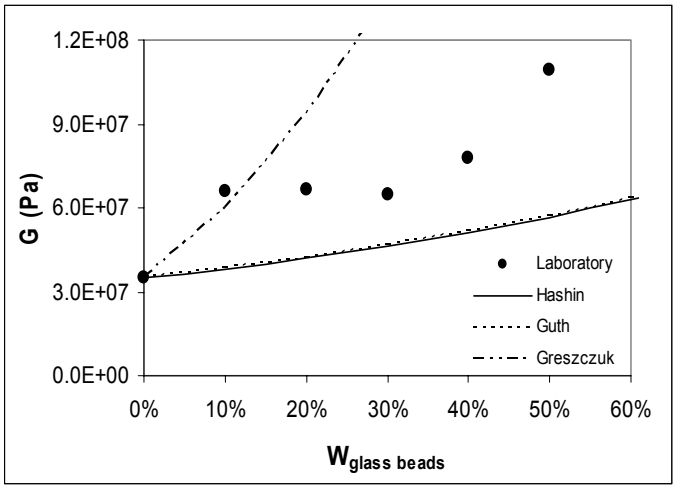

Figure 7.8 G of the Kaolinite –Glass Beads Mixtures at 100 kPa

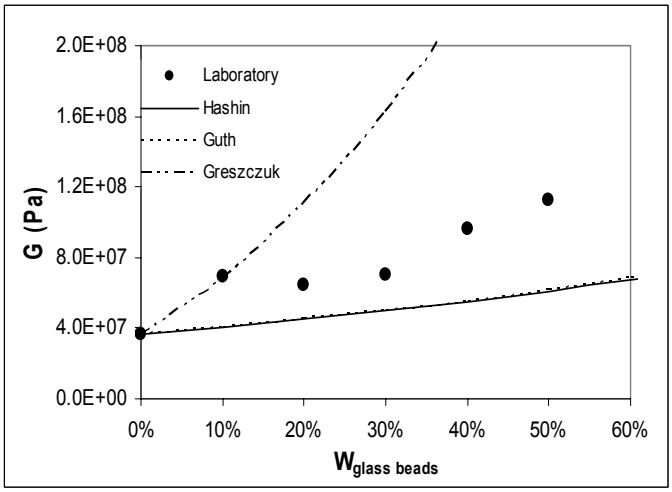

Figure 7.9 G of the Kaolinite –Glass Beads Mixtures at 200 kPa

The observed underprediction on the elastic moduli E and G can be analyzed from a change in the properties of the matrix material. When increasing the concentration of the glass beads, the spaces between the disperse particles starts to reduce and stress concentration around these particles is developed. This causes a compaction of the matrix material. In this way, the Kaolinite starts to behave as a new more rigid matrix. This was explained in chapter 4, when the influence of the vertical pressure on the elastic moduli of pure Kaolinite samples was analyzed. In this way, the elastic moduli in those mixtures containing more than certain fraction of glass beads cannot be predicted using the theoretical models since a change in the matrix behavior and the structure of the mixture is produced.

7.2 Tests on Mixtures of Sand 16 and Glass Beads (10mm)

In order to study how the theoretical models perform when the matrix material of the mixture is composed by big particles, mixtures of coarse sand number 16 and glass beads of 10 mm in diameter were tested. These mixtures had a size ratio equal to 8.5, ratio that is considerable small compared to the size ratios of the previous tests. Three different vertical pressures were used.

Figure 7.10 shows the density of the tested samples. The maximum density at each pressure was obtained at a sand particles concentration of 40%. It should be noticed that the density of each sample at the three different vertical pressures was almost the same, since the sand and the glass beads did not present a significant volume reduction when increasing the vertical pressure.

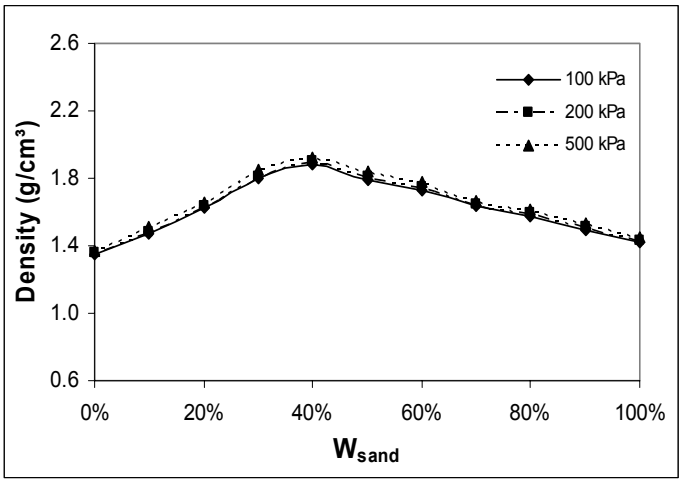

Figure 7.10 Density of the Sand –Glass Beads Mixtures

The maximum values for Vp and Vs were recorded at a sand particles concentration between 20% and 30%. The obtained results are showed in figures 7.11 and 7.12. The sand particles concentration where the maximum velocities took place did not correspond with the concentration found in the density curves. The disagreement of these tow points, 40% and one number between 20% and 30%, show that the change in the mixture structure was a gradual process, and it did not take place at one specific concentration.

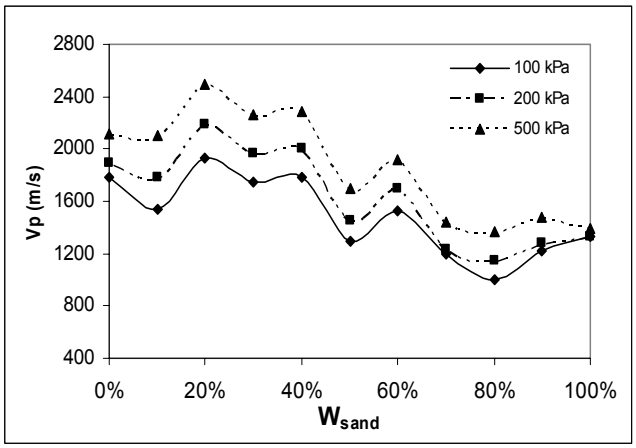

Figure 7.11 Vp of the Sand –Glass Beads Mixtures

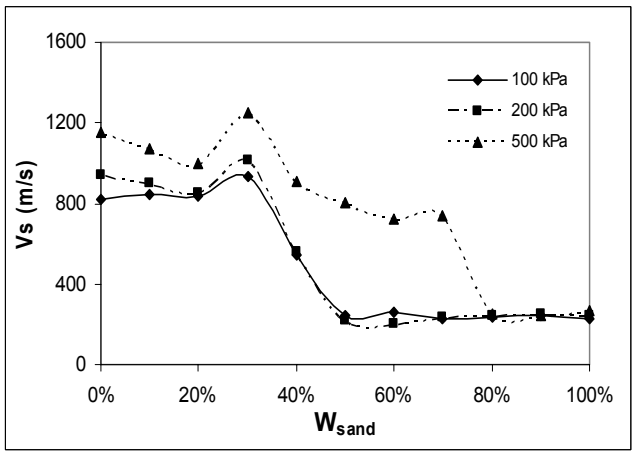

Figure 7.12 Vs of the Sand –Glass Beads Mixtures

Since it was not clear what concentration could be considered as the limit for theoretical simulations, the porosities of the samples were calculated. Figure 7.13 shows that the minimum porosity took place at a fine particles concentration of 40%. This value corresponds to the optimum found in the density curves. In this way, the theoretical simulations were carried out until this critical concentration.

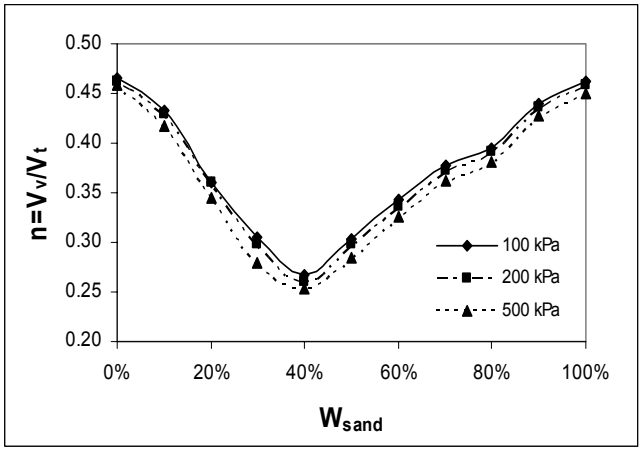

Figure 7.13 Porosity of the Sand –Glass Beads Mixtures

Figures 7.14, 7.15 and 7.16 show the laboratory results and the theoretical simulations for the Poisson's ratio of the samples. It was found that at each vertical pressure, the Poisson's ratio tended to remain constant when the percentage of glass beads was increased. A constant average value of 0.47 was found at 100 kPa and 200 kPa. The average value at 500 kPa was 0.43. At every vertical pressure, it was observed that beyond the considered interval, the Poisson's ratio started to decrease until it reached the value of the pure glass beads (close to 0.33).

At every vertical pressure and every concentration of disperse particles, the Hashin's model accurately predicted the Poisson's ratio of the mixtures. On the other hand, the Guth's model and the Greszczuk's model tended to overpredict and underpredict the laboratory results. Nevertheless, the agreement between the laboratory data and the values predicted by the Greszczuk model at 500 kPa was really good.

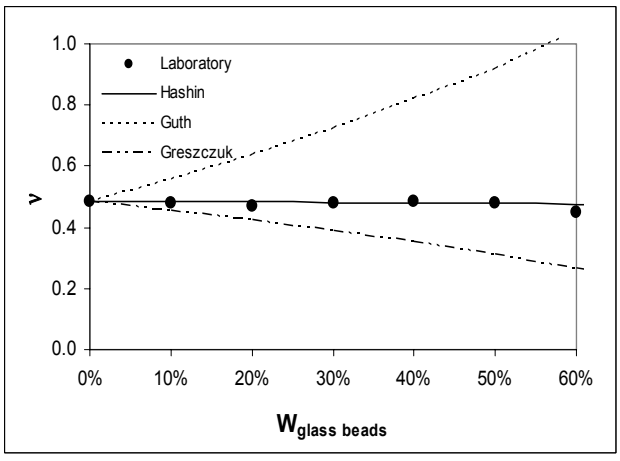

Figure 7.14 Poisson's ratio of the Sand –Glass Beads Mixtures at 100 kPa

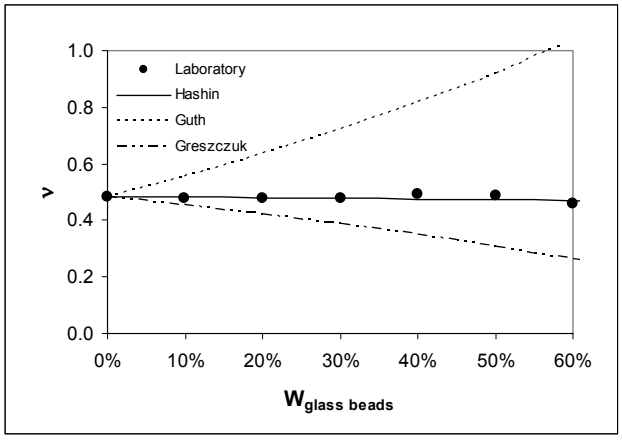

Figure 7.15 Poisson's ratio of the Sand –Glass Beads Mixtures at 200 kPa

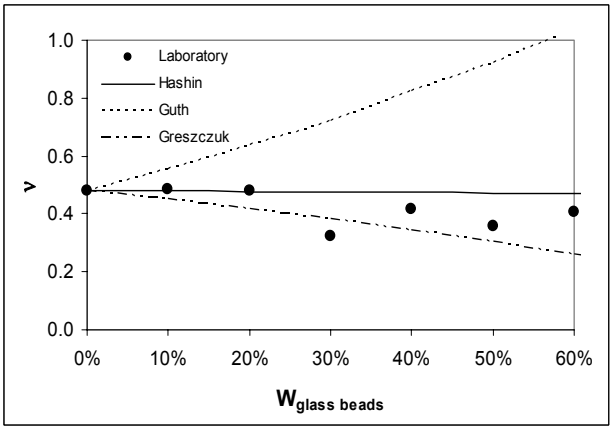

Figure 7.16 Poisson's ratio of the Sand –Glass Beads Mixtures at 500 kPa

Figures 7.17 and 7.18 show the laboratory results and the values predicted by the theoretical models for the elastic modulus E at 100 kPa and 200 kPa. The Hashin and Guth models accurately predicted the elastic modulus E at 100 kPa, although it should be noticed that during the last concentrations of the considered interval, the laboratory values started to separate from the predicted values. At 200 kPa, this separation was increased and the models started to separate from the laboratory data even early, generating a significant overprediction. At these vertical pressures of 100 kPa and 200 kPa, the values predicted by the Greszczuk model strongly differed from the laboratory results.

The situation that took place at 500 kPa was totally different; Figure 7.19 shows the obtained results. It can be noticed that the Hashin and Guth models satisfactory predicted the laboratory results during lower concentrations of glass beads, but after a certain point, the laboratory results jumped to higher values and the theoretical models stayed

apart. On the other hand, the values predicted by the Greszczuk model were not so far from the laboratory results, but their trend was different.

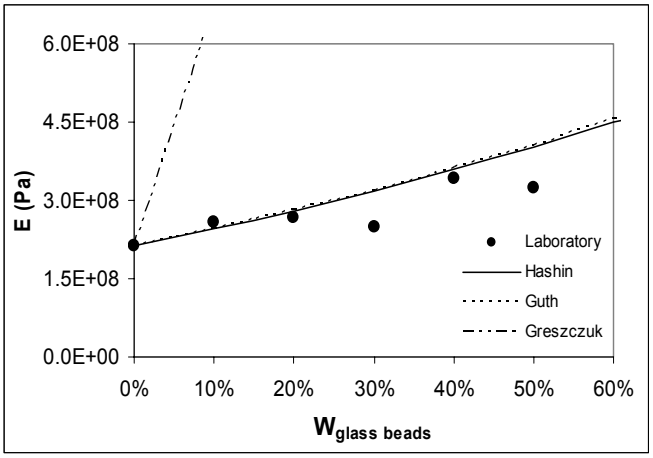

Figure 7.17 E of the Sand –Glass Beads Mixtures at 100 kPa

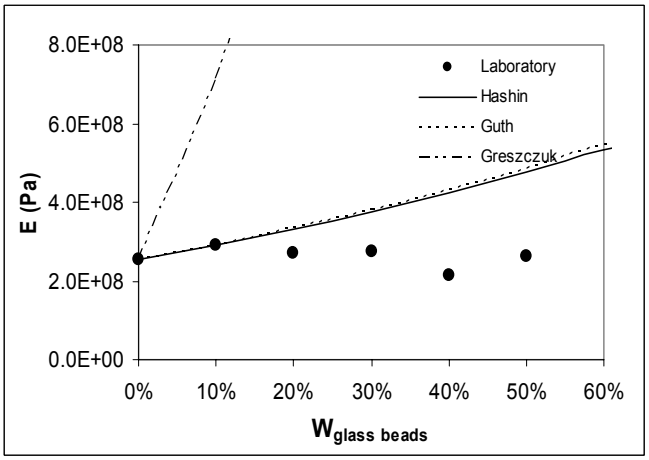

Figure 7.18 E of the Sand –Glass Beads Mixtures at 200 kPa

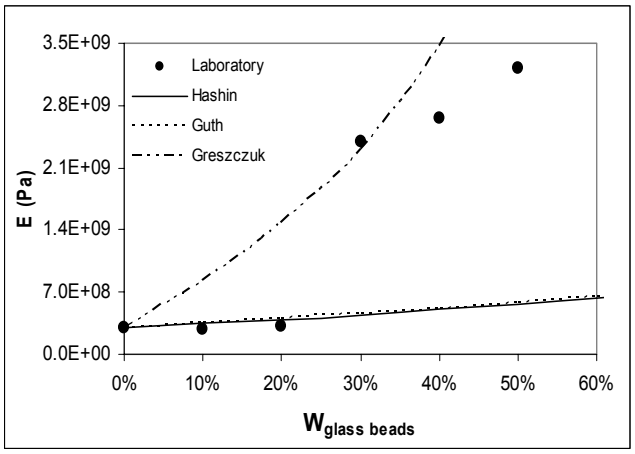

Figure 7.19 E of the Sand –Glass beads Mixtures at 500 kPa

The exhibited trend for the elastic modulus E was repeated again in the results of the elastic modulus G. Figures 7.20, 7.21 and 7.22 show the obtained results. At a vertical pressure of 100 kPa, the Hashin and the Guth models satisfactory predicted the elastic shear modulus of the samples, although a small overprediction of the laboratory results was observed at the end of the considered interval. The amount of this overprediciton was increased at 200 kPa, and it started even early. At these vertical pressures the Greszczuk's model strongly overpredicted the laboratory results.

At 500 kPa, a strong difference between the laboratory results and the values predicted by the Hashin and the Guth models was observed. These models considerably underpredcited the laboratory results. On the other hand, the Greszczuk model predicted close values to those obtained in the laboratory, but they had a completely different trend.

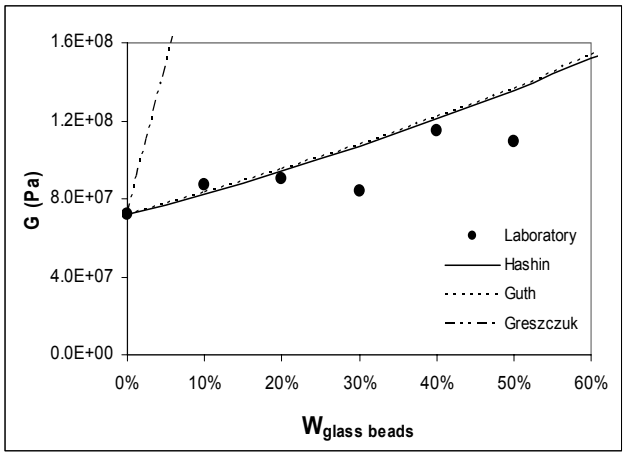

Figure 7.20 G of the Sand –Glass Beads Mixtures at 100 kPa

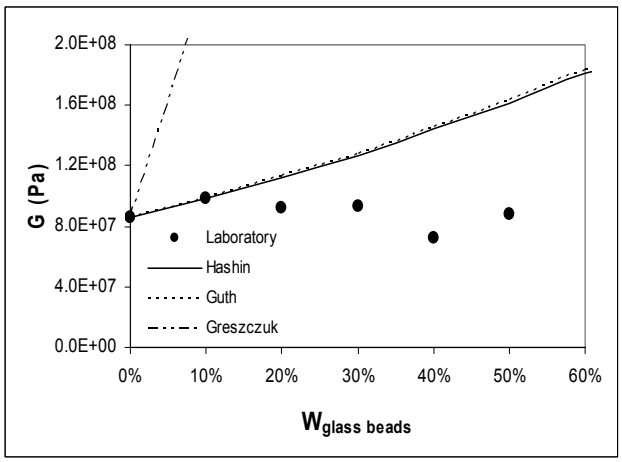

Figure 7.21 G of the Sand –Glass Beads Mixtures at 200 kPa

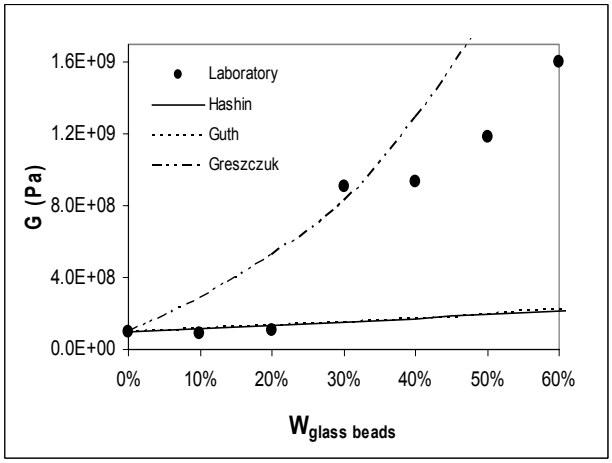

Figure 7.22 G of the Sand –Glass Beads Mixtures at 500 kPa

7.3 Particle Interference and Crushing

Analyzing the presented results for the elastic moduli E and G in the last section, two important and opposite phenomena can be noticed. During the tests developed at 100 kPa and 200 kPa, it is clear that some kind of structure interference took place after a certain concentration of glass beads was reached, affecting the accuracy of the theoretical models since they tended to overpredict the laboratory results. On the other hand, during the tests at 500 kPa, the laboratory results showed a dramatic change beyond a certain concentration of glass beads, and the theoretical simulations started to dramatically underpredict the recorded values. This last phenomenon can be explained by the fact that the coarse sand started to crush at this pressure.

7.3.1 Particle Interference

Particle interference is a topic that has been deeply explored under the powder technology. Ahmad and Smalley [29] present the Weymouth's model for particle interference that satisfactory explains how this kind of structure interference is developed in a dry binary mixture. When increasing the fraction of the oversized particles in the mixture, the packing of the fine particles is not affected until one point, where the spaces between the large particles are not big enough to allow the arrangement of the fine particles [30]. It should be noticed that at this point, not all the large particles are making contacts between them, and they can still be considered as disperse particles. Figure 7.23 illustrates this process:

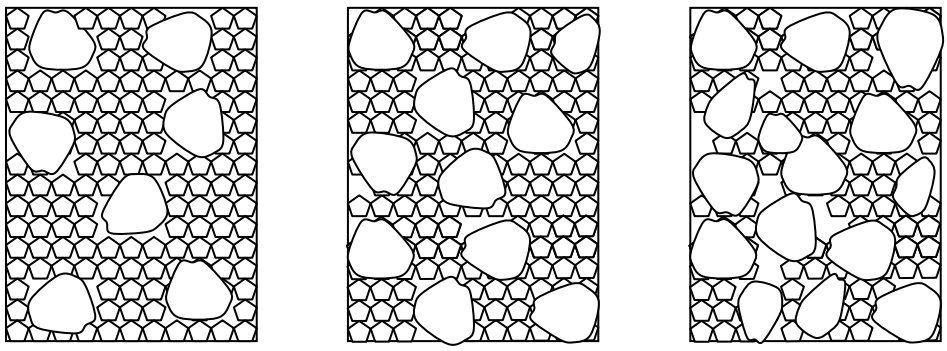

Figure 7.23 Weymouth's Model for Particle Interference
(Adapted from Ahmad and Smalley [30])

Figure 7.23 shows the process of increasing the fraction of the disperse particles in a binary mixture. According to Ahmad and Smalley [30], the stage A is produced when the separation between the large particles is bigger than the average diameter of the smaller particles. Then, the stage B takes place when the large particles are separated just for a distance equal to the average diameter of the fine particles. Until this moment the uniformity of the voids defined by the fine particles has not been affected. The Stage C is the point when the arrangement of the fine particles is disturbed by the large particles, since the separation of the large particles is smaller than the average diameter of the small particles, making impossible that the fines can uniformly fill the spaces between the disperse particles.

Ahmad and Smalley [30] refer to T.C Powers, who state that particle interference is expected only when the components of the mixture are geometrically similar. This explains why this kind of phenomenon was not observed in the previous tests that were developed on binary mixtures having strongly higher size ratios.

Particle interference causes a change in the packing of the matrix material, producing a new setup with a high voids content. Therefore, the theoretical models cannot be used when the mixtures present particle interference, since they assume that the matrix of the mixture is not affected when increasing the concentration of disperse particles.

7.3.2 Crushing

The change in the soil properties due the crushing of the particles is a complex new field. According to Billman [31], the main effects that the crushing has on the properties of granular materials can be summarized in the next points:

1. When grain crushing occurs, a large volume reduction takes place. Therefore, the axial strength required to reach the failure of the composite is increased.
2. The produced grain splitting increases the percentage of fines in the composite; thus, the permeability is reduced.
3. The principal effective stress ratio at failure (σ'_1/σ'_3) decreases when increasing the confining pressure.

Billman has found that most of the grain degradation takes place in the medium and small sized particles of the composite. Also, conducting experimental tests he found a log-log relation between the grain diameter and the tensile strength of the particles; the bigger was the diameter of the particle, the smaller was the tensile strength. On the other hand, Lowrison [32] reported that the ultimate strength is inversely proportional to the square root of the grain size. Although the functions proposed by these authors are different, they have a similar trend.

The objective of this section is just to gain an insight about how the crushing of the matrix particles can affect the elastic moduli of the mixtures. During the tests made on mixtures of coarse sand and glass beads at a vertical pressure of 500 kPa, some noises were reported. It sounded like if the particles were breaking. The processes that one of these samples could have when it was subjected to a constant pressure can be depicted using the next figure.

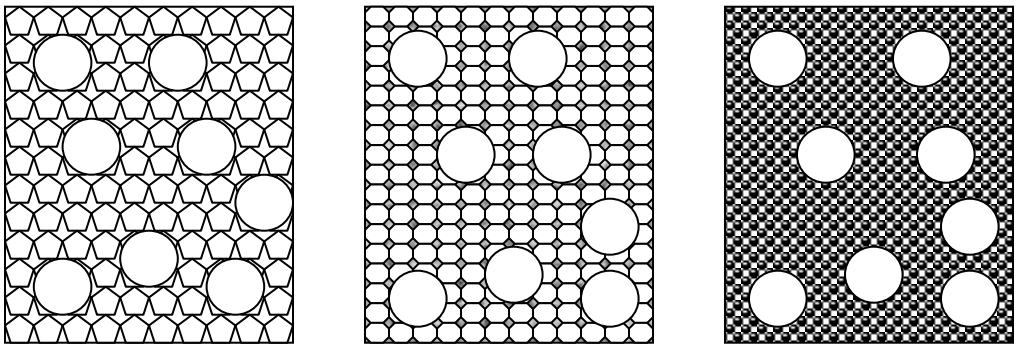

Figure 7.24 Change in the Matrix Particles Shape Due the Crushing

Figure 7.24 shows how the matrix material is crushed (assuming that the disperse particles are rigid and do not break). The stage A illustrates the original setup of the mixture. The stage B show how when some significant stresses are induced, the irregular particles presented in A start to break, producing smoother particles and some smaller debris that fill the voids between them. Thus, the stage C is reached when all the original particles are reduced to a powder compound. Obviously, the stage C requires and extremely high confining pressure and a lot of time to allow the process.

Since the oversized particles of the mixtures concentrate stresses, the level of crushing of the matrix material depends on the disperse particles concentration. In this way, if the tested samples of coarse sand and glass bead had

different levels of crushing under a vertical pressure of 500kPa, their matrix could have totally different properties and the theoretical models cannot be applied.

7.4 Summary

Tests in mixtures of Kaolinite clay and glass beads, and mixtures of coarse sand and glass beads, were carried out in order to understand the influence that the size of the matrix particles has on the accuracy of the theoretical models. The same glass beads, which had 10mm in diameter, were used in both sets of tests. It was found that not just the size ratio between the matrix particles and the disperse particles is important, since the kind of the material composing the matrix can influence the agreement between the laboratory results and the theoretical simulations.

The Kaolinite-glass beds mixtures were intended to simulate mixtures with an extremely high size ratio (2381). These tests showed that when increasing the concentration of the large particles, the spaces between the glass beads started to reduce and due the stress concentration around these particles, a compaction of the Kaolinite clay took place. This compaction completely changed the properties of the matrix. The theoretical models assume that the elastic properties of matrix material do not change when increasing the concentration of disperses particles. Thus, the Hashin and Guth models underpredicted the observed results for this kind of mixtures.

The tests that were carried out on mixtures of coarse sand number 16 and glass beads were intended to study the influence that a small size ratio has on the performance of the theoretical models. It was found that particle interference was generated when increasing the concentration of the large particles. This interference disturbed the packing of the matrix material, incrementing the voids ratio of the mixture, and strongly affecting the properties of the matrix. Consequently, the theoretical models overpredicted the elastic moduli of these samples. It was observed that when these mixtures were subjected to a higher vertical pressure, crushing of the matrix particles was produced. This crushing changed the properties of the matrix material, and since the level of crushing was not the same at each concentration of the disperse particles, the theoretical models tended to incorrectly predict the laboratory results.

In this way, properties as the particle size ratio and the compressibility of the matrix material have to be known prior to apply the theoretical models. If the interaction between the matrix particles and the disperse particles disturbs the setup of the matrix material, the theoretical models cannot be applied since the assumptions that they have will not be satisfied.

8.0 INFLUENCE OF THE DISPERSED PARTICLES SIZE

This Chapter presents tests that were developed in order to study the influence that the size of the disperse particles has on the elastic moduli of soil mixtures, and how this influence is included in the theoretical simulations. Mixtures of 70% Kaolinite clay and 30% Ottawa sand were used as the matrix of the samples. Glass beads of 2mm, 5mm, and 10 mm in diameter were used as the disperse particles. The average size ratio was 11.1 for the mixtures containing glass beads of 2mm in diameter, 27.8 for those containing glass beads of 5mm, and 55.6 for those containing glass beads of 10 mm. The tests were carried out at three different vertical pressures: 100 kPa, 200 kPa and 500 kPa. However, the results at 200 kPa are not presented since they exhibited the same trend that those obtained at 100 kPa.

This chapter continues the discussion about the effects of particle interference and matrix compaction that was started in the previous chapter.

8.1 Tests on Mixtures of Kaolinite-Ottawa Sand and Glass Beads

Figure 8.1 shows the density of the mixtures at 100 kPa. The maximum densities were obtained at a fine particles concentration between 10% and 30%. Figure 8.2 shows the density of the same samples when they were subjected to 500 kPa. At this last vertical pressure the maximum densities were obtained at a fine particles concentration between 20% and 40%. This increment in the optimum concentration obeys the fact that the matrix of the samples was composed by a mixture with a high percentage of Kaolinite clay, material that has an important volume reduction when it is subjected to a high confining pressure. It must be noticed that at the two different vertical pressures, the mixtures containing the smaller glass beads had the higher densities.

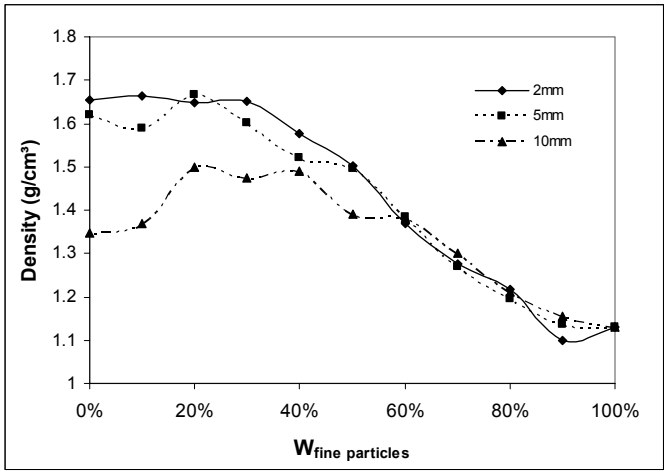

Figure 8.1 Density of the Mixtures at 100 kPa

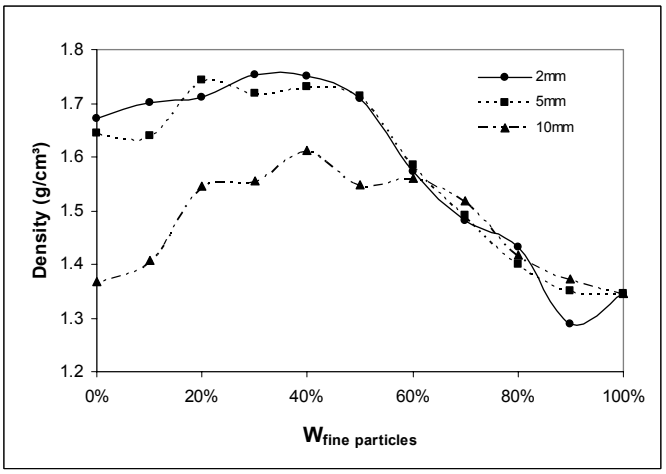

Figure 8.2 Density of the Mixtures at 500 kPa

Figures 8.3 and 8.4 show the recorded Vp and Vs at 100 kPa and 500 kPa. The ranges where the maximum values took place were close to those ranges obtained on the density curves. At each pressure, it can be noticed how when increasing the disperse particles diameter, the maximum velocity (both Vp and Vs) significantly increases too.

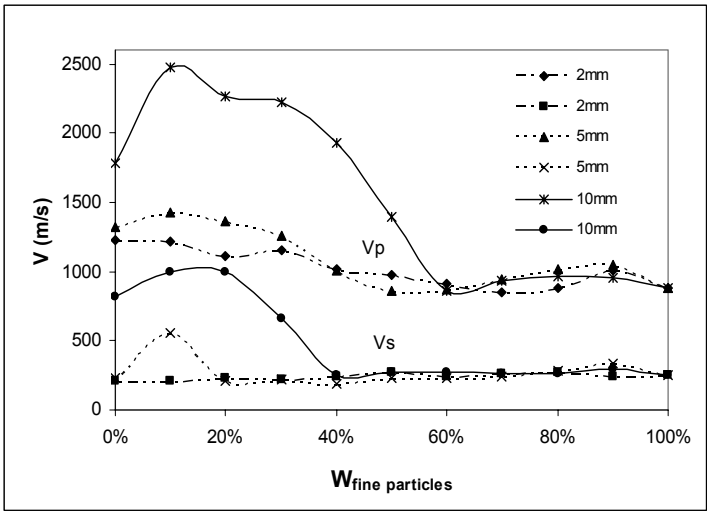

Figure 8.3 Vp and Vs of the Mixtures at 100 kPa

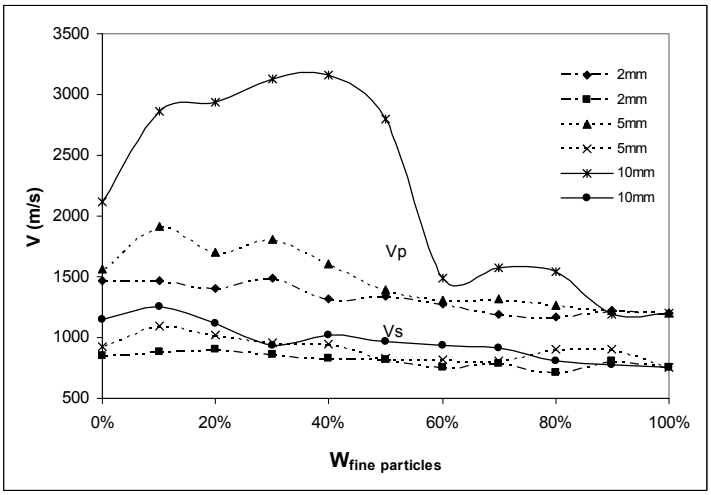

Figure 8.4 Vp and Vs of the Mixtures at 500 kPa

Figures 8.5 and 8.6 show the elastic modulus E of the samples at vertical pressures of 100 kPa and 500 kPa respectively. At each vertical pressure, the mixtures containing the bigger glass beads had the higher elastic moduli. However, the exhibited trends at 100 kPa and 500 kPa were slightly different. When the samples were subjected to 100 kPa, a steep transition between the maximum value and the surrounding points took place. On the other hand, when the samples were subjected to 500 kPa, the observed transition was more uniform.

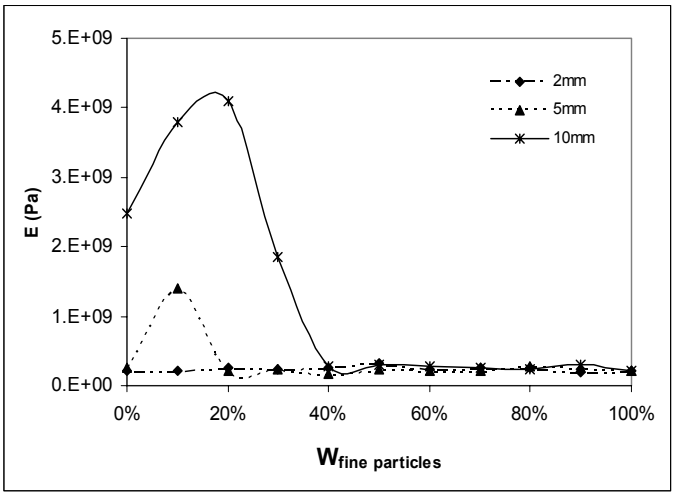

Figure 8.5 E of the Mixtures at 100 kPa

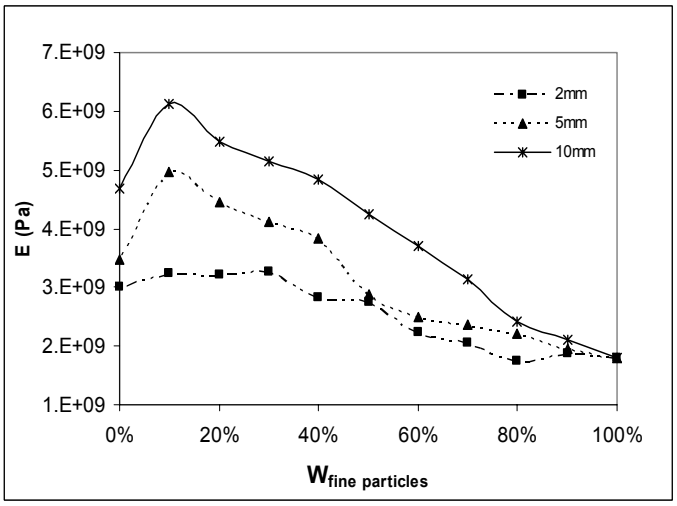

Figure 8.6 E of the Mixtures at 500 kPa

The trend exhibited in the elastic modulus G was similar to the trend exhibited in the elastic modulus E. Figures 8.7 and 8.8 show the obtained results. The higher values were obtained on the samples containing the glass beads of 10mm in diameter. Also, the transition to those values was more uniform when the samples were subjected to a higher vertical pressure.

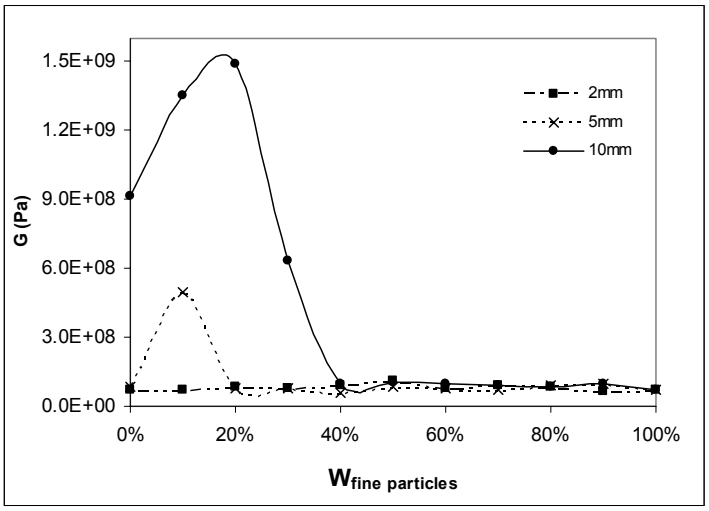

Figure 8.7 G of the Mixtures at 100 kPa

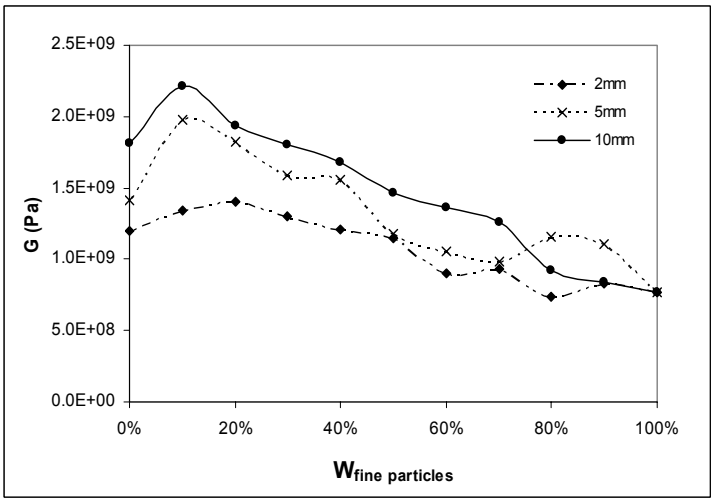

Figure 8.8 G of the Mixtures at 500 kPa

8.2 Theoretical Simulation

Since the Hashin, Guth, and Greszczuk models are based on the elastic properties of the matrix and only the concentration by volume of the disperse particles, it could be thought that the size of the disperse particles is not included as a variable in these models; however, somehow the effect of the disperse particles size is implicit in the concentration by volume of these particles. As showed in Chapter 4, the concentration by volume of the disperse particles can be expressed as the concentration by weight times the ratio between the density of the composite and

the density of the disperse particles. Similarly, the density of the composite depends on the disperse particles size as showed in Figures 8.1 and 8.2.

Trough out the previous chapters, the Hashin's model has been the most accurate model in predicting the Poisson's ratio and the elastic moduli of the tested mixtures; thus, in order to simplify the presentation of the theoretical simulations, only the results predicted by this model are provided. The following graphs show the obtained laboratory results compared to those values predicted by the Hashin's model. It should be noticed that the Hashin's model at each different pressure is slightly affected when increasing the size of the glass beads, and some times it is hard to distinguish the three sets of predictions.

The comparisons between the values obtained in the laboratory and the values predicted by the Hashin's model for the Poisson's ratio of the samples are showed in figures 8.9 and 8.10. At each vertical pressure, the values predicted by the Hashin's model when using different sizes of glass beads cannot be clearly differentiated. Figure 8.9 show that this model satisfactory predicted the values measured in the laboratory when the samples were subjected to a vertical pressure of 100 kPa. A constant value of 0.45 was observed as the average Poisson's ratio of the samples at this pressure. On the other hand, the results obtained at 500 kPa showed that the Hashin's model satisfactory predicted the Poisson's ratio of the samples only when these had glass beads of 2mm or 5mm as the disperse particles of the mixture. The average Poisson's ratio of the samples at this pressure was very close to 0.2.

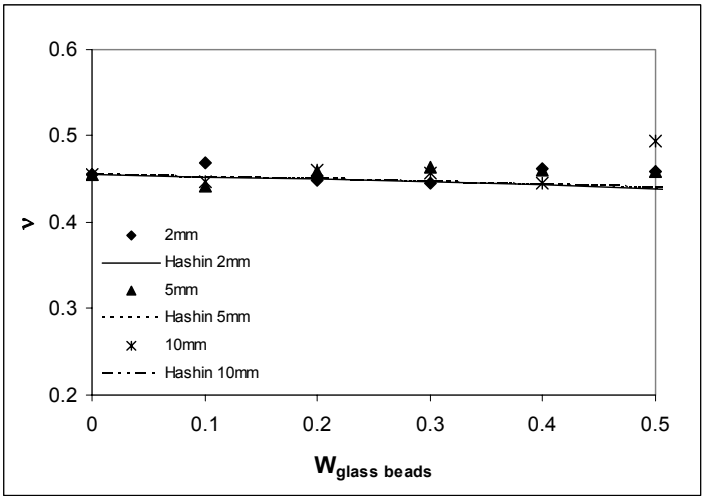

Figure 8.9 Poison's ratio Simulation at 100 kPa

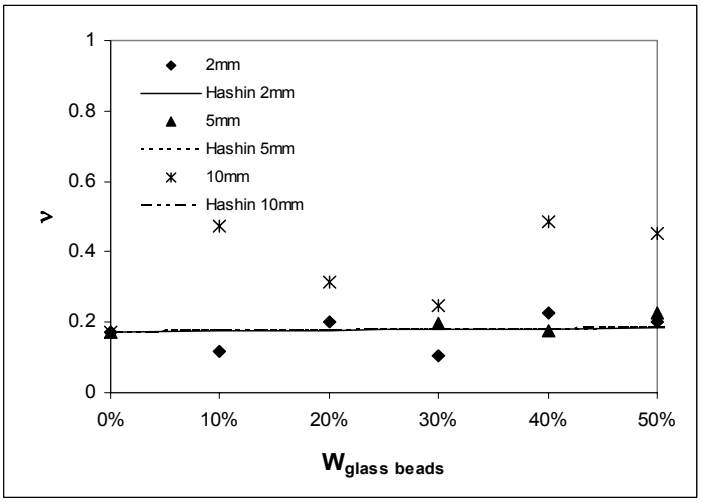

Figure 8.10 Poisson's ratio Simulation at 500 kPa

Figures 8.11 and 8.12 show the results for the elastic modulus E. At each vertical pressure, the values predicted by the Hashin's model when using different sizes of glass beads could hardly been differentiated. At 100 kPa, the Hashin's model tended to overpredict the laboratory result, although it can be noticed that the amount of the overprediction was related to the size of the used glass beads. In this way, this model satisfactory predicted the elastic moduli of the samples containing glass beads of 10 mm in diameter. The observed trend in the results at 500 kPa was totally different. Beyond a glass beads concentration of 20 %, the Hashin's model strongly underpredicted the elastic moduli of the samples containing glass beads of 10 mm. On the other hand, this model tended to slightly overpredict the elastic moduli E of the samples containing glass beads of 2 mm and 5 mm. It should be noticed, that this overprediction was bigger on the samples containing glass beads of 2 mm.

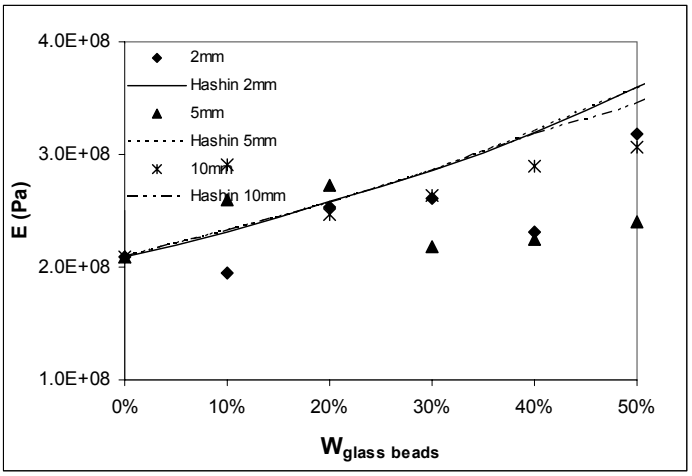

Figure 8.11 E Simulation at 100 kPa

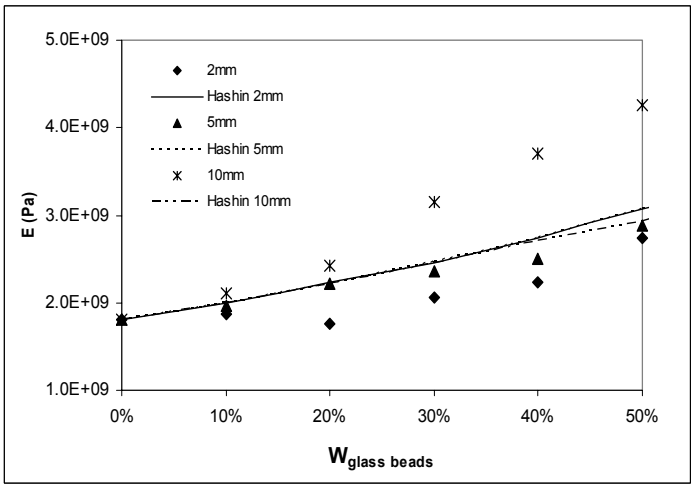

Figure 8.12 E Simulation at 500 kPa

The exhibited trend in the elastic modulus G was similar to the exhibited trend in the elastic modulus E. Figures 8.13 and 8.14 show the obtained results. At each vertical pressure, the Hashin's model predicted almost the same group of values for each kind of mixture. When the samples were subjected to a vertical pressure of 100 kPa, the theoretical model tended to overpredict the laboratory results, and again the smaller error was obtained when using glass beads of 10mm in diameter. At a vertical pressure of 500 kPa, the model overpredicted the laboratory results for the mixtures containing glass beads of 2mm and 5mm, while it underpredicted the measured values for the mixtures containing glass beads of 10 mm.

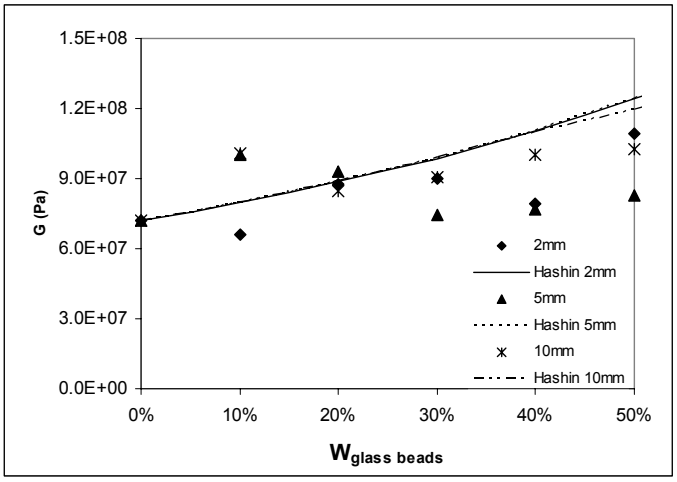

Figure 8.13 G Simulation at 100 kPa

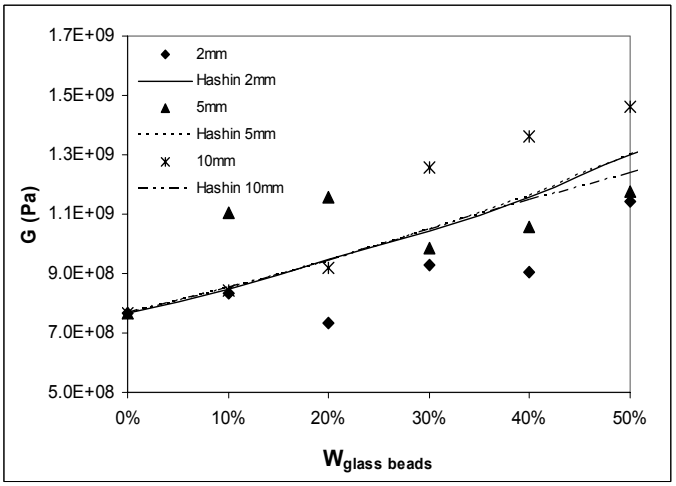

Figure 8.14 G Simulation at 500 kPa

8.3 The Effects of Matrix Compaction and Particle Interference

During the previous chapter, the separate effects of matrix compaction and particle interference were studied. In summary, it was concluded that when the size of the matrix particles and the disperse particles is similar, particle interference is generated when increasing the concentration of the disperse particles, since the separation of these particles does not allow the fine particles to maintain their package. This phenomenon was observed to take place in mixture of coarse sand No.16 and glass beads of 10 mm in diameter. On the other hand, the matrix compaction was

observed in mixtures containing Kaolinite clay and glass beads of 10 mm in diameter. The particle size ratio of this kind of mixtures was extremely high. The effects of particle interference and the matrix compaction are totally different. Particle interference causes the overprediction of the laboratory results while the matrix compaction causes the underprediction of those values. The test presented in this chapter will be analyzed under this approach, intended to gain more insight about how these tow effects affect the theoretical models.

The mixtures containing glass beads of 2mm in diameter had an average size ratio of 11.1, value that is close to the size ratio obtained in the mixtures of coarse sand No.16 and Glass beads of 10 mm (tested on the previous chapter). So, it was not surprising that these mixtures presented particle interference too. It can be noticed how for both elastic moduli E and G, the Hashin's model tended to overpredict the laboratory results regardless the used confining pressure. Similarly, The mixtures containing glass beads of 5 mm in diameter showed particle interference since the Hashin's model overpredicted the laboratory results. These mixtures had an average particle size ratio of 27.8.

An interesting phenomenon could be observed in the theoretical simulations for the mixtures containing glass beads of 10 mm in diameter. On both E and G simulations, the theoretical model slightly overpredicted the laboratory results when the samples were subjected to a vertical pressure of 100 kPa, but it strongly underpredicted the measured values when the vertical pressure was increased to 500 kPa. The amount of the underprediction when the samples were subjected to 100 kPa was really small, and it can be explained since the average particle size ratio was 55.6. As it was explained in the last chapter, the effect of particle interference tends to disappear when the particles size ratio is really high. On the contrary, the amount of underprediction when the samples were subjected to 500 kPa leaded to a significant error. As in the previous chapter, matrix compaction took place. However, the obtained error was small when compared to that obtained during the tests on pure Kaolinite clay and glass beads of 10 mm (presented in the previous Chapter). Thus, during the tests presented in this chapter, the matrix did not compress as much as it did in the previous tests; although the matrix was affected for the matrix compaction effect, the inclusions of Ottawa sand helped to avoid a bigger variation in the elastic properties of this medium.

8.4 Summary

Tests were carried out in dry mixtures containing a matrix composed by Kaolinite clay and Ottawa sand, and glass beads as the disperse particles. Three different sizes of glass beads were used. It was observed that when the size of the disperse particles is several times bigger than the size of the fine particles, the effect of particle interference is minimized while the effect of matrix compaction is maximized. In this way, the elastic moduli of these mixtures tend to be higher. On the other hand, as explained in the previous chapter, the presented theoretical models assume that the properties of the matrix material do not change when increasing the concentration of the disperse particles. Thus, if particle interference or matrix compaction takes place, the theoretical models cannot be applied.

The tests that were carried out on mixtures containing glass beads of 2mm and 5mm in diameter confirmed the effect that the particle interference has on the agreement between the values measured in the laboratory and those predicted by the theoretical models. Similarly, the tests made on the samples having glass beads of 10 mm as the disperse particles provided valuable information in order to understand the effect of matrix compaction.

In conclusion, although the Hashin's model indirectly includes the size of the particles, it does not include the variations in the matrix properties than can be induced. Thus, previous knowledge about the feasibility that a mixture has to develop particle interference or matrix compaction has to be known in order to correctly apply the theoretical models.

9.0 FEASIBILITY OF PREDICTING THE STATIC ELASTIC CONSTANTS USING THE TEORETICALL MODELS

Until this chapter, the Hashin, Guth, and Greszczuk models have been used in predicting the elastic properties of soil mixtures under different conditions. In this way, the influence that the moisture content, the vertical pressure, and the particles size have on the performance and accuracy of these models has been studied, producing satisfactory results. Nevertheless, all the tests presented until this moment have measured the dynamic elastic constants of the samples. This chapter attempts to study whether or not these models can be used in predicting the static elastic properties too.

Experimental tests developed by Marrion [8] have shown that the ratio between the static and the dynamic moduli depends on the used confining pressure. He found that the value of this ratio is increased when the samples are subjected to high confining pressures. According to Marrion, the dynamic moduli only reflect the elastic part of the deformations, while the static moduli comprise both the elastic and the inelastic deformations. Since the theoretical models are based on the principles of elasticity, some of the assumption that they have will not be satisfied if the soil mixtures present important inelastic deformations.

9.1 Triaxial Measurements

W. Su [33] presented the results obtained on triaxial tests that were carried out on soil mixtures containing gravels. The maximum size of the oversized particles was 1 inch. The confining pressure used on the tests was 150 kPa. Su presented the axial strength- deviator stress curves and the axial strength-volumetric strain curves, for mixtures having a large particles concentration between 0% and 60%. Also, he provided the density of the samples. Figure 9.1 shows these values as a function of the concentration of the large particles.

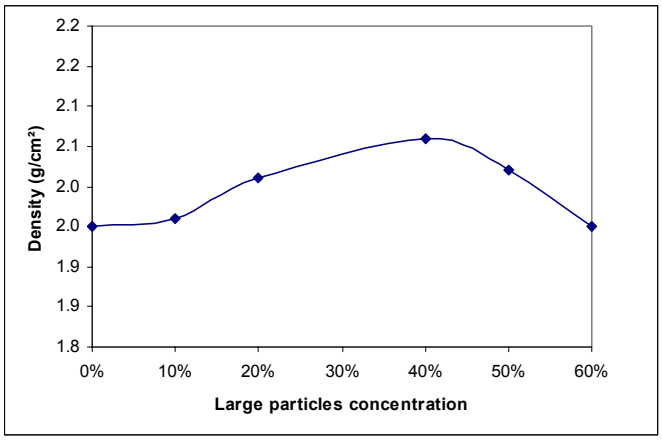

Figure 9.1 Density of the Su Samples

It must be noticed that beyond a concentration of large particles equal to 40%, the density of the mixtures started to decrease, indicating that the change in the kind of structure was taking place, and the large particles were no longer the disperse particles of the mixture.

Using the curves provided by Su (depicting the deviator stresses, the axial strains and the volumetric strains), the static elastic moduli and the Poisson's ratio of the mixtures were calculated by using the follow procedure:

1. From the definition of the Poisson ratio ($\mu = \varepsilon_t / \varepsilon_a$), the next expression can be deduced

$$\mu = 0.5 - 0.5(\varepsilon_v / \varepsilon_a) \qquad (9\text{-}1)$$

Where ε_v and ε_a are defined as the volumetric strain and the axial strain. Su provided both values.

2. In order to calculate the elastic modulus E, the follow equation proposed by Bishop and Henkel [34] can be used

$$-\varepsilon_v = [\,(1 - 2\mu)/E\,][\,\Delta\sigma_1' + \Delta\sigma_2' + \Delta\sigma_3'\,] \qquad (9\text{-}2)$$

Where all the terms were defined previously, and $-\varepsilon_v$ is describing a decrease in volume. Since the triaxial tests were CD tests, the increments in σ_2' and σ_3' were zero, and the elastic modulus E could be solved since the rest of the terms were known.

3. Since the Poisson's ratio and the elastic modulus E were solved, the shear modulus G could be easily found.

By using this procedure, the static elastic properties of the mixtures containing a large particles concentration of 0%, 10%, 20%, 40%, 50%, and 60% were calculated. Table 10.1 shows the obtained results.

Table 9.1 Triaxial measurements (Su tests)

C_{fw}	C_{fv}	ρ(g/cm³)	ε_a	ε_v	σ_3 (kPa)	$\Delta\sigma$(kPa)	μ	E (kPa)	G (kPa)
0.00	0.00	1.95	4%	-0.9%	150	550	0.61	1.38E+04	4.26E+03
0.10	0.08	1.96	3%	-0.9%	150	680	0.65	2.27E+04	6.87E+03
0.20	0.15	2.01	3%	-0.9%	150	710	0.65	2.37E+04	7.17E+03
0.40	0.32	2.06	3%	0.0%	150	770	0.50	2.57E+04	8.56E+03
0.50	0.39	2.02	3%	-0.5%	150	710	0.58	2.37E+04	7.47E+03
0.60	0.45	1.95	3%	-0.9%	150	650	0.65	2.17E+04	6.57E+03

It should be noticed that the tested samples had Poisson's ratios between 0.5 and 0.65. The fact that these values were higher than 0,5 was not surprising since the volumetric deformation of the samples (ε_v) took negative values. According to Sechler [35], a sample can have a Poisson's ratio higher than 0.5, if it presents a volume increment when it is subjected to an increasing pressure. Mal and Singh [36] have shown that under the approach of the elasticity theory, the Poisson's ratio can only take values between –1 and 0.5. Although mathematically it is possible to have an element with a negative Poisson's ratio, this situation is not very often found in the laboratory practice. Analyzing the equation for the Poisson's ratio in terms of the wave velocities (equation 4.2), it can be noticed that only if the shear wave velocity is several times higher than the compression wave velocity, the sample will have a negative Poisson's ratio. On t he other hand, a Poisson's ratio equal to 0.5 is presented only in fluids or incompressible solids.[36]

9.2 Theoretical Simulations

The Hashin, Guth and Greszczuk models were applied to the data obtained in the previous section. Figure 9.1 (density curve) showed that the change in the mixture's structure took place at a large particle concentration of 40%. In this way, the values calculated using the theoretical models are only valid between a large particles concentration of 0% and this critical concentration. Figure 9.2 shows the values measured in the laboratory for the Poisson's ratio of the samples and those values predicted using the theoretical models.

The values predicted by the Hashin's model satisfactory agree with the laboratory results. However, at the critical concentration of large particles (40%), this model overpredicted the value measured in the laboratory. On the other hand, the Guth model constantly underpredicted the Poisson's ratio of the samples while the Greszczuk model slightly underpredicted these values.

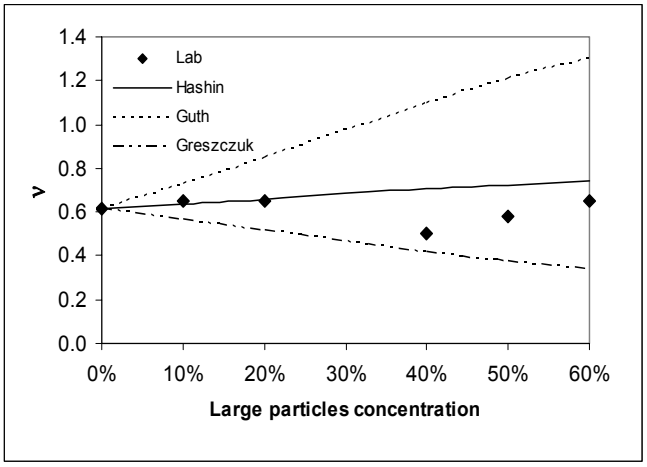

Figure 9.2 Poisson's ratio Simulation for the Su Mixtures

The comparison between the laboratory results and those values predicted using the theoretical models for the static elastic modulus E of the samples is showed in figure 9.3. Again, the values predicted by the theoretical models were only valid bellow a large particles concentration of 40%. The Hashin and Guth models satisfactory predicted the laboratory results until this concentration was reached. On the other hand, the results obtained by using the Greszczuk's model did not have any sense, since this model predicted decreasing values that even became negative when the large particles concentration was higher than 20%. This can be explained since the Poisson's ratio

of the matrix was bigger than 0.5. As explained in Chapter 3, the Greszczuk's model is based on deformation compatibility, isotropic condition and other assumptions that clearly are not satisfied when the matrix of the mixture presents a Poisson's ratio bigger than 0.5.

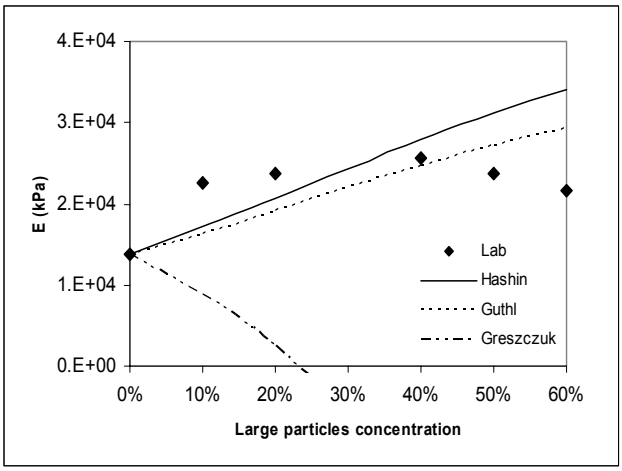

Figure 9.3 Static E Simulation for the Su mixtures

Figure 9.4 show the comparison between the measured static elastic modulus G of the samples and those values predicted using the theoretical models. Again, the Hashin and Guth models satisfactory predicted the laboratory results between a large particles concentration of 0% and 40%. On the other hand, because the reasons explained before, the Greszczuk's model predicted absurd values.

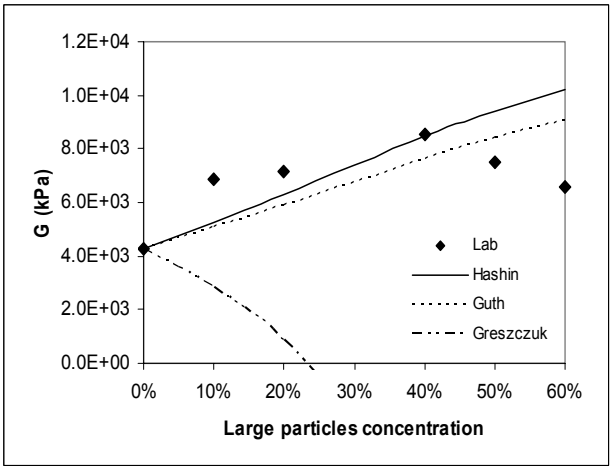

Figure 9.4 Static G Simulation for the Su Mixtures

In conclusion, experimental results showed that the Hashin and Guth models could satisfactory be applied in order to predict the static elastic moduli of soil mixtures. However, only the Hashin's model could accurately predict the Poisson's ratio of these composites. It should be noticed that not all the constrains that these models have were completely satisfied, but it seems like this fact did not lead to a significant error. On the other hand, the poor agreement between the laboratory values and those predicted using the Greszczuk's model showed that this model cannot be applied in predicting the static elastic moduli. Further investigation in this topic is recommended.

10.0 STATISITICAL ANALYSIS

Through out this investigation, the Hashin's model has proved to be the most accurate model in predicting the elastic properties of the tested mixtures. It was showed that this model can be applied in order to predict the elastic constants of soil mixtures under different conditions of vertical pressure, moisture content and particles size ratio. On the other hand, it was found that the Guth's model is an accurate model that can be used in predicting the elastic moduli, but it cannot be used in order to predict the Poisson's ratio since this model tends to overpredict the laboratory results. Similarly, it was found that the Greszczuk's model can only be used under certain conditions since small alterations in the constrains that this model has, can cause important overpredictions. In this way, the statistical analysis presented in this chapter was carried out using only the data obtained with the Hashin's model.

Analyzing the graphs presented during the previous chapters, the accuracy of the Hashin's model can be appreciated from the good match between the measured values and those obtained using this model. However, it is necessary to have statistical descriptors in order to mathematically assess this agreement. A frequency analysis was carried out using the laboratory results for the elastic properties of the samples, and those values predicted using the Hashin's model. The laboratory results provided by other authors were not included in this analysis. Also, those cases when matrix compaction or crushing of the matrix material took place were excluded. The statistical analysis was done separately for the Poisson's ratio and the elastic moduli E and G. The following procedure was applied for each one of these elastic properties:

1. The values measured in the laboratory and those obtained using the Hashin's model were separated according to the vertical pressure used on the tests. In this way, three different groups were obtained (100 kPa, 200 kPa, 500kPa). The group of the tests developed under a vertical pressure of 100 kPa had 40 couples, the group of the tests developed at 200 kPa had 40 couples, and the group of the tests developed at 500 kPa had 16 couples.

2. Each one of the values obtained using the Hashin's model was divided by the correspondent value measured in the laboratory.
3. The obtained ratios were sorted and a frequency analysis was carried out. The used class length was 5%. Using these data, a frequency histogram was plotted.
4. The mean value and the standard deviation for each distribution were calculated.
5. Using the results of the frequency analysis, the percentage of ratios between 0.7 and 1.3 were calculated.

The obtained results are presented in the follow sections.

10.1 Statistical Analysis for the Poisson's ratio

The frequency histograms for the ratio between the Poisson's ratios predicted by the Hashin's model and the Poisson's ratios measured in the laboratory are showed in Figure 10.1. The results for the considered three groups (according to the used vertical pressure) are showed in the same figure. The group conformed by the tests developed at 100 kPa had a mean equal to 0.991, with a standard deviation of 0.036. It can be noticed that all the values in this group were higher than 0.85 and lower than 1.10. In the same way, the group of the tests developed at 200 kPa presented satisfactory results, having a mean of 0.990 with a standard deviation of 0.021. Although the tests developed under a vertical pressure of 100 kPa had a mean closer than 1, the tests developed at 200 kPa had a better standard deviation. It can be noticed that all the ratios of this group were higher than 0.90 and lower than 1.05.

The group of the tests that were developed under a vertical pressure of 500 kPa had a mean of 0.952 with a standard deviation of 0.288. This group had the worst mean and the worst standard deviation of the three groups. Only 75% of the considered samples had a ratio between 0.7 and 1.3, showing a significant spread.

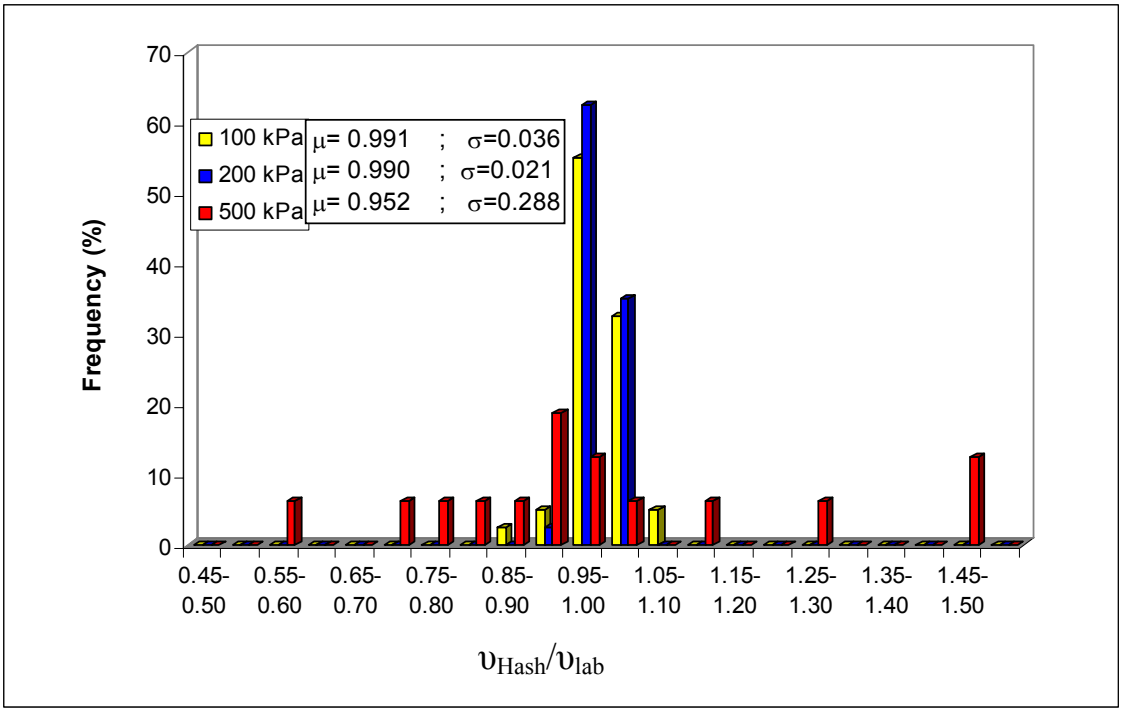

Figure 10.1 Frequency Histogram for the Poisson's ratio

In this way, based on the results presented before, it can be concluded that the Hashin's model satisfactory predicted the Poisson's ratio of the tested mixtures.

10.2 Statistical Analysis for the Elastic Moduli E and G.

Figure 10.2 shows the frequency histograms for the elastic modulus E. Again, the results for the different groups are showed in the same graph. The group conformed by the tests that were developed at a vertical pressure of 100 kPa had a mean of 1.041 with a standard deviation of 0.251. Similarly, the group of the tests developed at 200 kPa had a mean of 0.996 with a standard deviation of 0.209. Thus, it can be noticed that the agreement between the predicted and the obtained values was improved when the vertical pressure was increased. While only the 75% of the samples from the first group had an EHash/Elab ratio between 0.7 and 1.3, 86% of the samples from the second group had this ratio between these limits.

The group of the tests developed under a vertical pressure of 500 kPa had a mean of 1.023 with a standard deviation of 0.167. This was the smallest standard deviation of the three groups. Also, It can be noticed that when the vertical pressure was increased from 100 kPa to 500 kPa, the percentage of samples having a ratio between 0.7 and 1.3 increased from 75% to 96%.

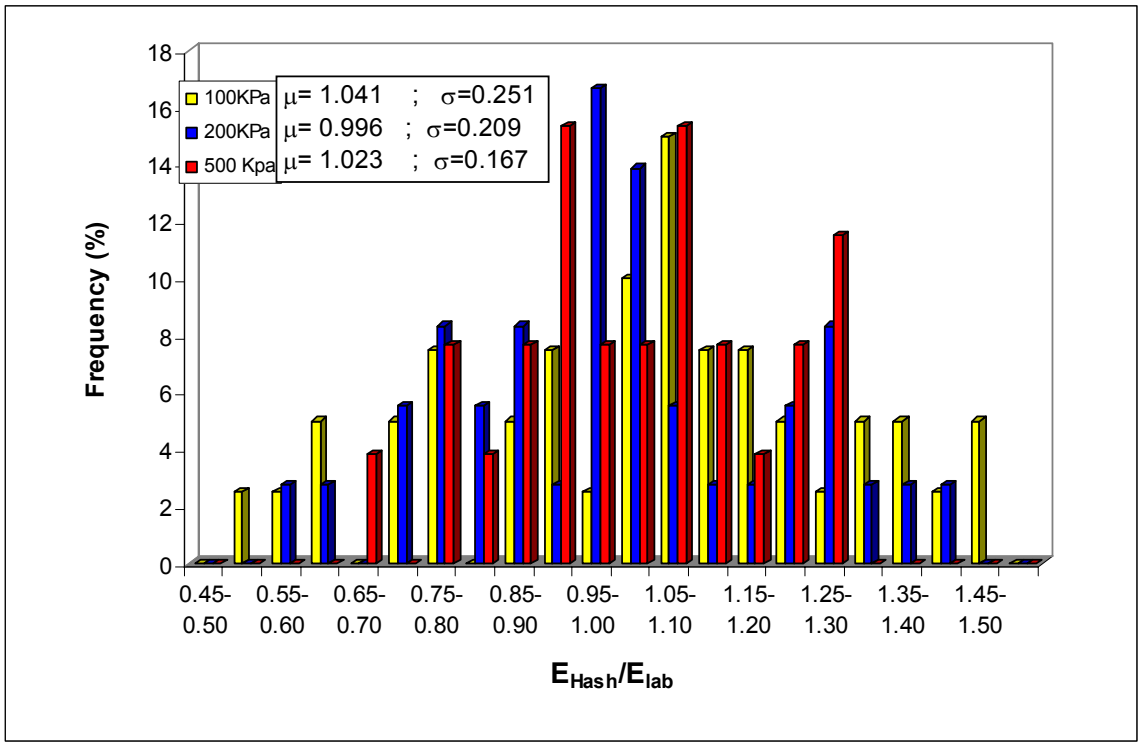

Figure 10.2 Frequency Histogram for the Elastic Modulus E

Figure 10.3 shows the results obtained for the elastic modulus G. The group of the tests developed at 100 kPa had a mean of 1.044 with a standard deviation of 0.258. The group of the tests developed at 200 kPa had a mean of 0.986 with a standard deviation of 0.224. Thus, although the standard deviation was better in the second group, the mean of the distribution was better in the first group. The group containing the tests developed at 500 kPa had a mean of 0.961 with a standard deviation of 0.188. Although this group had the worst mean of the three groups, it had the best standard deviation.

As in the case of the elastic modulus E, when the vertical pressure was increased from 100 kPa to 500 kPa, the percentage of samples having ratios between 0.7 and 1.3 was increased too; in this case from 73% to 96%. However,

in this case the mean of the distribution started to decrees and tended to be less than 1, from 1.044 at 100 kPa to 0.961 at 500 kPa.

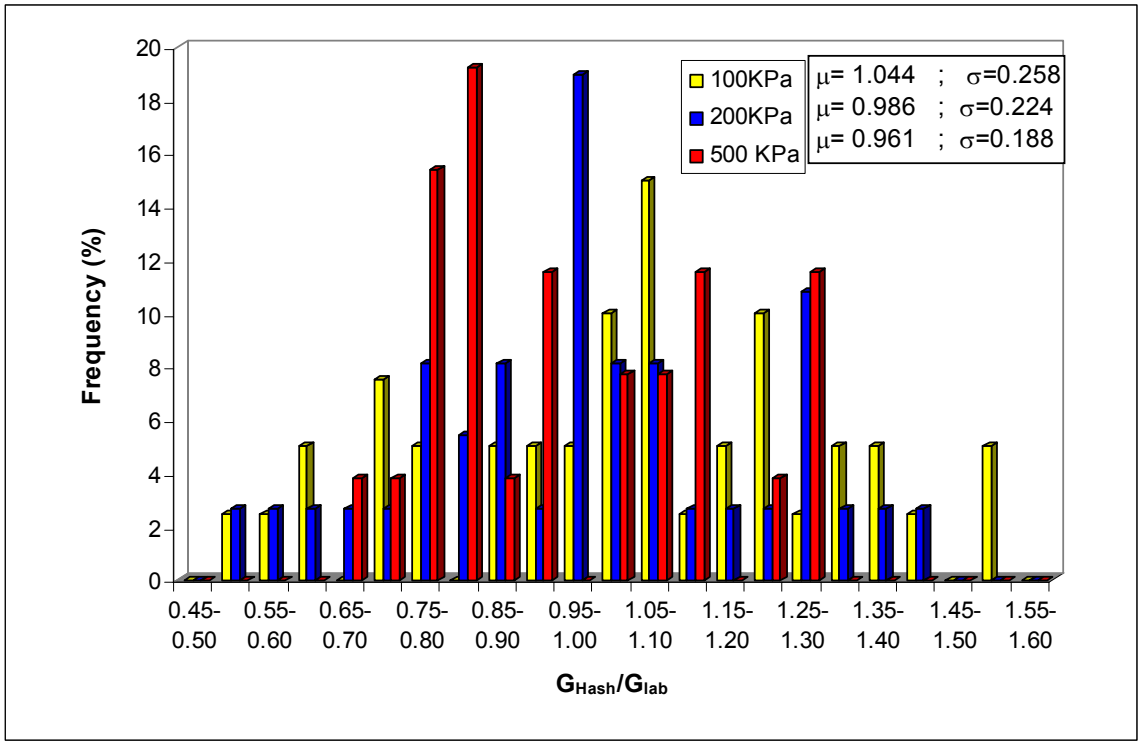

Figure 10.3 Frequency Histogram for the Elastic Shear Modulus G

In this way, it can be seen that the Hashin's model is able to satisfactory predict the elastic moduli of soil mixtures.

10.3 Summary

A frequency analysis was carried out for the ratios (υ, E and G) between the values predicted using the Hashin's model and the values measured in the laboratory. The results for the Poisson's ratio had the best mean values and standard deviations of the whole analysis. It was found that the agreement between the measured and the predicted Poisson's ratio of the samples was better for the test that were carried out under vertical pressures of 100 and 200 kPa than for those carried out at 500 kPa. The fact that those distributions had the 100 % of their samples between 0.85 and 1.10 show the accuracy of the Hashin's model.

The analysis for the elastic moduli showed that the agreement between the laboratory results and those values predicted using the model was improved when the vertical pressure was increased. Nevertheless, only 16 samples could be considered for the statistical analysis of the results obtained under a vertical pressure of 500 kPa, while 40 samples were used for the analysis of the tests developed at 100 kPa and 200 kPa. This leads to the conclusion that although the agreement between the laboratory results and the predicted values improved with the vertical pressure, the risk that matrix compaction or crushing takes place improved too.

In conclusion, if the results presented in this section are compared to the traditional factors of safety used in the Geotechnical practice, it can be seen that the Hashin model is a theoretical model that satisfactory predicts the elastic properties of soil mixtures.

11.0 CONCLUSIONS

Theoretical models that can be used in order to predict the elastic properties of soil mixtures were presented. Using ultrasonic velocity tests on more than 50 different mixtures, the elastic properties measured in the laboratory and those values predicted by the theoretical models were compared. The effects that the external pressure, the moisture content, and the size ratio have on the performance of these models were studied, leading to the follow conclusions:

- The Hashin model and the Guth model satisfactory predict the elastic moduli of dry mixtures regardless the used confining pressure. Also, the Hashin model can be satisfactory used on predicting the Poisson's ratio under the same conditions. On the other hand, the Greszczuk model has to be treated with some restrictions, since it overpredicts the elastic moduli and underpredicts the Poisson's ratio of the composites when the normal stresses are less than 500 kPa. It can be concluded that the assumption of deformation compatibility that this model has is not fulfilled when using low vertical pressures.

- The results of the tests carried out on unsaturated mixtures lead to the conclusion that the Hashin and Guth models can be satisfactory used in order to predict the elastic moduli of unsaturated mixtures regardless the applied normal stresses. Again, only the Hashin's model should be used in order to predict the Poisson' ratio of the mixtures, and the Greszczuk model can only be used when the normal stress is higher than 500 kPa. It was found that these models should not be used when a soil composite is saturated or its degree of saturation is close to 1, and it is subjected to higher vertical pressures.

- Prior to apply the theoretical models on soil mixtures, knowledge of the particle size ratio and the compressibility of the matrix material is required. If the size ratio of the particles is around 10 or 20, particle interference will take place. Particle interference causes that the theoretical models overpredict the elastic moduli of the mixtures, since it changes the elastic properties of the matrix material. It should be noticed that

particle interference could lead to significant errors. Further investigation in finding the critical size ratio when the particle interference can be neglected is highly recommended.

- On the other hand, when the size ratio of the particles is extremely high, the stress concentration around the bigger particles can lead to the matrix compaction. This effect of matrix compaction changes the elastic properties of the matrix material and leads to a significant underprediction of the real elastic moduli. In this way, the theoretical models should not be used under these conditions.

- The theoretical models cannot be applied when the matrix material presents crushing since this crushing changes the elastic properties of the matrix. The level of crushing in the matrix is a function of the large particles concentration.

- The Hashin and Guth models can be used in order to predict the static elastic properties, although not all the constrains that these models have are completely satisfied. On the other hand, the Greszczuk's model should not be used if the principles of elasticity are violated. It was found that important errors are produced when using this model under these circumstances.

- In general, it was found that the Hashin's model is the most accurate model in predicting the elastic properties of soil mixtures. The use of the Hashin method is very valuable because it needs only the knowledge of the elastic properties of the soil matrix and the concentration by volume of the large disperse particles. Based on the statistical results presented in the last chapter, it can be concluded that this model can be satisfactory used in the geotechnicall practice; thus, time and money is saved by the use of this method.

BIBLIOGRAPHY

BIBLIOGRAPHY

1. Vallejo, L. E., and Mawby, R., "Porosity Influence on the Shear Strength of Granular Material Clay Mixtures", *Engineering Geology*, 58, (2000), pp. 125-136.

2. D'Appolonia, D.J., Poulos, H.G., and Ladd, C.C., "Initial Settlement of Structures on Clay," *ASCE Journal of the Soil Mechanics Division*, 97(10), (1971), pp.1359-1377.

3. Fragaszy, R.J., Su, W., and Siddiqi, F.H, "Effects of Oversize Particles on the Density of Clean Granular Soils,".*Geotechnical Testing Journal*, 13(2), (1990), pp.106-114.

4. Fragaszy, R.J., Su, J., Sidiqqi, F.H., and Ho, C.L., "Modeling Strength of Sandy Gravel.", *ASCE Journal of Geotechnical Engineering*, **118**(6), (1992), pp. 920-935.

5. Iannacchione, A, "Shear Strength of Saturated Clays with Floating Rock Particles" (unpublished Ph.D. Dissertation, Scholl of engineering , University of Pittsburgh, 1997).

6. Yin, H, "Acoustic Velocity and Attenuation of Rocks" (unpublished Ph.D. Dissertation, Stanford University, 1993).

7. Vallejo and Mawby, Op.Cit., p.127.

8. Marion, D, "Acoustical, Mechanical, and Transport Properties of Sediments and Granular Materials" (unpublished Ph.d. Dissertation, Stanford University, 1990).

9. Kolterman, E., and Gorelick, S. M., "Fractional Packing Model for Hydraulic Conductivity Derived from Sediment Mixtures", *Water Resources Research,* 31, (1995), pp. 3283-3297.

10. Vallejo and Mawby, Op.Cit., p.130.

11. Kolterman and Gorelick, Op.Cit., pp. 3285,3286.

12. Vallejo and Mawby, Op.Cit., p.135.

13. Kolterman and Gorelick, Op.Cit., pp. 3283,3284.

14. Vallejo and Mawby, Op.Cit., pp.127-132.

15. Ibid., pp. 129-134.

16. Das, B. M., *Principles of Geotechnicall Engineering* (fourth edition; N.Y : Thomson Publishing, 1998), pp. 172-177.

17. Kolterman and Gorelick, Op.Cit., pp. 3290,3291.

18. Ibid., pp. 3288,3289.

19. Guth, E., "Theory of Filler Reinforcement", *Applied Physics,* 16*,* (1944), pp.20-25.

20. Ibid., pp. 20-22.

21. Greszczuk, B., "Effect of Foreign Inclusions on Properties of Solids", *Engineering Mechanics Division*, 6*,* (1966), pp. 63-77.

22. Ibid., p.65.

23. Ibid., pp.65,66,67.

24. Hashin, Z., "The Moduli of an Elastic Solid Reinforced by Rigid Particles", *Bulletin Research Council of Israel,* 56*,* (1955),pp 46-59.

25. Ibid., p.46.

26. Ibid., p.57.

27. Das, B. *Principles of Soil Dynamics* (Boston: PWS- Kent publishing, 1993), p. 520.

28. Agarwal, B.D., and Bpoutman, L.J., *Analysis and Performance of Fiber Composites* (New York: Wiley).

29. Ahmad, K., and Smalley, I.J., "Observation of Particle Segregation in Vibrated Granular Systems", *Powder Technology*, Vol. 8, (1973), pp. 69-75.

30. Ibid., p. 70.

31. Parry, H.G.., *Stress-Strain Behavior of Soil*, " Some Aspects of the Behavior of Granular Materials at high Pressures, by J. Billman" (Oxfordshire: Foulis and co, 1971), pp. 69-79.

32. Lowrison, G.C., *Crushing and Griding* (Cleveland: OH, 1974), pp. 28-30.

33. Su, W, "Static Strength Evaluation Of Cohesionless Soil With Oversize Particles" (unpublished Ph.D. Dissertation, Department of Civil Engineering, Washington State University, 1989).

34. Bishop, A.W, and Henkel, D.J., *The Measurement of Soil Properties in The Triaxial Test* (London : William Clowes and Sons, 1969),pp. 5-6.

35. Sechler, E.E., *Elasticity in Engineering* (New York : Wiley and Sons, 1952), pp. 56-58.

36. Mal, A.K, and Singh, S.J., *Deformation of Elastic Solids* (New Jersey: Prentice Hall, 1991), pp.10-15.